Promyelocytic leukemia protein function in normal, tumor and senescent human cells

LENKA ROSSMEISLOVÁ

PhD thesis

Charles University
3rd Faculty of Medicine

Institute of Molecular Genetics, v.v.i.
Academy of Sciences of the Czech Republic

Supervisor: Doc. RNDr. Pavel Hozák, DrSc.

Prague 2007

I would like to thank my supervisor Doc. RNDr. Pavel Hozák, DrSc. for advice and support during my PhD studies. I am especially grateful to MUDr. Zdeněk Hodný, CSc. for his help with planning experiments, practical advice and helpful discussions. Also I would like to express my endless gratitude to my former supervisor, MD. Steven R. Smith, PhD. for being my friend and „boss" at the same time. I greatly appreciate the technical assistance of Věra Lukešová and Iva Jelínková. And I do not want to miss the opportunity to say that I have felt very fortunate to meet, work and have fun with my colleagues, especially Jana, Zorka, Katka, Michal, Rasťo and Tibor.

Last, but absolutely not at least, I would like to thank Martin, my husband, and my parents for their unconditional love and encouragement priceless at times when nothing was working, deadlines were approaching, supervisors were upset or too busy and when the science did not seem to be fun.

LIST OF ABBREVIATIONS

APNC actinomycin- induced PML nucleolar cap
APL acute promyelocytic leukemia
AraC arabinosylcytosine
ATM ataxia telangiectasia mutated kinase
ATP adenosine triphosphate
ATR ATM and Rad3 related kinase
BLM Bloom syndrome helicase
BRCA1 breast cancer type 1 susceptibility protein
BrdU 5-bromo-2'-deoxyuridine
BrU 5-bromouridine
BrUTP 5-bromouridine triphosphate
CDS coding sequence
C/EBP CCAAT/enhancer binding protein
Chk1 check kinase 1
Chk2 check kinase 2
DMA distamycin A
DMEM Dulbecco's modified Eagle's medium
DFC dense fibrillar center
DTT dithiothreitol
ERK extracellular signal-regulated kinase
EtBr ethidium bromide
FBS fetal bovine serum
FC fibrillar center
FITC fluoresceinisothiocyanate
GAPDH glyceraldehyde-3-phosphate dehydrogenase
GAS IFNγ-activated site
GC granular component
HAUSP herpesvirus associated ubiquitin specific protease
HDAC histone deacetylase
HeLa human cervical carcinoma cells
HIPK2 homeodomain interacting protein kinase 2
hMSCs human mesenchymal stem cells
IF indirect immunofluorescence
IFN interferon
IGF insulin-like growth factor
IRF1 interferon regulatory factor 1
ISG interferon-stimulated genes
ISRE interferon stimulated response element
MAPK mitogen-activated protein kinase (ERK1/2)
MDM2 mouse double minute 2 protein
MEF mouse embryonic fibroblasts
MRE11 meiotic recombination 11 homolog
mRNA messenger ribonucleic acid
NBS1 Nijmegen breakage syndrome protein 1
NCoR nuclear co-repressor
NER nucleotide excision repair
NES nuclear export signal
NLS nuclear localization signal
PAGE polyacrylamide gel electrophoresis

PBSphosphate buffer saline
PCNAproliferating cell nuclear antigen
PMLpromyelocytic leukemia protein
PML NBsPML nuclear bodies
PML-NDSPML-nucleolus-derived structure
PMSFphenylmethylsulfonyl fluoride
Pol IRNA polymerase I
Pol IIRNA polymerase II
Pol IIIRNA polymerase III
PPARperoxisome proliferator-activated receptor
pRbretinoblastoma protein
PVDFpolyvinylidene difluoride
qRT-PCRquantitative real time polymerase chain reaction
RAretinoic acid
RARretinoic acid receptor
rDNAribosomal deoxyribonucleic acid
RNaseribonuclease
RPA1replication factor-A protein 1
rRNAribosomal ribonucleic acid
RT-PCRreverse transcription polymerase chain reaction
SDSsodium dodecylsulfate
SIRTsir2-like protein
S/MARsscaffold/nuclear matrix attachment regions
STATsignal transducer and activator of transcription
SUMOsmall ubiquitin-like modifier
TGFßtransforming growth factor ß
TIFtranscription initiation factor
TNFαtumor necrosis factor α
TSAtrichostatin A
TZDthiazolidinedione
UBFupstream binding factor
WBWestern blotting
WRNWerner helicase

TABLE OF CONTENT

1 Abstract

Promyelocytic leukemia protein (*PML*) gene encodes a nuclear protein localizing into the nucleoplasm and distinct nuclear bodies, referred to as PML nuclear bodies (PML NBs). *PML* is now considered as a gene with tumor-suppressive properties since it is implicated in many nuclear functions affecting cellular proliferation, apoptosis and senescence.

The presented work is a part of a larger project that aims to clarify the regulation of promyelocytic leukemia protein expression and investigates the role of PML protein in cellular senescence. The specific goals of my PhD project were to evaluate new *in vitro* models for the study of PML, to elucidate the effects of histone deacetylase inhibitors on *PML* gene expression, and to investigate the association of PML with the nucleolus.

First section of the results is dedicated to the validation of human mesenchymal stem cells (hMSC) as a new model for the study of human adipogenesis, i.e. the commitment and terminal differentiation. This model has been later used for the study of PML protein expression in terminally differentiated cells. hMSC are renewable source of non-committed precursors that are able to differentiate into mature adipocytes under the proper hormonal and pharmacological stimuli. After the optimization of culture protocol supporting the adipogenic differentiation, we determined that the inhibition of MAPK activation, which is increased in later passages of hMSC, facilitated adipogenic conversion of hMSC. Since the pattern of genes expressed during hMSC differentiation into adipocytes (adipsin, aP2, PPARγ, C/EBPß, GLUT4 and leptin) was similar to that observed in other *in vitro* adipocyte models, we concluded that hMSC represent a new and valuable model for the study of human adipogenesis.

Next, we demonstrated that the response of two structural components of PML nuclear bodies, PML and Sp100, to interferon-α was abolished in cells simultaneously treated with histone deacetylases inhibitors. Specifically, trichostatin A blocked the IFNα-induced increase of PML NBs numbers, and up-regulation of both mRNA and protein PML levels in several human cell lines and skin fibroblasts. This effect was not caused by the block of nuclear transport of STAT2, a component of transcription factor ISGF3 responsible for IFNα/β-induction of PML expression. Moreover, chromatin immunoprecipitation with STAT2 antibody confirmed binding of STAT2 to ISRE element of PML promoter after IFNα-stimulation even in the presence of trichostatin A. These data

indicate that the deacetylation is a necessary event for a full transcriptional activation of PML and Sp100 gene, however its effect is not mediated exclusively via ISGF3.

Lastly, we described the expression and localization of PML in growing and senescent hMSC. In particular, we focused on and characterized various forms of a novel nuclear PML compartment associated with nucleoli. This novel compartment was found under growth-permitting conditions also in skin fibroblasts but not in several immortal cell lines. In addition, we observed that PML translocated to the nucleolus also upon inhibition of polymerase I transcription. In HeLa cells, the PML affinity to either active or inactivated nucleoli was restored by a treatment causing premature senescence (i.e. simultaneous administration of 5-bromo-2'-deoxyuridine and distamycin A). These findings indicate that PML may be involved in nucleolar functions of normal non-transformed or senescent cells and that PML association with the nucleolus might be important for cell cycle regulation.

In summary, this work has brought new details on the regulation of *PML* gene expression that can be potentially important in human medicine. Using new *in vitro* models to investigate PML function and behavior, we have collected data showing that PML interacts with the nucleolus and that this interaction is linked with the nonimmortalized or senescent stage of the human cells. In addition, the model of human mesenchymal stem cells has been used to follow the destiny of PML nuclear bodies during terminal differentiation.

2 General Introduction

2.1 *Promyelocytic leukemia protein*

Promyelocytic leukemia protein (*PML*) gene was originally identified as a fusion partner of retinoic acid receptor alpha (*RAR*) in chromosomal translocation found in acute promyelocytic leukemia (APL) [1,2]. Wild type gene encodes a nuclear protein localizing into nucleoplasm and distinct nuclear bodies, referred to as PML nuclear bodies or ND10 (nuclear domain 10) [3].

Human *PML* gene is located on chromosome 15q24.1; PML locus is approximately 52 kb in length and is subdivided into 9 exons [4]. Primary PML transcripts may undergo extensive alternative splicing [5,6]. It results in the production of at least 11 different mRNA species coding PML protein isoforms that share N-terminal region but differ in central and C-terminal regions. *In vivo* translation of these spliced mRNAs generates proteins with predicted molecular weight from 48-97 kDa and migration speed up to 180 kDa, which is the result of various posttranslational modifications [6,7] (Tab. 1).

From its discovery in 1991 [8], PML protein was found to be implicated in many nuclear functions indicating its significant role in the regulation of viral infections, cellular proliferation, apoptosis and senescence (for a review, see [9-12]). Based on these observations, *PML* is now considered as a gene with tumor-suppressive properties.

2.1.1 Regulation of PML transcription

The observation that certain hormones and cytokines strongly affect PML expression initiated the studies of the *cis*-regulation of PML expression. Indeed, PML promoter and its first exon and intron contain recognition elements for several transcription factors **(Fig. 1)**.
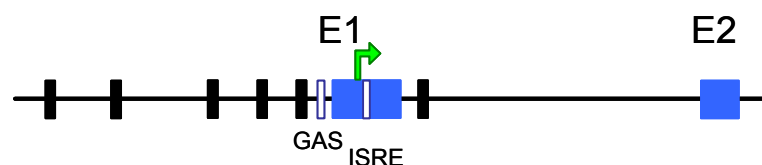

Fig.1. Scheme of promoter and proximal part of human *PML* gene. Exons are represented by blue boxes, putative p53 response elements are indicated by black and GAS/ISRE elements by white boxes. Transcription start is indicated by the arrow. Adapted from de Stanchina et al [24].

The most potent and also first discovered inducers of PML expression are interferons (IFNs) [13-15]. They strongly stimulate PML transcription through the ISRE and weakly through the GAS elements **(BOX #1)** that have been identified within the promoter including first untranslated exon of *PML* gene [16]. PML mRNA induction by interferons is rapid and independent of *de novo* protein synthesis [14], and can be further enhanced by the simultaneous treatment with retinoic acid [17]. In kinetic studies, the peak of transcriptional stimulation was detected between 4 and 8 hours of IFNα- or IFNγ-treatment, then the levels of PML mRNA declined steadily for following 12 hours [16]. In addition, we have shown that the ability of IFNs to induce PML transcription depends on the activity of histone deacetylases (HDAC) as demonstrated in the Experimental part II. Since interferons are cytokines produced mainly by immune cells in response to viral infection, *in vivo* activation of immune system leads indeed to PML up-regulation [12,16,18]. Importantly, expression of several other PML NBs-associated proteins (Sp100, Sp140, Sp110, ISG20 and PA28) is also stimulated by IFNs, which suggests the role of PML bodies as whole structures in IFN and antiviral response [12,15,19-21].

BOX #1 Interferons and IFN-induced gene expression

Type I IFN (IFNα, ß, ω) are synthesized and secreted in response to viral infection and dsRNA treatment. IFNα and ω are products of leukocytes, while IFNß is secreted by fibroblasts. **Type II IFN** (IFNγ) is expressed in T-lymphocytes and natural killer cells upon induction by antigens or mitogens.

IFN inducible gene promoters are characterized by the presence of one of the two consensus elements, IFN-stimulated response element (**ISRE**) and/or the IFNγ-activated site (**GAS**). ISRE element is recognized by the IFN-stimulated gene factor 3 (**ISGF3**), which consists of phosphorylated STAT1, STAT2 and the DNA-binding protein p48 (IRF9), or by STAT1 homodimers. **STAT**s (STAT1, 2, 3) are phosphorylated by Jak1 and Tyk2 kinases in response to type I IFN. In response to IFNγ, only STAT1 is phosphorylated by Jak1 and Jak2 and forms homodimers that can bind to the GAS motif. IFN I and II signaling pathways are interconnected through transcription factor **IRF1**. IRF1 is transiently but strongly induced by IFNγ through the GAS element in its promoter. Once in the nucleus, it binds the ISRE thus directly activating IFNα/β-stimulated genes (in other words, IFNγ can stimulate the expression of genes lacking GAS sites via the induction of IRF1 [12,16]).

PML expression could be also stimulated by estrogens as the highest expression of PML in the endometrium is during the proliferative (estrogenic) phase, and minimal during the luteal (secretory) phase [22,23]. However, no estrogen response element has been described within *PML* gene so far and no molecular mechanism of estrogen stimulation of PML expression has been suggested.

In addition, PML has been shown to be a transcriptional target of p53 [24] **(BOX #2)**. There were several p53 response elements found within the promoter and the first intron of *PML* **(Fig. 1)**. Intriguingly, only activated p53 can bind into these elements, and the p53 activation depends on the acetylation occurring within PML bodies [24,25]. Therefore, PML and p53 influence expression or activity of each other in a positive-feedback loop.

PML expression is also cell cycle dependent and affected by various stress conditions as heat shock, ionizing irradiation, and DNA damage [26]. However, the exact molecular mechanisms of initiation of PML transcription by these conditions are currently unknown. Neither there are any data available about maintaining basal PML expression under conditions of normal cellular growth.

2.1.2 Species and tissue specificity of PML expression

PML expression is restricted to higher eukaryotes as no *PML* gene homolog is found in S. cerevisiae, Drosophila or Arabidopsis genomes [27]. This is in agreement with the view that antiviral and tumor suppressive pathways evolved during the evolution of multicellular organisms with renewing tissues that have to be protected against uncontrolled cell proliferation.

In vitro, PML is expressed ubiquitously in cells of different origin while its expression *in vivo* is more restricted. PML expression is generally suppressed in tissues with high proliferative index (including tumor cells) and certain terminally differentiated cells [18,28]. Specifically, PML NBs are absent in rapidly growing epithelia (normal breast, colon, stomach, parathyroid, lung), large neurons and other cells of neuronal lineage such as neuroblastoma cells [18,29]. PML expression is however reestablished in neurons under certain pathological conditions which might suggest involvement of PML bodies in the repair processes after axonal injury [30]. Importantly, PML seems to be prevalently down-regulated in tumor cells, although certain tumor types exhibit normal or high PML expression [23,30,31]. On the other hand, the highest PML levels were found in macrophages, which corresponds with the PML inducibility by interferons **(BOX #1)** [23,30].

2.1.3 PML protein structure

PML protein can be divided into several functional domains. Four of them form together the RBCC/TRIM motif that is highly conserved among a large family of proteins involved in the regulation of transcriptional activity [32]. RBCC motif consists of C_3HC_4 RING finger motif, two cysteine/histidine-rich B boxes (B1 and B2), and an α-helical coiled-coil domain **(Fig. 2)**. RING finger domain mediates protein-protein interactions, B-boxes bind zinc ions while changing conformation, and coiled-coil domain is responsible for PML multimerization [6]. Mutational analysis of PML RBCC domain showed that the RBCC/TRIM motif is essential for PML nuclear body formation as well as for PML

tumor-suppressive, apoptotic and anti-viral activities [6,33-36].

Prevalent localization of PML into the nucleus is due to the presence of nuclear localization signal (NLS). Nuclear localization signal is located in exon 6 that might be skipped during transcription, yielding cytoplasmic PML isoforms. Nuclear export signal is present between aminoacids 700-718 suggesting that the function of PML isoforms carrying this signal may be dependent on the ability to shuttle between nucleus and cytoplasm [37].

R-ring finger (45-105AA)
B1-B1 box(124-166 AA)
B2-B2 box (184-230AA)
CC-coiled coil (229-323AA)
NLS-nuclear localization signal (487-493AA)
D-degron (498-524AA)
S/P- serine/proline –rich region (503-570AA)
SUMO-B-SUMO binding domain (508-511AA)
NES –nuclear export signal (700-718AA)

▲ SUMO
▲ Phospho-group
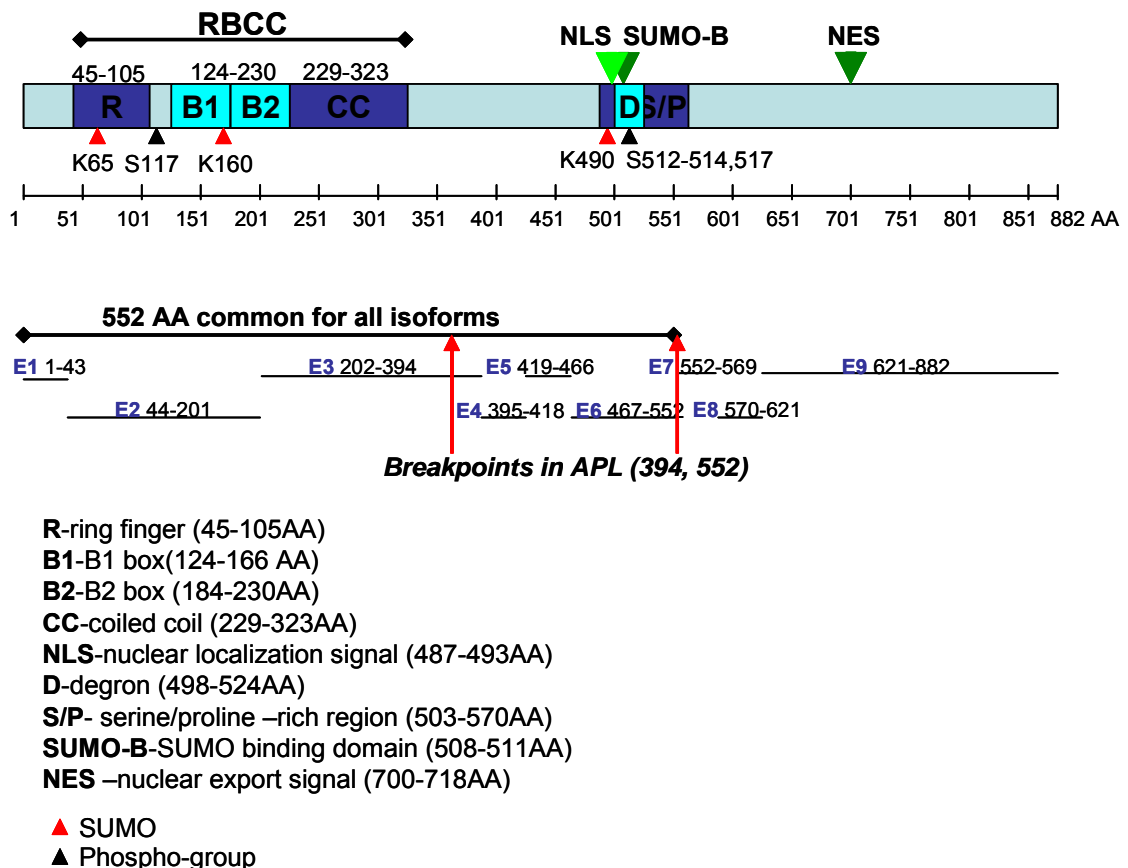
Fig. 2. PML protein structure. The distinct domains and known modification sites are shown. The localization of exons with numbers of delimiting aminoacids is shown in the lower part of the picture. Breakpoints in APL are highlighted by red arrows.

2.1.4   PML protein modification

When specific antibodies against PML protein were developed they revealed multiple protein entities that did not completely correspond to predicted molecular mass of PML isoforms [6]. This provided first although indirect evidence about PML posttranscriptional modifications that could explain the broad pattern of PML mobility in the electric field. And indeed, it has been shown over the years that after translation, PML

protein is subjected to numerous posttranscriptional modification events that include sumoylation and phosphorylation.

Probably the most important for the integrity and formation of PML bodies is the sumoylation - i.e. the covalent binding of small ubiquitin-like modifier (SUMO-1, 2, 3) [38-40]. PML harbors three sumoylation sites: in the RING finger domain (K65), in the first B-box (K160), and in the nuclear localization signal (K490, **Fig. 2**) [41,42]. Sumoylation is carried out by UBC9, a SUMO-conjugating enzyme (an E2 enzyme in the sumoylation pathway) that was found to be bound by PML RING domain [7,38]. On the other hand, at least three SUMO-specific proteases (SENP-1, SENP-2 and SENP-5) are responsible for the removal of SUMO from PML, suggesting that the sumoylation status of PML can be finely tuned [43,44].

PML sumoylation was proved to be essential for PML localization into bodies and it has thus a major role in the maturation of PML bodies including specific recruitment of other proteins into these nuclear domains [45]. Consistent with this, the soluble nucleoplasmic fraction of PML is not SUMO-modified [12,16]. However, it is still unclear whether the sumoylation affects PML antitumor function since a PML mutant deficient in sumoylation still has the growth-suppressive potential when overexpressed [46].

In addition to PML sumoylation sites, PML contains also SUMO binding domain enabling non-covalent interaction with SUMO or sumoylated proteins including PML itself [47]. This domain is localized at the position 508-511 and thus it is shared among all PML isoforms except PML-VIIb. Intriguingly, also this domain was found to be necessary for PML NBs formation. Given the importance of both covalent and non-covalent SUMO binding to PML for PML bodies' formation, a new model was proposed implying that PML sumoylation and noncovalent binding of PML to sumoylated PML through the SUMO binding motif represents the nucleation event for subsequent recruitment of sumoylated proteins and proteins containing SUMO binding motifs to PML NBs [47].

Phosphorylation is generally one of the most dynamic protein modifications; consistent with this view, in case of PML it regulates its behavior during mitosis, redistribution upon DNA damage and also PML degradation. Phosphorylation of PML occurs presumably on acidic C-terminal portion of PML containing multiple tyrosine and cysteine residues. It is thought that differences in the phosphorylation status of PML are important for the disintegration of PML bodies during mitosis because the highly labile mitosis-specific PML variant was *in vitro* stabilized by inhibitors of phosphatases. On the other hand, dephosphorylation of PML is necessary for the restoration of PML bodies in

the early stages of G1 [48].

In addition, PML protein is phosphorylated in response to DNA double-strand breaks by Chk2 (check kinase 2) and in response to global DNA damage by ATR (ATM and Rad3 related) [49,50] **(BOX #3)**. Phosphorylation of PML by ATR was found to be necessary for its DNA damage-induced relocalization into the nucleolus [50]. It was shown very recently by Dellaire et al. that both ATM (ataxia telangiectasia mutated) and ATR activity is needed for the PML bodies redistribution upon DNA damage [51]. However, it remains unclear if this effect of ATM/ATR kinase activity on PML protein is direct or mediated by ATM/ATR substrates (effector kinases, **BOX #3**).

Finally, it was shown that PML contains predicted N-terminal and C-terminal PEST domains typical for proteins that are rapidly degraded upon phosphorylation. By deletion analysis PML *degron* was mapped between amino acids 498-524; while phosphorylation of Ser517 promotes ubiquitin-mediated degradation of PML, mutant PML resistant to phosphorylation at this site exhibits longer half-life connected with increased tumor-suppressor abilities [52]. The kinase responsible for this PML phosphorylation is CKII (casein kinase II), a serine-threonine kinase frequently activated in human cancers. Intriguingly, there is a negative correlation between CKII kinase activity and PML protein levels in human lung cancer-derived cell lines and primary specimens [52]. This suggests that the PML protein down-regulation found in the majority of human tumors is not caused by the decreased transcription but rather increased degradation of PML. This is in line with previous findings showing that mRNA for PML is present in human tumors while the protein is mostly undetectable [22,31,53].

2.1.5 PML isoforms

After the extensive research on PML that was frequently irrespective of the fact that PML has many isoforms, more effort is now dedicated to systematic examination of individual isoforms. Isoform specific antibodies were developed and expression of individual isoforms on the wild or PML-/- background was employed to nail down the functional and structural differences among them. However, a careful analysis of endogenously expressed PML isoforms is still needed since the overexpression of PML may lead to the formation of artificial PML aggregates and may disrupt the balance between PML bound to the bodies and its free nucleoplasmic form [10]. Also, as different endogenous PML isoforms multimerize, the study of individually expressed PML isoforms

might not be relevant as single isoform does not necessarily have natural interaction partners. Nevertheless, the overexpression studies still provide a valuable tool for deciphering the PML function.

When expressed in HepG2 cells, each of the individual PML isoforms exhibits distinct immunofluorescence staining patterns that are different also from the pattern of endogenous PML in untransfected cells. The differences are noted in the number, size, and shape of the bodies, and also in the intensity of diffuse nuclear staining [7]. The existence of different patterns could be explained by the variation in sumoylation of individual isoforms. It is also possible that variable C-terminal domains distinct for each isoform **(Fig. 3)** can preferentially interact with different spectrum of proteins or can exert direct steric effect on PML NB assembly. Another hint suggesting different role of individual isoform is the level of their expression: the longest isoforms PML-I and -II exhibit the highest expression levels, while PML-III, PML-IV and PML-V are quantitatively minor isoforms [7]. Details on particular isoforms are summarized bellow and in Table 1.

Table 1. PML protein isoforms

Name of the isoform (GeneCard)	Name of the isoform (Jensen)[6]	Size of protein	Number of amino acids	Size of mRNA	Range of CDS (nucleotides)	Size of CDS	GeneBank#
PML 1	PML-I	97 kDa	882 AA	5600 bp	141-2789	2648 bp	NM_033238
PML 2	PML-V?	67 kDa	611 AA	3751bp	141-1976	1835 bp	NM_033240
PML 3	PML-II	90.6 kDa	824 AA	3073 bp	141-2615	2474 bp	NM_033242
PML 5	PML-VI	61.6 kDa	560 AA	3171 bp	141-1823	1682 bp	NM_033244
PML 6	PML-IV	69.6 kDa	633 AA	2254 bp	141-2042	1901 bp	NM_002675
PML 7	PML-VIb	47.6 kDa	423 AA	1851 bp	141-1412	1271 bp	NM_033246
PML 8	PML-VIIb	48.6 kDa	435 AA	1797 bp	141-1448	1307 bp	NM_033247
PML 9	PML-II	90.7 kDa	829 AA	3088 bp	141-2630	2489 bp	NM_033239
PML 10	PML-IVa	64.4 kDa	585 AA	2110 bp	141-1898	1757 bp	NM_033249
PML 11		85.7 kDa	781 AA	2944 bp	141-2486	2345 bp	NM_033250
PML 12	PML-V?	67.2 kDa	611 AA	3736 bp	141-1976	1835 bp	NM_033245
	PML-III		641 AA				

PML-I possesses all C-terminal motifs and domains, including nuclear export signal and destabilization motifs for p53, MDM2 and HDAC. It was found to locate both in the nucleus and cytoplasm. Notably, the C-terminal sequence of PML-I is much more conserved from mouse to man than the RBCC motif, suggesting that it has an important but to this point unknown function. Moreover, PML-I mRNA represents a very significant fraction (40-80%) of the total PML mRNA in nontransformed cells or normal tissues while it is much less prevalent in transformed cell lines. This suggests that the diminished PML-I expression may be linked with tumor transformation [7].

Besides numerous bodies [54], PML-II exhibits an unusual thread-like staining. In addition, its expression results in appearance of thin bubble-like structures close to the nuclear membrane and of its lamin-like lining. Thus, it can be speculated that the function of this isoform may be dependent on the interaction with the nuclear membrane [7].

PML-III was found to associate with the centrosome via an interaction with the kinase Aurora A. This PML-III localization appeared to be important for the centrosomal stability and duplication since RNAi mediated PML-III deficiency resulted in centrosome instability [55]. However, this conclusion remains speculative since another research group could not confirm the presence of PML-III within centrosomes [7].
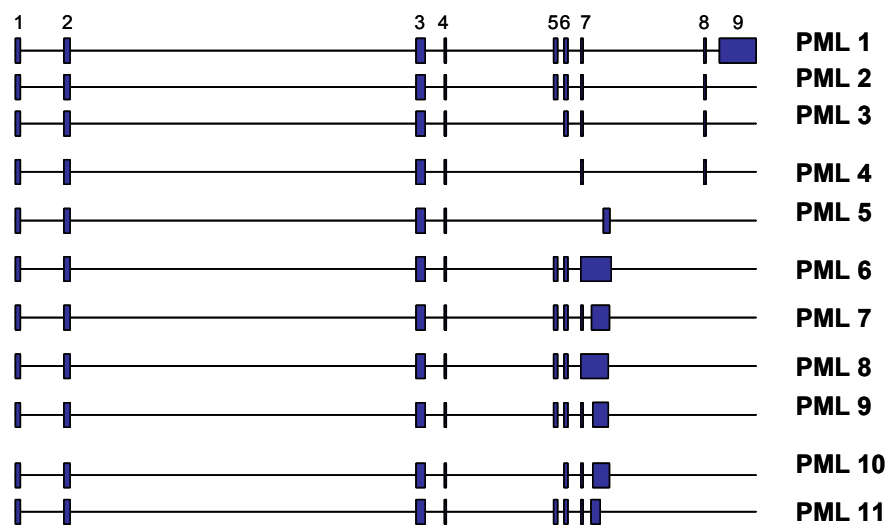
Fig. 3. Exon-intron structure of PML hnRNA isoforms. Exons are shown in blue. Based on the data from GeneCards [4].

The most studied PML isoform is PML-IV. It consists of 633 aminoacids and contains a C-terminal domain necessary for the interaction with p53. When overexpressed, PML-IV builds up a large number of small irregular bodies [54] and it was also occasionally detected in the nucleolus. Only this isoform was found to be able to trigger senescence when overexpressed in the PML+/+ MEFs but not in PML-/- MEFs. This suggests that only heteromultimers of PML can efficiently promote senescence [46]. Peculiarly, it was shown recently that the endogenous PML-IV is expressed only weakly in comparison to the longest isoforms PML-I and –II [7].

PML-V expression leads to the assembly of very large and dense bodies [7].

PML-VI expression yields in a reduced number of round PML NBs maybe because most of the protein remains diffusely dispersed in nucleoplasm [54]. PML-VIb variant lacks

the NLS so it is expected to be cytoplasmic similarly to PML-VIIb. First observations of PML localization in cytosol have been ascribed mainly to PML bodies that were released from the nucleus during mitosis and were not yet translocated back [48]. Thus, it was not expected that PML serves any special function in cytosol. Nevertheless, Lin et al. showed that cytoplasmic isoform PML is essential for the TGFß signaling since TGFß cannot induce growth arrest, cellular senescence and apoptosis in absence of PML. This was illustrated by the inability of cells lacking PML to up-regulate p21 and p15 in response to activation of TGFß signaling pathway [56]. However, as noted above, cytoplasmic localization may be typical also for PML-I due to the presence of nuclear export signal in C-terminal part of PML-I and therefore also this isoform might be potentially involved in some kind of cytoplasmic signaling.

2.1.6 PML nuclear bodies

PML protein distribution within the nucleus has its unique pattern - a majority of PML protein is concentrated within structures belonging to the group of so called nuclear bodies [57]. Nuclear body is a discrete proteinaceous structure denser than surrounding chromatin defined by specific markers. PML nuclear bodies were originally discovered as targets of autoantibodies in patients suffering from the autoimmune disease, primary biliary cirrhosis [58,59]. Cells typically contain between 5-30 PML bodies per nucleus [57]. The size (ranging from 0.2 to 1 µm in diameter) and the number of the bodies vary with the cell cycle and other factors changing the overall expression of PML protein. It remains controversial which cell cycle phase is associated with the highest PML NBs number; while one group using synchronized HeLa cells found the highest number of PML NBs in G1 phase [26], other groups showed that PML NBs number is increased after DNA replication, i.e. in S [60] or G2 phase [23,48].

PML nuclear bodies are usually spherical and under certain conditions ring-shaped. Different electron and light microscopy techniques revealed that PML protein is located usually on the surface of the body, while the core is filled with other proteins [61]. Although there are reports that nascent RNA is associated with PML NBs, RNA was not found inside the core of the bodies [61,62]. DNA was detected only within a subpopulation of PML bodies in G2 phase [63], nevertheless, PML bodies make multiple contacts with the surrounding chromatin [64]. In addition, chromosome painting provided evidence that PML NBs are located in the interchromatin domain. Live imaging of cells ectopically expressing PML-GFP demonstrated that PML bodies are positionally stable over several hours [65].

After stress (heat shock, Cd^{2+} exposure, adenovirus E1A expression), however, PML nuclear bodies partially disassemble by fission mechanism producing PML microstructures. Since the relative sizes and positioning of parental PML bodies observed before heat shock are preserved after recovery, it has been suggested that there are pre-determined locations for PML nuclear bodies assembly [65]. It is therefore quite interesting that PML NBs were found to be preferentially localized in the vicinity of several active gene loci, including both the MHC-I [66] and histone gene clusters [67].

Up to date, 77 proteins have been identified as transient or permanent components of PML bodies [68]. Functionally, these proteins belong to transcription factors (Sp100, Daxx, pRb, p53 [45]), proteins with DNA-repair function (BLM, hRAD51, WRN, hMre11/Rad50/NBS1 [11,45,69-71]), telomere-binding proteins (TRF1, TRF2 [72]), chromatin-modifying/remodeling proteins (HDAC, CBP/p300 [73,74]) and other groups.

Because of the heterogeneity of proteins located into PML NBs, it has been proposed that they may serve as depots, releasing or binding different proteins upon the actual needs of the cell thus maintaining suitable nucleoplasmic levels of particular factors [75]. The bodies may also provide an optimal environment for posttranslational modification of associated proteins. This model is based on the observation that in the absence of PML, proteins normally associated with PML bodies not only acquire aberrant localization patterns but they also cannot reach the proper activity that is dependent on posttranslational modifications normally occurring in PML NBs [25,74,76,77]. In a third model, PML nuclear bodies may function as sites of specific nuclear events as transcription or DNA synthesis [62,65,78-80].

Even though our knowledge of PML and PML bodies is still not exact and complete, there is no doubt that PML function is dependent on its potential to interact with different proteins. Following paragraphs are dedicated to examples of PML interactions and processes, which PML is involved in, that have been further studied as a part of my PhD project.

2.1.7 APL and *PML* gene ablation

The first studies of PML had been stimulated by the fact that PML was found to be involved in the development of acute promyelocytic leukemia. APL, characterized by the inability of promyelocytic precursors to differentiate, is caused by a reciprocal chromosomal translocation of chromosomes 15 and 17 resulting in the production of fusion protein of RAR and PML [1,2]. Inactivation of one copy of *PML* gene by its fusion to *RAR*

alters the normal localization of PML from NBs to microdispersed tiny dots presumably because wild-type PML heterodimerizes with PML-RARα [81] and thus is unable to form PML nuclear bodies. PML-RARα retains both DNA and RARα-ligand binding domains but compared to wild-type RARα, fusion protein aberrantly recruits corepressors (i.e. NCoR, nuclear co-repressor) and histone deacetylases [82], which leads to the transcriptional silencing of recognized promoters through DNA hypermethylation [83] and heterochromatin formation. In detail, binding of retinoic acid (RA) to its wild-type receptor RARα triggers dissociation of the NCoR-HDAC complex and activation of gene transcription, while PML-RARα forms complexes with NCoR-HDAC that are stable even in the presence of physiological doses of RA (10^{-9}-10^{-8} M). Thus, PML-RARα acts as a constitutive transcriptional repressor of retinoic acid-dependent genes [82].

Treatment with supraphysiological levels (10^{-7}-10^{-6} M) of all-trans retinoic acid (ATRA) destabilizes PML-RARα-corepressor binding. Moreover, fusion protein is selectively degraded through the proteasome pathway, while wild-type PML is released [84]. This results in the restoration of the normal pattern of PML nuclear bodies together with the release of the differentiation block. Thus, both aberrant recruitment of the NcoR-HDAC complex and disintegration of PML nuclear bodies is believed to play a key role in the development of APL. However, treatment of APL patients with ATRA leads to complete but frequently only short-lived remission [12]. Therefore, it is usually necessary to combine the treatment with histone deacetylase inhibitors to further lower the impact of the aberrant HDAC binding to RARE-containing promoters [83,85]. HDAC inhibitors can, however, affect also sensitivity of PML to interferons as discussed in the Experimental part II.

To define the function of PML protein on the whole-organism level, *Pml* (-/-) mice were generated. The protein itself proved to be nonessential as *Pml* (-/-) mice are viable though extremely sensitive to spontaneous botryomycotic infections and they succumb to the infection within the first year of their life. However, *Pml* (-/-) mice and cells are protected from apoptosis triggered by a number of stimuli such as ionizing radiation, interferon, ceramide, Fas ligand and TNFα [86]. Therefore, since the PML loss leads to inability to remove damaged cells from the organism, it was surprising that *Pml* (-/-) mice were not more tumor prone compared to their wild type littermates when young (the detailed long-term evaluation of tumor susceptibility was compromised due to premature infection-caused mortality of mutant mice). However, when the carcinogenesis was

induced chemically, *Pml* (-/-) mice were found to develop significantly more tumors than their wild type littermates [87], supporting and extending the evidence of PML tumor suppressive properties.

The involvement of PML in the regulation of cellular proliferation is further illustrated by data on *in vitro* cultured *Pml* (-/-) cells. *Pml* (-/-) MEFs grow substantially faster than their wild type counterparts and they cannot be growth-arrested upon treatment with RA. Moreover, *Pml*-deficient MEFs exhibit enhanced ability to form colonies and they reach much higher cellular densities. However, they are still unable to grow in a semi-solid medium like fully transformed cells [87]. Altogether, the loss of wild type PML represents an important but not the only step leading to full tumor transformation.

2.1.8 PML links to tumor suppressor pathways

In agreement with the proposed PML tumor-suppressive potential, when overexpressed, PML exhibits strong growth suppression that is connected with the establishment of cellular senescence or with the induction of apoptosis or necrosis [56,88-91]. *In vivo*, this is manifested by lower potential of PML overexpressing cells (breast and prostate cancer cells) to initiate tumor formation when injected into nude mice [92,93]. *In vitro*, the cells (HeLa, breast cancer cell line) overexpressing PML accumulate in G1 phase and their entry into S phase is delayed due to the decreased expression of cyclin D/E and Cdk2 [94]. Intriguingly, the decreased expression of cyclin D1 may be at least partly directly regulated by PML through its interaction with eIF4E (eukaryotic initiation factor 4E) that is responsible for the transport of cyclin D1 mRNA from the nucleus to the cytoplasm [95-98]. An elegant study demonstrated that PML is an essential regulator of this eIF4E function as an interaction of eIF4E with PML reduces the affinity of eIF4E to m7G-cap of cyclin D1 mRNA that subsequently leads to nuclear retention of cyclin D1 mRNA and the abrogation of its translation [27]. Nevertheless, more general effects of PML on the cell cycle progression are now attributed to the ability of PML to interact with or influence the proteins involved in p53 and pRb tumor suppressor pathways **(BOX #2)** [99].

The activity of p53 is dependent on its phosphorylation and acetylation status [100]. It is known that the acetylation enhancing the activity of p53 is carried out by acetyltransferase CBP/p300 [100]. Quite intriguingly, a fraction of CBP is found within PML NBs and, moreover, CBP is able to acetylate p53 only in cells with functional PML nuclear bodies [74]. The acetylation of p53 can be reverted by SIRT1 (Sir2-like protein 1), a molecule enhancing resistance of cells to stress, that is targeted into PML nuclear bodies

upon PML overexpression or up-regulation [101]. SIRT1 thus may antagonize PML-induced-p53-dependent senescence. Another protein responsible for p53 activation that is located into PML nuclear bodies is HIPK2 (homeodomain-interacting protein kinase 2). HIPK2 phosphorylates p53 at Ser46 and this modification stimulates p53 proapoptotic activities [76,102,103]. However, the most compelling evidence that points at the link between PML and p53 growth-suppressive pathway were brought by Pearson et al. studying Ras-induced senescence [25]. They showed that only PML expressing cells but not *Pml* (-/-) cells can respond to Ras overexpression by the activation of p53, recruitment of p53 into PML bodies, and the induction of premature senescence. In fact, *Pml* (-/-) cells were resistant to Ras-induced senescence despite the presence of wild type p53. Thus, at least in mice, PML is required for the efficient activation of p53 in response to aberrant oncogene signaling. Besides oncogene stimulation, p53 is recruited into PML NBs following the treatment with arsenic trioxide and gamma- or UV-irradiation [11,70,104]. Importantly, only certain PML isoforms can recruit p53 into bodies since p53 interaction with PML is mediated by C-terminal domain that is not shared by all PML isoforms [77].

BOX #2. Tumor suppressors

p53 is a transcriptional factor that masters apoptotic, senescent and repair programs in response to cellular stresses. It transcriptionally activates or represses target genes involved in the regulation of the cell cycle; this primarily leads to block of proliferation of damaged cells. The stability of p53 is predominantly mediated by the interaction with **MDM2**. MDM2 is E3 ubiquitin ligase targeting p53 for proteasome-dependent degradation. Upon induction of DNA damage, oncogene activation or other stresses, p53-MDM2 binding weakens; p53 is stabilized, and accumulates in the nucleus. Active **p53 is phosphorylated and acetylated** on multiple residues and these modifications and their combinations influence the effects of p53 on its **target genes** including *p21$^{WAF1/CIP1}$*, *14-3-3σ, GADD45, PCNA, cyclin D1, cyclin G, BAX, Bcl-L, FAS1, FASL* and *MDM2*. For instance, the posttranslational p53 modifications found in senescent cells are mostly distinct from p53 modification typically induced by DNA damage [105]. **Mutations in *TP53***, the gene that encodes the p53 protein, are found in 50% of human cancers. Furthermore, p53 is inactivated by **E6 protein** of high-risk HPV18 [100,106].

pRb was discovered as a protein whose loss results in the development of **retinoblastoma**, a rare childhood tumor of the eye. pRb belongs to a group of so called pocket proteins including also **p107 and p130** sharing with pRb 30-35% identity. The primary function of pRb is to **inactivate the transcription factor E2F** and thus block E2F-dependent transcription. E2F release from this inhibiting complex with pRb is dependent upon pRb hyperphosphorylation directed by cyclin-dependent kinases CDK 4 and CDK6 during G1 phase. E2F then binds to promoters of genes necessary for the progression through G1 phase and entry into S phase. CDK4 and 6 themselves are inactivated by **inhibitors such as p16, p15, p18 and p19** and under these conditions pRb is maintained in its active hypophosphorylated form. This usually occurs after DNA damage and during cellular senescence. In contrast, pRb inactivation is strongly linked with the development of cancer [107].

PML affects not only the activation but also the stability of p53 through the interaction with MDM2 and HAUSP (herpesvirus-associated ubiquitin specific protease). It was demonstrated that PML directly interacts with MDM2, the key p53 negative regulator [104,108]. This interaction occurs predominantly in the absence of PML sumoylation

of Lys160, so it can be expected that it is the free nucleoplasmic PML form that binds MDM2 [108]. On the other hand, the activity of HAUSP is linked to PML nuclear bodies; HAUSP is able to remove ubiquitin residue from p53 molecule thus protecting it from proteasome-dependent degradation [109,110].

Moreover, as discussed in the Chapter 2.1.1, the relationship between PML and p53 is reciprocal since p53 transcriptionally activates PML expression and may also inhibit CKII-dependent PML destabilization [52]. Together, these two tumor suppressor proteins potentiate activity of each other in a positive feedback loop that reinforces their downstream effects leading to the establishment of the growth arrest including senescence or the induction of apoptosis.

Although the role of p53 in the processes initiated by PML overexpression is evident, several studies have implicated that the essential protein in PML-triggered apoptosis or senescence in human cells is in fact the pRb. This was suggested since at least in liver tumor cells, the ability of PML to induce cell cycle arrest was not related to the status of p53 [111]. Similarly, the inactivation of p53 in human fibroblasts was not sufficient to block senescence induced by PML overexpression while the inactivation of pRb prevented it [88]. It remains still unclear how exactly PML and pRb are interconnected functionally though it was shown that they can physically interact [99]. To complicate the whole picture even more, endogenous PML retains a growth suppressive activity also in pRb-ablated cells indicating that PML is likely to simultaneously affect multiple pathways involved in cell-cycle regulation [99].

PML nuclear bodies attract not only tumor suppressors but also proto-oncogene c-Myc [112]. Myc is a transcription factor that binds and regulates a large number of genes including many that encode ribosomal proteins, rRNA processing factors and translation factors. Furthermore, Myc is a potent direct activator of tRNA and 5S rRNA synthesis [113]. How PML affects the function of c-myc, which is targeted into PML bodies upon myc overexpression, was not deciphered. It should not be underestimated as the deregulation of the c-myc proto-oncogene is believed to play a role in the genesis of up to 30% of all human cancers [114].

2.1.9 PML and DNA damage

Maintaining of DNA integrity is the basic presumption of proper cellular functions and organism homeostasis. As the DNA is being constantly damaged by environmental and intrinsic factors, sophisticated array of DNA repair and cell cycle checkpoint

mechanisms have evolved to ensure the continuity of unchanged genetic information **(BOX #3)**. The exact involvement of PML and PML bodies in the DNA repair/checkpoints is not completely determined yet. But it is already clear that PML is important for or at least modulates the response of cells to DNA damage.

PML is a target of phosphorylation by Chk2 (serine 117) [49] and also the substrate for ATM-directed phosphorylation [50]. Interestingly, both kinases are targeted to PML NBs following the DNA damage [11]. It was observed that following irradiation a subset of PML NBs colocalize with the sites of new DNA synthesis, which is considered as a marker for active DNA repair [115], as well as with γH2AX, a marker of single and double strand DNA breaks [70]. Similarly, a subset of PML NBs colocalize with BLM, a member of the RecQ DNA helicase family, at sites of nucleotide excision repair (NER) induced by UV-C radiation [69,115]. Another RecQ DNA helicase, WRN, whose loss results in premature aging (Werner syndrome), moves upon DNA damage caused by irradiation from its regular location in the nucleolus into nucleoplasmic foci containing Rad51 and RPA that partially overlap with PML NBs [11,71]. Lastly, PML colocalizes and associates with the DNA damage response protein TopBP1 in response to ionizing irradiation [116].

BOX #3 DNA damage-repair and checkpoints

DNA repair mechanisms include **direct, base and nucleotide excision repair and double-strand break repair by homologous recombination or non-homologous end joining** that are carried out by specialized enzymes or enzymes primarily involved in DNA replication [117]. At the same time as DNA damage is recognized and DNA repair takes place, DNA damage activates so called **DNA damage checkpoint-pathways** that delay or arrest cell cycle progression for the time necessary to fully repair the damage [118]. They are not activated only during certain stages of the cell cycle but they constantly monitor the integrity of the genome and their activity is enhanced when the extent of DNA damage rise above certain threshold level. They consist of proteins that are able to recognize the damage (sensor proteins) and convey the signal from the sensors to the effector molecules that control the transition to following cell cycle phase **(Fig. 4)**.

ATM and ATR kinases belong to the most important sensor molecules. ATM is activated by the damage caused by γ irradiation, i.e. dsDNA breaks [119], while ATR is activated by replicative stress or UV light causing mainly base damage [120]. When activated, they phosphorylate signal transducer kinases **Chk2** (ATM) and **Chk1** (ATR) and other proteins including p53, NBS1, BRCA1 (ATM) [117,121]. Chk1 and Chk2 phosphorylate and thus inactivate **Cdc25 phosphatases** crucial for the activation of cyclin dependent kinases promoting transition into the next cell cycle stage [122].

The outcome of the synchronized activation of both DNA repair and checkpoint mechanisms is the removal of the DNA damage before the cell can enter the next cell cycle phase. When the damage is unreparable or too extensive, effector molecules ensure that the affected cell is removed from the proliferative cellular pool by apoptosis or by entering the senescence.

Although the above discussed data do not explicitly prove the direct involvement of PML bodies in DNA repair, it is well accepted that several proteins important in all aspects of DNA repair processes alter their activity upon the transition through PML bodies. ATR, Chk2, MRE11, NBS1, BLM belong to them; they pass through PML NBs in a temporally regulated manner [45,69,70,123]. Also p53, one of the effector molecules necessary to maintain

G1/S cell cycle arrest, is stabilized and activated in PML NBs through acetylation by CBP and phosphorylation by HIPK2 and Chk2 that both co-accumulate in PML NBs in response to DNA damage [11,102,124,126]. What is even more intriguing, following UV irradiation, PML, MDM2 and p53 form a trimeric complex at PML NBs, where PML interaction with MDM2 prevents MDM2-dependent p53 ubiquitination [104,124]. In agreement with this, PML-ablated cells fail to induce p53-dependent gene expression in response to genotoxic stress [125].
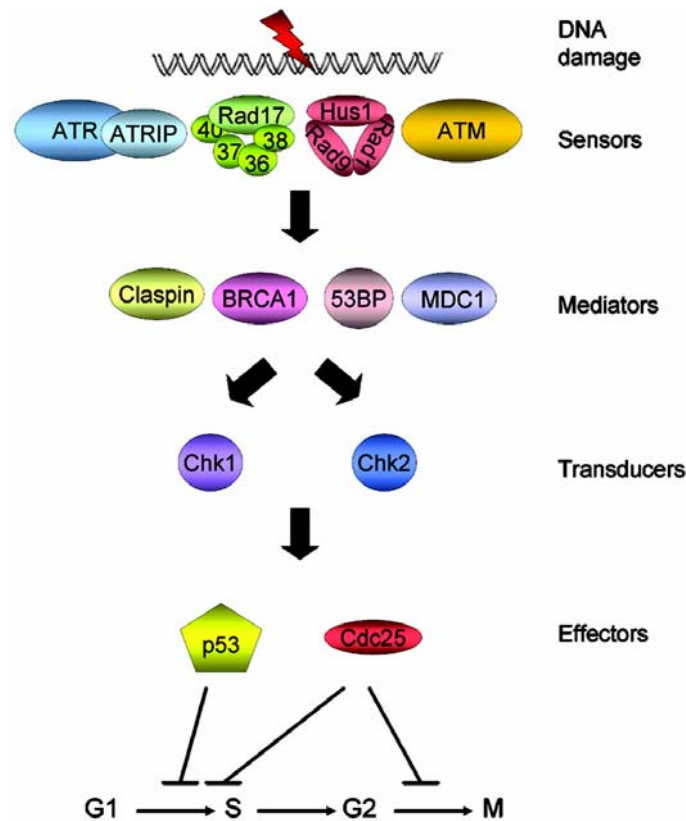
Fig. 4. Components of the DNA damage checkpoints in human cells [115].

Remarkably, PML NBs numbers increase significantly shortly after gamma-irradiation [11]. The molecular mechanism of this increase has been proposed recently; PML NBs react to DNA damage by rapid disassembly and thus serve as dynamic sensors of cellular stress [51]. It was suggested that PML NBs may sense the DNA damage due to their numerous contacts with chromatin. Following extensive DNA damage including the double-strand DNA breaks, PML bodies appear to be literally torn apart by chromatin fibres that are pulled away from the bodies; this process is then manifested by an appearance of PML microstructures, i.e. increase in PML NBs number. Interestingly, it has been proposed that the dissociation of PML bodies is probably prerequisite to the release of associated factors to the sites of damage. Moreover, the activation of DNA repair

24

machinery results in chromatin relaxation and expansion of interchromatin domains, so PML bodies that have lost contact with chromatin may migrate within these spaces which could explain observation of PML bodies translocating to the sites of DNA damage and repair [51].

DNA damage checkpoints are activated also by shortened and deprotected telomeres [126] **(BOX #4)**. Cancer cells prevent this cell cycle block by the reactivation of telomerase. Those cancer cells that do not express telomerase may maintain the acceptable length of telomeres by alternative telomere lengthening mechanism (ALT) [127]. Molecular mechanisms of ALT remain obscure; however, some results suggest that recombination events are involved [128]. Importantly, ALT is connected with a subset of PML bodies that are enriched in telomeric DNA, the telomere binding proteins TRF1 and TRF2, and several proteins important for DNA repair and homologous recombination (e.g. BRCA1, NBS1, Rad1/Rad9/Hus1, Rad17, RPA1, Rad51 and Rad52) [80,129]. These bodies are therefore referred to as ALT-associated PML bodies (APBs) [130]. APBs can be detected almost exclusively in late S-G2 phase [72]. Generally, they appear in cell population as soon as ALT-mechanism is established and the length of telomeres stabilized, suggesting that APBs are functionally connected with the ALT mechanism. Interestingly, this is probably the only so far known PML activity that is not primarily growth-suppressive.

BOX #4. Telomeres

Telomeres are specialized **chromatin structures** at the end of linear chromosomes. Telomeric DNA consisting of many double-stranded **TTAGGG repeats and a 3'-single strand overhang** is in complex with telomere-binding proteins. They form a cap structure that protects the ends of telomeric DNA against degradation and chromosomes against end-to-end fusions. Due to the inability of DNA polymerase to replicate DNA ends, telomeres get shorter with each cellular division. This **telomere attrition** accelerated also by oxidative and other stresses is believed to cause replicative senescence as it inevitably leads to activation of DNA damage checkpoints (deprotected ends of telomeric DNA are recognized as double strand breaks [126,131]) and genomic instability caused mainly by the fusion and subsequent rearrangement of chromosomes. It is possible that telomere shortening represents an evolutionary solution for multicellular organisms with cycling cells preventing cells with deregulated cell cycle checkpoints to proliferate indefinitely and thus it suppresses tumorigenesis. Embryonic, stem and certain other cells have the potential to maintain the telomere length by expression of **RNA-dependent enzyme telomerase** [132]. Moreover, cancer cells that do not express telomerase may maintain the acceptable length of telomeres by so called **alternative telomere lengthening mechanism (ALT)** [127].

In summary, PML and PML bodies are involved in the regulation of cellular proliferation, DNA damage repair and senescence, and exhibit overally strong growth and tumor suppressive potential. Although extensive progress in the deciphering of PML interactions that might be responsible for these properties has been made, further investigation of complete pathways involving PML is necessary.

2.2 The nucleolus

The nucleolus is the most prominent subcompartment of the higher eukaryote nucleus. The nucleolus is primarily dedicated to ribosome synthesis; it is a place, where rDNA is transcribed, precursors of rRNA are spliced and modified, and where the assembly of preribosomal particles occurs. In last years, however, the novel functions of the nucleolus have been discovered- the nucleolus has been implicated in the regulation of the cell cycle and the aging process. The reappraisal of these nucleolar functions is based on the accumulating evidence that the nucleolus can serve as a very sensitive sensor of cellular fitness and the impairment of its function and structure induced by stress condition (as the lack of nutrients or growth factors and DNA damage) is one of the primary stimuli for the activation of cell cycle and DNA damage checkpoints.

2.2.1 Structure of the nucleolus

The structure of the interphase nucleolus is highly dependent on transcription activity and associated ribosome assembly; hence it has been proposed that the nucleolus is "an organelle formed by the act of building a ribosome" [133]. The nucleolus is organized around clusters of rDNA genes that are arranged as tandem head-to-tail repeats on several chromosomes (in humans, there are about 400 rDNA genes on chromosomes 13, 14, 15, 21, 22). These clusters form so called nucleolar organizing regions (NOR).

In trancriptionally active nucleolus, three morphologically distinct domains can be discriminated: fibrillar centers (FCs), dense fibrillar component (DFC) and granular component (GC) **(Fig. 5)**. FCs are composed of fine (4-5 nm) fibrils and are attached to the NORs. The number of fibrillar centers usually positively correlates with the rDNA transcription activity of the cell and RNA polymerase I (Pol I) and UBF are considered as typical markers of FC. Since the active transcription of ribosomal genes occurs preferentially at the border of FC and DFC, it is possible that FCs are in fact storage places for inactive transcription factors that are recruited to active rDNA genes upon need. This is supported by the finding that less than 10% of nucleolar Pol I is engaged in transcription and the density of Pol I in FCs accounts for more than this proportion [134]. Dense fibrillar component surrounds FCs. It is characterized by the presence of fibrillarin, although fibrillarin may be present also in granular component that consists of small granules representing prevalently ribosome precursors [135].
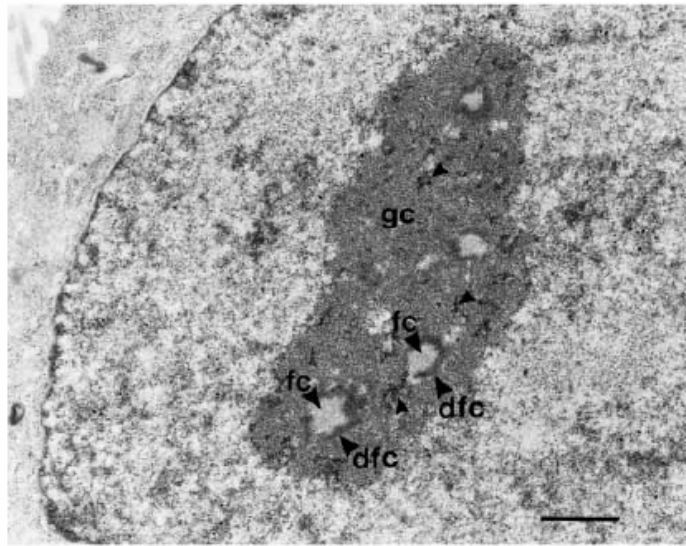
Fig. 5. The nucleolus on the ultrastructural level. Distinct domains are indicated by arrowheads. Bar, 1 μm. From Hozak et al [220].

In the absence of rDNA transcription caused by actinomycin D **(BOX #5)** or during very low metabolic activity of the cells (for example in hibernating carps [136]), nucleolar structure rearranges and three functional nucleolar domains become segregated from each other [137]. FC and DFC segregate into two distinct types of nucleolar caps, while the remnants of GC form so called central body. When both Pol I and Pol II are inhibited, certain nucleoplasmic proteins (especially those involved in mRNA binding or processing) segregate into another type of caps located on the surface of the segregated nucleolus. The segregation is reversible until certain point and segregated nucleolus may regain the normal structure when the actinomycin block is released.

BOX #5. Actinomycin D
Actinomycin D (AMD) is the antibiotic produced by *Streptomyces antibioticus*. It is known for its ability to **inhibit Pol I and Pol II transcription** [138]. Pol I transcription is inhibited by low doses of AMD (0.001-0.05 μg/ml, i.e. 0.8-40 nM), while both polymerases are inhibited when higher concentration of AMD is used. Its action is quite rapid; transcription (its elongation phase) is fully blocked within 10-20 minutes. **AMD binds to DNA duplexes**, mainly to pGpC and ß conformation that is usually present in gene promoters. High concentrations might cause DNA breaks probably due to the poisoning the topoisomerase enzymes [139,140]. Long-term exposition to AMD induces cell cycle arrest and senescence [139].

2.2.2   rDNA transcription

To better understand how the nucleolus is engaged in the regulation of the cell cycle, the main components and steps of nucleolar transcription have to be described, since their regulation is prerequisite of the change in the cellular growth status. Transcription of

rDNA genes, representing about 70-90% of overall cellular transcription, is carried out by RNA polymerase I. The rRNA genes for 18S, 5.8S and 28S rRNA are present in a single transcription unit, representing unique eukaryotic polycistrone. Its transcription yields a 47S rRNA precursor that is co- and post-transcriptionally cleaved and modified to produce the mature rRNA species [141,142]. The modifications consist of 2'-O-methylation of ribose groups and the conversion of uridine to pseudouridine and are directed by more than 150 different snoRNAs that pair with specific target sequences [143]. The last rRNA species, 5S rRNA, is transcribed by RNA polymerase III in nucleoplasm and is then transported to the nucleolus where it is incorporated into newly assembled preribosomes together with 78 ribosomal proteins [142].

BOX #6 Nucleolar proteins and their function in the ribosome synthesis

RNA polymerase I - a complex enzyme composed of at least 14 subunits (mammalian Pol I) of size over 500 kDa; Pol I is initiation competent only when associated with TIF-IA.

SL1 (TIF-IB) - human selectivity factor 1, consists of TBP and at least three TAFs (TBP associated factors) that are necessary for the promoter recognition (because TBP does not bind to DNA); SL1 interacts with UBF [144].

UBF - upstream binding factor; recruits Pol I to the rDNA promoter, stabilizes binding of SL1 and competes with nonspecific DNA-binding proteins such as histone H1 thus activating rDNA transcription [145].

TIF-IA - forms a bridge between Pol I and SL1 and thus it is required for the assembly of a productive transcription initiation complex. Moreover, it is indispensable for the formation of the first phosphodiester bond in nascent rRNA molecule [146].

Fibrillarin - is a part of snoRNP and exhibits a methyltransferase activity. In view of that, it is expected to be responsible for 2'-O-methylation of rRNA [141].

Nucleophosmin (B23) - is a 32 kDa protein, prevalently localized into GC. It is important for late processing of pre-rRNA as it cleaves 47S rRNA within ITS2. In the phosphorylated form, it binds RNA, non-phosphorylated form is dispersed freely in nucleoplasm; however, it can also migrate into cytosol, acting as a chaperone protein [147].

Nucleolin (C23) - is a 76 kDa prevalently nucleolar protein, that shuttles between nucleolus, nucleoplasm, cytosol and cell surface. It is involved in early stages of rRNA maturation (it probably binds 5'-region of pre-rRNA and facilitates recruitment of processing components), ribosome assembly, nucleo-cytoplasmic transport, and cell proliferation. It exhibits DNA and RNA helicase activity. Its activity is regulated through phosphorylation [148].

Transcription begins with the recruitment of SL1 and UBF **(BOX #6)** to rDNA gene promoter (core element and upstream control element resp. **(Fig. 6)**). SL1 and UBF interact with each other and with DNA while forming a stable pre-initiation complex (PIC). PIC attracts an initiation-competent subfraction of Pol I, defined by the presence of TIF-IA, to the transcription start site and thus converts into a productive initiation complex [149]. After initiation, TIF-IA is released from the ternary complex and becomes available for binding to another preinitiation complex. SL1 also dissociates from the template upon transcription, whereas UBF remains bound to the upstream promoter element, thus most likely facilitating the reinitiation of transcription.
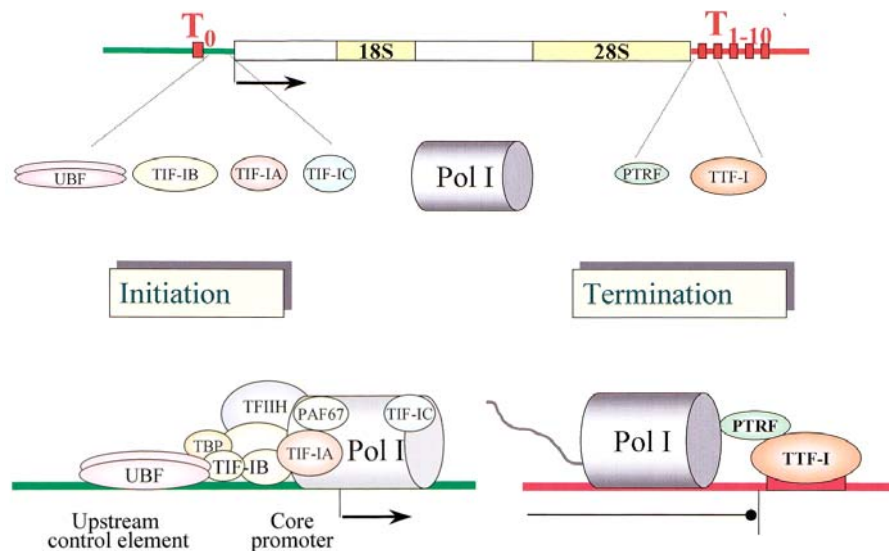
Fig. 6. Schematic representation of regulatory elements in the rDNA transcription units. Promoter is preceeded by single terminator element, while ten terminator elements are found downstream rDNA unit. Proteins involved in initiation and termination of transcription are shown in the lower part of the scheme. Adapted from [145,147].

Due to the dense loading of the Pol I complexes on active rDNA genes, the elongation phase is very sensitive to any type of DNA damage as there is a high probability of a polymerase encountering, and stalling at, a site of DNA damage. Stalled Pol I then represents a strong signal for activation of DNA damage checkpoint. To avoid the cell cycle arrest, Pol I transcription is coupled with repair, which is illustrated by the presence of DNA-repair proteins TFIIH, CSB (Cockayne syndrome B) and xeroderma pigmentosum group G (XPG) in a complex with Pol I involved in rDNA transcription [144].

Transcription is terminated upon cooperation of Pol I, TTF-I and transcript-release factor PTRF at the termination site resulting in dissociation of the elongating PolI and nascent transcript from the template DNA [144].

2.2.3 Regulation of ribosome production

Given that the overall rate of protein synthesis is limited by ribosome availability as the number of mRNA molecules exceeds the number of ribosomes, the impact of an attenuation of the nucleolar metabolism induced by stress conditions is major; for instance, 50% decrease in translation causes fibroblasts to exit the cell cycle and quiesce. On the other hand, cells that have defective cell cycle checkpoints (for example fibroblasts from p53 KO mice) or cancer cells, are characteristic by markedly elevated rDNA transcription [150]. Thus, in normal cells, a fine equilibrium is maintained between the growth status of the

cell and the production of rRNAs, which is the limiting step in ribosome accumulation.

The amount of rRNA is regulated mostly at the level of rDNA transcription [144]. Indeed, the activity of several proteins essential for the initiation of rDNA transcription can be effectively regulated. UBF activity is positively correlated with its phosphorylation that enhances UBF affinity to DNA and mediates its interactions with other proteins [149]. On the other hand, in quiescent cells, UBF is hypophosphorylated and transcriptionally inactive. UBF can be phosphorylated by CKII, ERK1/2, Cdk4 and Cdk2 and this phosphorylation leads to an immediate upregulation of rDNA transcription. Interestingly, both CKII and ERK are constitutively activated in many cancers [150]. Furthermore, UBF interacts with hypophosphorylated pRb that accumulates in the nucleolus when the demand for rRNA production is low, for example in the growth arrested or differentiating cells [151]. This interaction prevents UBF from recruiting SL1 and CBP to rDNA promoter. Similar effect on UBF activity has also another pocket protein p130 **(BOX #2)** [113]. In addition, interaction between SL1 and UBF is destabilized by the direct binding of p53 with SL1 [150]. Furthermore, SL1 activity may be decreased through the deacetylation of one of the TAFs **(BOX #6)**, TAF_l68, by Sir2 [145].

TIF-IA represents another molecule whose activity can be finely tuned in response to extra- and intracellular conditions. Compelling evidence was gathered that in mammals the growth-dependent cessation of rDNA transcription is attributable to a drop in TIF-IA amount or activity [149]. Upon stress, TIF-IA is phosphorylated by c-Jun N-terminal kinase 2 (JNK2) at threonine 200. This modification hampers the TIF-IA interaction with Pol I and leads to the translocation of TIF-IA from the nucleolus to the nucleoplasm. The exclusion of TIF-IA from the nucleolus is also triggered by the phosphorylation of TIF-IA Ser 199 induced by the mTOR inhibitor rapamycin [152]. On the other hand, phosphorylation of TIF-IA by activated ERK potentiates TIF-IA association with Pol I [153]. When TIF-IA is inactivated, normal nucleolar structure is disrupted and several nucleolar and ribosomal proteins including UBF, B23, ARF and L11 are released to the nucleoplasm [154]. The impact of such delocalization of nucleolar proteins is explained in detail in the following chapter.

2.2.4 The nucleolus as a sensor of cellular fitness- the nucleolus and its relationship with p53 tumor suppressor pathway.

Besides its essential role in ribosome synthesis, the nucleolus has been recently shown to perform unexpected tasks in cell cycle regulation, control of aging, nuclear

export pathways and telomerase function [148]. The fact that nucleolar functions are affected by growth factor and nutrients availability, various stress factors and DNA damage, together with its potent sequestration function, leads to the growing awareness that the nucleolus is predisposed to serve as a sensitive sensor of overall cellular fitness.

Probably the most powerful molecule dependent on the nucleolar activity is p53. p53 turnover is mostly dependent on the p53 association with MDM2 **(BOX #2)** and the block of this association leads to p53 stabilization. Several nucleolar proteins have been shown to interact with MDM2 and inhibit its binding to p53. Intriguingly, the interaction of these proteins and MDM2 can occur only upon impairment of nucleolar functions permitting the release of nucleolar proteins into the nucleoplasm as discussed bellow.

One of the first discovered regulators of p53 was ARF (alternative reading frame). ARF is a 19 kDa protein, transcribed from the same locus (INK4) as CDK inhibitor p16 through the use of alternative promoter [155]. *Arf* (-/-) mice are highly tumor prone, indicating that ARF is a *bona fide* tumor suppressor. It is found mainly in GC but it quickly reacts to even brief perturbations in cell cycle and in nucleolar function (induced for instance by the CDK, CKII and Pol II inhibitors) by translocation into nucleoplasm [156]. ARF tumor suppressive potential is mostly based on its ability to interact with MDM2. Firstly, it was suggested that ARF sequesters MDM2 from nucleoplasm to the nucleolus and thus inhibits MDM2-dependent p53 degradation [157]. However, p53 is stabilized also by mutant ARF unable to localize into the nucleolus [158]. Another study confirmed as well that the interaction of ARF protein with MDM2 occurs in nucleoplasm and not directly in the nucleolus [159]. Therefore, another model proposed that ARF forms a ternary complex with MDM2 (and p53) in nucleoplasm, thus preventing p53 nuclear export. This in turn leads to enhanced nuclear retention, stabilization and activation of p53. In contrast to ARF stabilization impact on p53, AFR can promote a polyubiquitination and thus destabilization of B23 **(BOX #6)**. This has a negative impact on the processing of preribosomal RNA which might explain how ARF inhibits synthetic nucleolar function [160]. Possibly for that reason, ARF expression in cycling cells is maintained at very low level but it is strongly induced by aberrant oncogene activation and pRb inactivation (due to the presence of E2F response element in the ARF promoter) [161]. Therefore, it has been proposed that the primordial role of ARF could be to block ribosome biogenesis that was triggered in response to the inadequate oncogene activation [113]. Also, ARF is crucial for the induction of p53 when pRb pathway is inactivated [161].

B23 is another protein involved in the modulation of p53 activity. Not only it prevents MDM2 binding to p53 but it also protects ARF from degradation, thus enforcing ARF-dependent p53 stabilization [162]. It interacts with p53 also directly and modifies its activity - it inhibits its premature activation. The observations that overexpression of B23 induced a cell cycle arrest and premature senescence in normal fibroblasts, and conversely that the depletion of B23 by siRNA treatment almost completely prevented p53 stabilization after X-ray irradiation [163], underscore the B23 function as an important regulator of p53.

Recently, similar p53 stabilizing properties as those of ARF and B23 have been ascribed to several ribosomal proteins. One of them is the ribosomal protein L11 that is normally a component of 60S ribosomal subunit. Under the conditions blocking the cell cycle progression (serum depletion, AMD-treatment), L11 cannot be bound in ribosomes and it is translocated from the nucleolus to the nucleoplasm. There it interacts with and inactivates MDM2 which leads to stabilization of p53 [164,165]. The same behavior was documented also for ribosomal protein L23 and L5 [166,167]. Interestingly, L5, L11 and L23 bind to separate sites of MDM2 (L23 interacts with the same domain as ARF) [167].

However, the most remarkable evidence of the crucial role of the nucleolus for the p53 activity has been presented by Rubbi and Milner [168]. In their experiments, they exposed cells to UV irradiation to induce p53 activation. Their experimental set-up allowed targeting of damaging light selectively to the nucleolus or to the remaining nucleoplasm. Strikingly, p53 was not activated when the nucleolus remained intact evenwhen the rest of the nucleus was substantially damaged. Thus they concluded that the nucleolar disruption is crucial for p53 stabilization induced by UV irradiation. Furthermore, when they integrated their data with other reports on p53 activation they found that also other treatments leading to p53 activation cause major changes in the nucleolar structure and therefore they proposed that the nucleolar disruption itself could be the main trigger for all p53 responses [113].

In summary, impairment of nucleolar function in response to different kinds of stress is accompanied by perturbation of nucleolar structure, cell cycle arrest and stabilization of p53. The other way around, the change of nucleolar structure may suggest an ongoing stress insult and/or the specific cellular response to it. We have found that the establishment of cellular senescence coincides with the formation of nucleolus-derived structures encircled by PML protein as described in the Experimental part III.

2.3 Cellular senescence

Aging is defined as a time-dependent decrease of organismal fitness inevitably resulting in the death. One of the major theories explaining the phenomenon of aging is the damage-based theory: the cellular and tissue damage accumulates over the lifespan of the organism until it impairs the effective functioning of crucial organ systems [169]. Cellular damage, which cannot be sufficiently eliminated but is not extensive enough to cause cell death, triggers cellular senescence that is characterized by the acquired and permanent insensitivity of the cell to mitogenic stimuli. Establishment of senescence is particularly important when damaged cells belong to proliferative pool and thus may potentially become malignant. Thus, both cell death and senescence eliminate the potentially dangerous cell from the affected tissue but at the same time the loss of cells hampers the tissue function. Together, it is expected that both processes protect organism against cancer but at the same time contribute to the aging of the organism.

2.3.1 Characteristics of cellular senescence

Cellular senescence is similarly to apoptosis established upon the execution of strictly controlled genetic program. Majority of *in vitro* cultured primary cells become senescent after extensive serial passaging. One of the molecular triggers of this so called replicative senescence has been already determined - it is the shortening of telomeres occurring with each cellular division **(BOX #4)**. Phenotypically, the senescent cell becomes flat and enlarged, produces different spectrum of extracellular matrix components, secretes cytokines unusual for its tissue of origin and exhibits distinct gene expression pattern [170]. Senescent cells can be detected due to the higher ß-galactosidase activity at pH 6.0 (so called senescence-associated ß galactosidase activity, SA-ß-GAL) [171].

Normal cells can enter a state similar to replicative senescence but independent of telomere shortening referred to as premature senescence. Premature senescence can be *in vitro* induced by ceramides, histone deacetylase inhibitors, oxidative stress, DNA topoizomerase inhibitors, activated c-*ras* gene inducing constitutive MAPK activation and other means. Independent of the trigger, the senescence-associated cell-cycle arrest is executed by cyclin-dependent kinase inhibitors that block progress through the cell cycle [172]. However, the molecular mechanisms preceding the accumulation of these inhibitors remain largely unknown. The selective induction of cellular senescence in tumor cells appears to be a promising approach to treat cancer. This expectation was supported by

recent reports demonstrating DNA-damaging treatment *in vivo* is accompanied by the induction of cellular senescence in tumor cells, which correlates with increased overall survival of the host [173]. One of the senescence inducers that is effective in most types of tumor cells is 5-bromo-2'-deoxyuridine (BrdU).

2.3.2 BrdU-induced premature senescence

5-bromo-2'-deoxyuridine is an analogue of thymidine, in which a methyl group is substituted by a bromine ion. BrdU is incorporated into DNA as 5-bromouracil instead of thymine [174]. The long-term exposition to BrdU and also other halogenated analogues of thymidine (5-chloro-2'-deoxyoridine, CldU; 5-iodo-2'-deoxyuridine) induces premature senescence in both normal and tumor derived cells [175,176]. BrdU-induced senescence resembles replicative senescence as shown by microarray analysis of gene expression of BrdU-treated and replicatively senescent cells [177]. Two thirds of genes upregulated in BrdU-treated cells are upregulated also in old versus young human fibroblasts [178]. In the Experimental part III we extended this analysis by description of BrdU effects on PML nuclear compartment. We found that BrdU-treatment restores the ability of PML to interact with the nucleolus that is nearly absent in untreated malignant cells. Thus this effect of BrdU might be connected with the induction of senescence. Moreover, we confirmed that BrdU induces expression of tumor suppressor genes such as pRb, p53 and p21.

The mechanism of BrdU action is not completely understood. While telomere shortening does not seem to be accelerated by BrdU [176], it was shown that BrdU has a mutagenic potential, since it can be converted into bromouracil that is not recognized by cellular repair enzymes and may pair with cytosine instead of adenine. This causes highly specific transition from AT to GC during subsequent replication. Only 4 days in the presence of 120 μM BrdU is sufficient time to induce this transition with frequencies between 9.8×10^{-6} to 3.9×10^{-5}. This represents approximately a 60- to 230-fold increase above the frequency of spontaneous mutation in the untreated control [174,179]. Nevertheless, the increased frequency of point mutations could hardly be the only mechanism responsible for fast and quite uniform induction of senescence by BrdU. Importantly, when exposed to light, BrdU is converted to uracil, removed by uracil glycosylase and the newly formed apyrimidic site may cause a nick or gap on DNA [178]. BrdU also substantially elevates the number of chromosomal aberrations and sister-chromatid exchanges [180]. This further underscores the fact that DNA damage is likely to be critical for both cancer and

aging. Conversely, Michichita et al. have suggested that the DNA damage is not involved in BrdU-induced senescence, as light-insensitive CldU that does not cause DNA damage when cells are exposed to light has the same effect as BrdU and no DNA damage inducible genes were found to be upregulated in BrdU-treated cells except for p21 [178]. Thus another model was proposed; it stems from the observation that BrdU promotes decondensation of constitutive chromatin and AT-rich Giemsa-dark bands in mitotic chromosomes and that the substitution of thymine with 5-bromouracil in AT-rich sequences lessen their bending and enhance their binding to the nuclear matrix. Taken together, this Japanese group postulated that BrdU affects a higher-order chromatin structure and this chromatin relaxation leads to the initiation of the expression of the senescence-associated genes in human cells. Although this model is based on the controversial results concerning the absence of DNA damage in BrdU-treated cells, it could possibly explain the striking synergism between BrdU and distamycin A in the induction of the senescence.

Distamycin A, a peptide-like antibiotic, binds to the minor grooves of AT-rich sequences similarly as Hoechst 33258, netropsin (DMA derivative) and the AT-hook protein [181,182]. It potentiates the effect of BrdU at low concentrations when BrdU alone does not exert significant effect [183]. It competes with DNA-binding proteins recognizing AT-rich sequences, namely S/MARs (scaffold/nuclear matrix attachement regions). S/MARs are AT-rich regions of several hundreds base pairs, preferentially located on G-bands and heterochromatin, and specifically associated with the nuclear matrix [184]. They strongly affect expression of genes and chromosome dynamics with S/MAR binding proteins in cooperation with other types of DNA-binding proteins such as histone H1 and high mobility group protein HMG-I. An example of gene whose expression is affected through changed dynamics of S/MAR is MYOD1 [185]. Human MYOD1 located on G-band 11p15.4 is expressed upon differentiation of satellite cells. Indeed, its expression is strongly inhibited by both BrdU and distamycin A suggesting that a change in chromatin structure is involved in the effect of BrdU on this gene.

Apart from the effect on the senescence-associated genes, BrdU was shown to induce production of alkaline phosphatase in a hybrid line [186], prolactin in rat pituitary tumor cells [187] and human fetal globin in normal adult erythroid cells [188]. On the other hand, BrdU down-regulates expression of the endogenous human papilloma virus type 18 E6/E7 **(BOX #7)** and this could explain high sensitivity of HeLa cells to BrdU treatment.

BOX #7. E6 and E7 HPV proteins

Papillomaviruses are DNA viruses that infect epithelial tissues. They usually cause benign warts but they can contribute to human tumorigenesis as high-risk HPV **E6/E7 proteins inactivate both major tumor suppressors pRb and p53** and dramatically augment genomic instability.

E7 proteins interact with the pRb and the related "pocket proteins" p107 and p130 and this interaction targets the pocket proteins to the proteasome-mediated **degradation**. E7 also affects transcription coactivators such as p300/ CBP. Moreover, HPV E7 expression has been shown to trigger primary centrosome and **centriole duplication errors** in normal diploid cells, thus increasing the genomic instability. Intriguingly, it has been demonstrated that E7 interact also with PML [89].

High-risk HPV E6 proteins eliminate safeguard mechanisms of the cell initiated by above described effects of E7 expression through inactivation of p53. E6 proteins do not interact with p53 directly but form a complex with the cellular E6-AP protein that consequently induces ubiquitination and **degradation of p53**. Moreover, E6 binds **c-myc** and this c-myc/E6 complex activates **hTERT** expression and thus facilitates the immortalization of human epithelial cells [189].

2.4 Human mesenchymal stem cells

The ability of the multicellular organism to survive during the extended period of time is given by the ability to repair cells and tissue that become damaged from extrinsic or intrinsic reasons. The maintenance of tissue homeostasis is dependent on the population of so called stem cells. These cells are characteristic by the potency to differentiate into multiple cell types as well as to self-renew and thus to maintain their cellular pool. They can reside in each tissue; however they can also migrate over long distances led by homing signals to colonize tissues that need to be repaired [190]. This property is important for natural but might be useful also for medicine-directed rejuvenation of the organism.

How exactly are stem cells maintained during the lifetime of the organism and what are the stimuli leading to their commitment and differentiation is not fully understood. Therefore, the *in vitro* research on the stem cells provides the opportunity to address these questions and to use this information also for human medicine to improve quality of life of the human population.

2.4.1 hMSC properties

Human mesenchymal stem cells (hMSC) can be isolated from bone marrow or adipose tissue using a density gradient that removes hematopoietic stem cells and already differentiated cells [191]. hMSC represent quite uniform population of cells that is positive for several surface markers (including SH2, SH3, CD29, CD44, CD71, CD90, CD106, CD120a, CD124). When in culture, they exhibit normal karyotype and also telomerase activity over several cell divisions. Depending of culture conditions and of the donor they can reach about 40 cell divisions before they become senescent [192].

The idea of human gene therapy is based on the introduction of a functional gene into cells within the body to correct a genetic defect. Importantly, hMSC represent a promising cellular vehicle for *in vivo* gene delivery given that they can be *in vitro* genetically manipulated without compromising the stem cell qualities. Using retroviral transduction, hMSC expressing GFP or human IL3 were generated and they maintained the transgene expression for extended period of time (up to several months), even when differentiated or when injected into nude mice [193].

hMSC secrete a number of cytokines such as IL6, IL7, IL8, IL11, IL12, IL14, IL15, LIF, M-CSF and GM-CSF. This secretory function of hMSC is important for other cells as it was shown that hMSC support hematopoietic differentiation *in vitro* [194]. They are truly

pluripotent cells because upon proper stimulation they can give rise to chondrocytes, osteoblasts, adipocytes, kardiomyocytes and even neurons while they do not differentiate spontaneously [195-200]. The commitment of hMSC into different lineages is dependent on nutrients availability, cell density, mechanical forces, growth factors, cytokines and interactions with the immediate environment [191,201]. The analysis of differentiation potential of 185 non-immortalized human MSC cell clones showed that hMSC were progressively losing their adipogenic and chondrogenic differentiation potential at increasing cell doublings while osteogenic potential was maintained even when cells exhibited features of senescence [192,202,203]. This, together with the observation that clones with a differentiation potential limited to the osteo-adipogenic or to the chondro-adipogenic phenotype were never detected, strongly supports the hierarchical model of hMSC differentiation pathway, where adipogenic potential is the first to be repressed [202]. Thus, it can be suggested that early phases of stem cell differentiation are associated with a successive restriction in the repertoire of genes that can be expressed [201].

2.4.2 Adipogenesis and adipogenic conversion of hMSC

Adipogenesis is connected with dramatic changes in the gene expression necessary for the establishment of highly specialized function of adipose cell, i.e. storage or mobilization of excessive energy in form of triglycerides and secretion of hormones and cytokines (for a review, see [204]). The key transcription factors involved in adipogenesis are C/EBPα and PPARγ; they govern the entire differentiation process acting on a single pathway, in which PPARγ appears to be the dominant factor. The importance of both of them was confirmed using KO mice models and overexpression approach. Loss of PPARγ results in the inability of cells to acquire any feature of adipose phenotype and, on the other hand, an overexpression of PPARγ in nonadipogenic mouse fibroblasts is sufficient to trigger the adipogenic program [205,206]. The ablation of C/EBPα in all tissue except liver (liver KO of C/EBPα leads to the embryonic lethality) resulted in complete loss of white adipose tissue proving that C/EBPα is required for the differentiation of white adipocytes [207]. All other transcription regulators, coactivators or repressors important in the adipogenic program affect these two master regulators.

Importantly, it seems that transcriptional programs leading to hMSC commitment into each lineage are mutually exclusive, i.e. factors activating adipogenic conversion block for example osteogenesis and *vice versa*. For example, the activity of MAP kinase ERK appears to be critical for the commitment to either adipogenic or

osteogenic program [208]. The treatment of hMSC with osteogenic supplements leads to sustained but time restricted ERK activation that coincides with differentiation manifested by the formation of bone-like nodules with a mineralized extracellular matrix. The block of this activation by PD98059, a specific inhibitor of the ERK signaling pathway, results in repression of the osteogenic conversion, while proportion of hMSC exhibits features of the adipogenic differentiation including the expression of adipose-specific mRNAs PPARγ2, aP2 and LPL. Molecular basis of this switch has been suggested - the ERK may phosphorylate PPARγ and it is known that this modification reduces PPARγ transcription activity [209]. In line with this, growth factors and cytokines, which activate MAP kinases, such as tumor necrosis factor α, are potent inhibitors of adipocyte differentiation [208]. The effects of ERK activation on adipogenic conversion of hMSC have been further evaluated in Experimenal part I.

Adipogenic conversion of cells is *in vitro* induced by medium containing hormonal cocktail (1-methyl-3/isobutylxanthine-inducer of cAMP, dexamethasone- glucocorticoid, insulin, and indomethacin) [210]. Phenotypically, cells start to accumulate cytoplasmic lipid droplets and become rounded; as a consequence the cell nucleus is pushed towards the cytoplasmic membrane. Fully differentiated adipocyte is characterised by one central lipid droplet and narrow cytoplasmic rim accommodating the nucleus. In Experimental part I, we describe conditions that support the adipogenic conversion of hMSC and validate them as an *in vitro* model for human adipogenesis.

2.4.3 Adipogenesis and tumor suppressors

Interestingly, to regulators of adipogenesis belong also pRb and several proteins primarily described to be important in the aging process. pRb role in adipogenesis is quite complicated – the inactivation of pRb through its hyperphosphorylation is necessary for E2F binding to PPARγ promoter. On the other hand, knock-out of pRb does not result in increased adipogenesis as could be expected. Quite contrary, pRb-/- MEF have a reduced capacity for differentiation into white adipocytes [211]. It is possible that complete loss of pRb hamper the exit from the cell cycle that is required for the terminal differentiation.

FOXO family of transcription factors has been implicated in the establishing of stress resistance that slows down aging [212]. Interestingly, FOXO1 negatively regulates adipogenesis and one of the roles of insulin in adipogenesis is to inactivate FOXO1 binding to promoters of its target genes [211]. FOXO1 transcriptional target is p21, so FOXO

inhibits adipogenesis at least in mice through blocking clonal expansion of preadipocytes [213].

There are essentially no data about PML role in adipogenesis or adipocytes. But it is noteworthy that PML is upregulated by interferons and retinoic acid - two factors that potently block adipogenesis. In the Experimental part III, we showed that PML is present also in fully differentiated adipocytes, although the number of PML bodies was somehow lowered.

2.4.4 hMSC and aging

As stem cells contribute to tissue homeostasis over the lifetime of organism, they must have molecular mechanisms that prevent senescence and maintain their "stemness". However, even these mechanisms might become partially insufficient upon accumulation of environmental insults and the aging of stem cells and the loss of their pluripotency may contribute to the deterioration of tissue function.

In vivo, most of the stem cells are maintained in mitotic quiescence that is distinct from permanent cell cycle exit. It has been suggested that it is the immediate environment- so called the stem cell niche - that is a source of the appropriate signals that keep stem cells in a quiescent state [201]. However, stem cells are able to react to mitotic stimuli and divide as many times as needed. They share the property of indefinite cell division with tumor cells. This raises the possibility that the tumor cells may have actually evolved from the stem cells with the deregulated cell cycle [214]; this deregulation presumably originates from unrepaired DNA damage and genomic instability. Therefore, the presence of stem cells in the body can represent also certain danger for the organism. Thus, the pathways directing stem cell cycle progression or growth arrest need to be thoroughly investigated to get the full picture of tumor development. However up to now, there is only little information on p53 and pRb tumor suppressor pathways in stem cells and there are virtually no data about PML and PML bodies and their role in stem cell biology. Thus, one of the goals of the Experimental part III was to bring new information about PML expression and behavior in *in vitro* cultured hMSC. We showed that PML expression is greatly dependent on the proliferative age of hMSC and that the senescence in hMSC is connected with newly described association of PML with the nucleolus.

3 Aims of the study

The general objective of the presented study was to contribute to the elucidation of the promyelocytic leukemia protein function and regulation in human cells. We aimed mainly to analyze the PML expression and behavior using the models of stem, tumor and senescent cells. This goal was preceded by the evaluation of these models including the characterization of adipogenic conversion of hMSC and was addressed in three experimental blocks.

The specific aims were:

1. To optimize the culture conditions enhancing adipogenesis in hMSC and then to validate hMSC as an *in vitro* model of human adipogenesis.

2. To examine the role of chromatin acetylation in the expression of *PML* gene.

3. To describe PML expression and nuclear compartmentalization in growing, differentiated and senescent hMSC and in other prematurely senescent cells.

4 Overview of used experimental methods

4.1 Cell culture

hMSC growth and differentiation
hMSC were subcultured 1:3 when they reached 80% confluence. For experiments, hMSC were used between passages 5 and 18. For differentiation, cells were grown to 100% confluence in the growth medium supplemented with 10% FBS specially selected to support hMSC growth. Two day post-confluent cells were incubated in Adipogenesis Induction Medium (AIM: DMEM-1 g/l glucose, 1 µM dexamethasone, 0.2 mM indomethacin, 1.7 µM insulin, 0.5 mM IBMX, 10% FBS, 0.05 U/ml penicillin, 0.05 µg/ml streptomycin) for 3 days, three days incubated in Adipogenesis Maintenance Medium (AMM: DMEM-1 g/l glucose, 1.7 µM insulin, 10% FBS, 0.05 U/ml penicillin, 0.05 µg/ml streptomycin) and then switched to AIM again. After third cycle, cells were fed with AMM up to 21 day of differentiation.

Induction and estimation of cellular senescence *in vitro*
Cells were treated by 10 µM BrdU, 10 µM DMA, or their combination for 5 - 7 days. Culture medium was changed with fresh additives every second day. Due to the sensitivity of BrdU-treated cells to light-induced DNA damage [215], cells were exposed to light only for minimal time interval necessary for cell handling. SA-β-galactosidase assay was performed according to Serrano et. al. [171] with modifications described in [216]. Images were captured at magnification 200x by fluorescence microscope Leica DMRXA equipped with digital camera.

Oil Red O staining
Cells were stained with Oil Red O to determine the extent of accumulation of lipids during differentiation [217]. Cells were fixed in 10% solution of formaldehyde in phosphate buffer for 1 hour or more, washed with 60% isopropanol and stained with Oil Red O solution (in 60% isopropanol) for 10 minutes. Excessive stain was removed by repeated washing with water. Cells were destained in 100% isopropanol for 15 minutes. The optical density of the solution was measured at 500 nm. An empty well treated in the same way was used as a blank.

4.2 Gene expression

Chromatin immunoprecipitation (ChIP)
HeLa cells (about 5×10^6 cells for each ChIP) were fixed with 1% formaldehyde for 10 min (reaction was stopped by 0.125 M glycine), harvested and lysed in cell lysis buffer (5 mM PIPES, pH 8.0, 85 mM KCl, 0.5% NP-40) for 10 min on ice. All buffers were supplemented with protease inhibitors (1 mM Pefabloc, 1 µg/ml pepstatin, 10 µg/ml leupeptin). The nuclei were resuspended in nuclei lysis buffer (50 mM Tris-HCl, pH 8.0, 10 mM EDTA, 0.2% SDS) and sonicated 8 times for 30 s (30 W; Sanyo Soniprep 150) on ice. Lysates were diluted and adjusted to contain all components of RIPA buffer (final concentration: 10 mM Tris-HCl, pH 8.0, 1 mM EDTA, 0.5 mM EGTA, 140 mM NaCl, 1% Triton X-100, 0.1% sodium deoxycholate, 0.1% SDS). Lysates were precleared with G-Sepharose beads equilibrated in RIPA buffer containing 1 mg/ml of BSA and 1 mg/ml of sonicated salmon sperm. Immunoprecipitation with desired antibody was performed at 4˚C overnight. The same total protein amount was used for each reaction. Immunocomplexes bound on beads were washed two-times with RIPA, four-times with LiCl buffer (10 mM

Tris-HCl, pH 8.0, 1 mM EDTA, 500 mM LiCl, 0.5% NP-40, 0.5% sodium deoxycholate), and once with TE buffer (10 mM Tris-HCl, pH 8.0, 1 mM EDTA). Protein-DNA complexes were eluted with 0.1 M NaHCO$_3$ and 1% SDS, decrosslinked in the presence of 200 mM NaCl for 5 h at 65˚C, and then treated with RNase A (f.c. 40 µg/ml, 20 min, 37˚C) and proteinase K (f.c. 200 µg/ml, 3 h, 50˚C). DNA was phenol/chloroform extracted, precipitated and PCR-amplified. The supernatant after G Sepharose beads collection was saved as reaction input; DNA was isolated, and 1/16000 of total input was amplified by PCR.

RNA analysis - qRT-PCR

Total RNA was isolated using Trizol or TriReagent and optionally applied to RNeasy minicolumns. RNA was dissolved in RNase free water and stored in –70°C until use. The concentration of RNA was determined using spectrophotometry. One-step qRT-PCR reaction with gene specific primers and TaqMan probe was carried out using the ABI PRISM 7700 SDS instrument. Gene specific primers and probes were designed using Primer Express software. For two-step qRT-PCR, 200 ng of total RNA was reverse transcribed using random hexamers as primers and for second step, an aliquot of cDNA corresponding to 10 ng was used. qRT-PCR was performed in ABI Prism 7000 or 7300 instruments employing master mix containing SYBR Green I. Every sample was measured in duplicates. Either standard curve or the ΔΔCt method was applied for quantification and appropriate house-keeping genes were used for normalization of the results [218].
For RT-PCR analysis, total RNA was isolated by cesium gradient centrifugation and dissolved in DEPC water. After the reverse transcription step, first strand of cDNA was amplified using specific primers. cDNA was analyzed after 35 cycles of PCR on agarose/EtBr gel.

Cell fractionation

Cytosolic and nuclear fractions were prepared according to a modified protocol of Dignam. Briefly, cells were scraped into ice-cold PBS, collected by centrifugation (500x g, 4˚C, 5 min), resuspended in cytosolic lysis buffer containing 10 mM HEPES (pH 8.0), 1.5 mM MgCl$_2$, 10 mM KCl, 10 mM iodoacetamide, 0.5 mM Pefabloc, 0.5 µg/ml pepstatin and 1 µg/ml leupeptin, and stroked several times through injection needle (29G). After incubation on ice (10 min), nuclei were pelleted by centrigufation, supernatant was removed and stored as cytosolic fraction. Nuclei were washed and resuspended in cytosolic lysis buffer. Both fractions were denatured in SDS sample buffer, boiled for 5 min and shortly sonicated before loading onto the gel.

Protein analysis-immunoblotting

Confluent cells were washed with PBS and scraped into RIPA buffer (10 mM Tris pH 8.0, 140 mM NaCl, 1% Triton X-100, 0.1% sodium deoxycholate, 0.1% SDS, 1 µg/ml pepstatin, 10 µg/ml leupeptin, 1 mM Pefabloc) or cell lysis buffer (50 mM Tris pH 7.4, 150 mM NaCl, 1% Triton X-100, 1% sodium deoxycholate, 0.1% SDS, 1 µg/mL pepstatin, 1 µg/mL leupeptin, 2 µg/mL aprotinin, 100 µM benzamidine) and briefly sonicated. Lysates were cleared by centrifugation. For MAPK experiments the lysis buffer was enriched with 10 mM activated sodium orthovanadate and 2 mM DTT. For detection of p53, p21 and pRb, cells were washed twice with ice-cold PBS supplemented with protease inhibitors (1 mM Pefabloc SC, 1 µg/ml leupeptin, 1 µg/ml pepstatin) and phosphatases inhibitors (1 mM sodium orthovanadate, 10 mM NaF) and then scraped into the same buffer and centrifuged at 2000 rpm, 5 min, 4°C. Cells were resuspended in 50 mM Tris (pH 6.8)/inhibitors of proteases and phosphatases, then lysed in 50 mM Tris (pH 6.8), 2% SDS, 10% glycerol and briefly sonicated. DTT and bromphenol was added to lysates to

final concentrations 100 mM and 0.01%, respectively. Protein concentration was determined using the bicinchoninic assay (Pierce, Rockford, IL, USA). Equal amounts of total protein were resolved on 8%, 13% or 8-16% gradient polyacrylamide minigels and electrotransferred onto nitrocellulose or PVDF membranes. After blocking, membranes were incubated overnight in a cold room with the primary antibody, and antigen-antibody complexes were detected using secondary antibodies coupled with horseradish peroxidase and the ECL detection system (Pierce).

4.3 Microscopy

Indirect immunofluorescence and nuclear run-on transcription assay
Cells were grown on 12 mm glass coverslips, washed twice with PBS and fixed/permeabilized in 3-4% formaldehyde/PBS/0.1% Triton X-100 for 20 minutes. Cells were then washed extensively with PBS and used immediately or stored in PBS/0.1% sodium azide at 4°C. Cells were incubated with primary antibodies diluted in PBS/0.05% Tween 20 for 1 hour at room temperature, then washed 3 times in PBS/0.05% Tween 20 and incubated with secondary antibodies conjugated with fluorescent dyes (FITC, Cy5, Cy3). To visualize RNA and nucleoli, cells were stained with 2 µM TOTO3 (Molecular Probes, Eugene, OR, USA). Coverslips were then mounted in MOWIOL with DAPI (0.8 µg/ml). Images were obtained using fluorescence microscope OLYMPUS VANOX-S or Leica confocal microscope TCS SP.

Run-on transcription assay
Detection of nascent RNA molecules was performed as described before [219]. In brief, cells were permeabilized by addition of 0.5 mg/ml saponin in physiological buffer (100 mM potassium acetate, 30 mM KCl, 10 mM Na_2HPO_4, 1 mM $MgCl_2$, 1 mM Na_2ATP, 1 mM DTT, pH 7.4 supplemented with 0.2 mM PMSF, 100 mg/ml BSA and 10 U/ml human placental RNase inhibitor), and transcription was initiated by adding a transcription mixture (final concentrations, 100 µM CTP, GTP, BrUTP, and 0.3 mM $MgCl_2$) into saponin-free physiological buffer. To enhance incorporation of BrUTP into rRNA transcripts, cells were incubated with 100 µg/ml α-amanitin for 5 minutes prior addition of transcription mixture and during the transcription itself. Cells were allowed to transcribe for 25 minutes at 35°C, then fixed and BrU was detected as described above.

Electron microscopy and immunogold labeling
For immunoelectron microscopy, cells grown on coverslips were fixed in 2% paraformaldehyde and 0.25% glutaraldehyde in Sorensen buffer (SB, 0.1 M sodium/potassium phosphate buffer, pH 7.3) for 1 hour at 0°C, and washed twice with SB (10 minutes each wash). The cells were dehydrated in series of ethanol solutions with increasing concentration of ethanol. Ethanol was then replaced in two steps by LR White resin, polymerized under UV light for 48 hours at 4°C, and 80 nm sections were immunogold labeled according to standard procedures [220]. Finally, sections were contrasted with a saturated solution of uranyl acetate in water (4 minutes) and observed in Morgagni electron microscope (F.E.I., The Netherlands) equipped with a CCD Mega View II camera (SIS, Germany).

4.4 List of used cells and cell lines

All cells were grown at 37°C under 5% CO_2 atmosphere.

Cells	Medium	Serum
hMSC	MSCBM, 1:1 mixture of DMEM-low glucose and M199	10% MSGS (FBS selected to support hMSC growth)
HSF	DMEM-high glucose	10% FBS
HeLa	DMEM-high glucose	5 or 10% FBS
U-2 OS	DMEM-high glucose	10% FBS
Jurkat	RPMI	10% FBS
K562	RPMI	10% FBS
SaOS-2	DMEM-high glucose	10% FBS
HEK293T	DMEM-high glucose	10% FBS
A549	Kaighn's modification of F-12K	10% FBS
H1299	RPMI	10% FBS

4.5 List of used primary antibodies

Antigen (clone)	Host	Dilution	Source	Method
Human PML (PG-M3)	mouse	1 µg/ml	Santa Cruz	IF
Human PML (5E10)	mouse	1:10	Dr. van Driel	WB
Human PML (H-238)	rabbit	0.5 µg/ml	Santa Cruz	IF,WB
Human Sp100 (Sp26)	rabbit	1:400	Dr. Sternsdorf	IF
Human Sp100 (SK54)	human	1:400	Institute of Rheumatology	IF
Human NDH II	rabbit	1:1000	Dr. Zhang	IF
Human B23	goat	2 µg/ml	Santa Cruz	IF
BrdU	mouse	10 µg/ml	Exbio	IF
γH2AX	mouse	1 µg/ml	Upstate	IF
Human SUMO-1	rabbit	1:200	Alexis	IF
Human DFC	human	1:100	Dr. Hernandez-Verdun	IF
Human PolI	rabbit	1:8	Dr. Grummt	IF
Human UBF	human	1:1000	Dr. Grummt	IF
Human p53	rabbit	1:1000	Dr. Vojtěšek	WB
Human p21$^{waf/sdi-1}$	mouse	0.5 µg/ml	Transduction Laboratories	WB
Human pRb	mouse	0.5 µg/ml	BD Pharmingen	WB
Human STAT2	rabbit	0.4 µg/ml	Santa Cruz	WB, ChIP
Human IRF1	rabbit	0.4 µg/ml	Santa Cruz	WB
Human PCNA	mouse	1:200	Dr. Vojtěšek	IF
Human C/EBPß (sc-150)	rabbit	1:400	Santa Cruz	WB
Human GAPDH	mouse	1:6000	Acris Antibodies	WB
Human GLUT4	mouse	1:1000	Dr.Pilch	WB
Human ERK phospho-Thr202/204 and total ERK1/2	rabbit	1:1000	NEB	WB
Human PPARγ(210-225-C100)	rabbit	1:500	Alexis	WB

4.6 List of used oligonucleotides

Primers for quantitative RT-PCR		
gene	forward	reverse
PML	CCGCAAGACCAACAACATCTT	CAGCGGCTTGGAACATCCT
GAPDH	GTCGGAGTCAACGGATTTGG	AAAAGCAG CCCTGGTGACC
PML	TGACCAGCATCTACTGCCG	AGCTCACTGTGGCTGCTGTC
actin	AGGCACCAGGGCGTGAT	TCGCCCACATAGGAATCCTT
18S rRNA	CGTTCAG CCACCCGAGATT	CGGACATCTAAGGGCATCACA
adipsin	CAGGGTCACCCAAGCAACA	CGCCAATTGCCCAGCTAA
cyclophilin B	GGAGATGGCACAGGAGGAAA	CGTAGTGCTTCAGTTTGAAGTTCTCA
leptin	TCACCAGGATCAATGACATTTCAC	CCCAGGAATGAAGTCCAAACC

TaqMan probes for qRT-PCR	
cyclophilin B	CATCTACGGTGAGCGCTTCCCCG
leptin	CGCAGTCAGTCTCCTCCAAACAGAAAGTCA

Primers for RT-PCR and ChIP		
gene	forward	reverse
GAPDH	CCACCCATGGCAAATTCCATGGCA	TCTAGACGGCAGGTCAGGTCCACC
leptin	GACTTCATTCCTGGGCTCCA	AGAGAAGGCCAGCACGTGA
aP2	GAGAAAACGAGAGGATGATAAACTGG	TGGGAGAAAATTACTTGCTTGCT
PPARγ	TGCCAAAAGCATTCCTGGTT	CGCTGTCATCTAATTCCAGTGC
ISRE-PML promoter	TAGAACCGCCCCCAGCTTCT	CCACCACAGCAAACCAACAAA

5 Results

5.1 *Experimental part I*

5.1.1 Introduction

Adipogenesis is a complex process including proliferation of precursor cells, their commitment to the adipogenic lineage, and terminal differentiation. Although the terminal differentiation of adipocytes is intensively studied and well described in the 3T3-L1/F442A murine cell lines, key information regarding the commitment of human precursor cells to the adipogenic lineage is still lacking.

Human pre-adipocytes derived from adipose tissue through collagenase digestion are widely used to study human adipogenesis; however, these cells are already committed to the adipogenic lineage[221]. Moreover, human pre-adipocytes have reduced proliferative ability, an unpredictable variability based on different donors and anatomical sites, and limited availability[222]. Human mesenchymal stem cells represent an alternative to this model. They are true multipotent precursors of several cell types. The variability between hMSCs from different donors was reported to be low[191]. hMSCs proliferate under *in vitro* conditions and retain their adipogenic, chondrogenic, and osteogenic potential that is reflected by simultaneous expression of genes characteristic of various mesenchymal cell lineages.

In the present study, we further characterize hMSCs and confirm their usage as a convenient model for the study of human adipogenesis, including the early stages of the differentiation process. We describe our efforts to optimize the differentiation of hMSCs in the presence of various pharmacological agents that impact signaling systems known to be important in adipocyte differentiation.

.

5.1.2 Results

hMSCs differentiated into adipocyte-like cells under all experimental conditions. In the absence of the hormonal cocktail no differentiation was observed.

Optimization of the Basal Differentiation Protocol.

Under standard differentiation conditions (suggested by hMSC supplier), only ~20% cells differentiated into adipocytes, compared with 95% described by Pittenger [191]. An important early event of adipogenesis is the exit from the cell cycle. hMSCs require hormonal stimulation for several cycles to achieve the commitment of cells to the adipogenic lineage. This suggested that only a certain number of cells were sensitive during each hormonal induction. We attempted to enhance differentiation by withdrawal of serum to synchronize the cell cycle [223]. With this idea in mind, for 5 days after they reached confluence, we fed cells with media containing different serum levels (0.5%, 2.5%, 5%, and 10% FBS) and then stimulated cells with AIM containing 10% FBS, one or three times, with 1 or 3 days of cultivation in AMM in between cycles **(Fig. 7)**. Serum starvation of cells (0.5% FBS), a maneuver that arrests cells in the G_0 phase, was less capable of stimulating adipogenesis compared with the serum-replete conditions. Surprisingly, cells that were allowed to rest between hormonal cycles for 3 days demonstrated improved morphology and differentiation efficiency **(Fig. 8)**. For this reason, we changed the originally described protocol to a "3 + 3" protocol and supplemented the medium with 5% FBS during post-confluence.

Previous studies suggested that the presence of serum inhibits differentiation of human adipocytes [221,224]. hMSCs seemed healthy when cultured in 0.5% FBS; however, 0.5% FBS was not sufficient to support differentiation, whereas 5% FBS was favorable **(Fig. 9)**.

Effect of insulin and glucose on differentiation of hMSCs.

Insulin is known to promote proliferation and differentiation of several pre-adipocyte cell lines, including 3T3-L1 or F442A cells [225]. High concentrations of insulin mimic the role of insulin-like growth factor-1 (IGF-1) and activate MAPK [226] and clonal expansion. We observed that high insulin concentrations were unnecessary for promoting adipocyte differentiation (the impact on differentiation was approximately the same as when 17 nM insulin was used). We found that 170 nM insulin was slightly more efficient (especially in combination with 5% FBS) in supporting differentiation of hMSCs **(Fig. 9).**

Next we compared the efficiency of different basal media (DMEM, 1 g/L glucose, minimum essential medium, and M199 without phenol red) to promote differentiation. M199 without phenol red (supplemented with FBS or rabbit serum and hormonal mixture) was modestly better compared with DMEM–4.5 g glucose/L media (data not shown).M199 contains 1 g/L of D-glucose, so we conclude that high concentration of glucose is not necessary for expression of the adipocyte phenotype.

Time-course of differentiation.

The main aim of our work was to validate hMSCs as a model for the early events in human adipogenesis. To compare the gene expression pattern of differentiating hMSCs to that of human pre-adipocytes known from the literature, we collected cells for RNA and protein analysis during differentiation. Soon after the onset of differentiation, cells started to accumulate lipids, whereas the most pronounced change in the phenotype was observed during the second cycle of hormonal induction. During the last week of differentiation, cells were maintained in AMM medium and continued to fill with lipids. After 21 days of differentiation using the base 3 + 1 differentiation protocol, ~20% of cells were fully differentiated into adipocytes. We used the RT-PCR technique to detect mRNA of PPARγ and adipsin genes [206,227] during differentiation of hMSCs. The examination of the relative mRNA levels revealed a pattern of gene expression in hMSCs similar to that described for human pre-adipocytes. PPARγ mRNA was detectable in confluent cells, rising markedly 12 hours after onset of differentiation and reaching a maximal level in the second cycle of hormonal induction. Adipsin mRNA was detected after a 48-hour incubation in AIM medium and persisted during differentiation **(Fig. 10A)**).

After optimization of differentiation protocol (3 + 3, 5% FBS, 170 nM insulin, and M199), we harvested cells from the second time-course experiment focusing on leptin mRNA [228] and C/EBPß, GLUT4, and PPARγ protein levels [229,230]. Leptin mRNA increased during differentiation, with the highest levels seen at the end of differentiation. Interestingly, the switch to AIM medium transiently inhibited leptin expression. At the end of each differentiation cycle, leptin levels were higher than in the previous cycle, suggesting the recruitment of responsive cells **(Fig. 10B)**. The highest leptin levels were approximately 5 to 10 times lower than in human subcutaneous fat tissue. When differentiated hMSCs were treated for 3 days in the presence of 1 μM dexamethasone, they

expressed levels of leptin mRNA similar to those seen *in vivo* (data not shown). This dexamethasone effect on leptin expression has been well documented in other cell models and *in vivo* [231-233].

GLUT4 protein was present at confluence and up-regulated in hMSCs after exposure to differentiation medium (data not shown). C/EBPß protein levels increased markedly and transiently within 24 hours and were greatly reduced at the end of the 21-day experiment **(Fig. 10C)** . PPARγ protein levels fluctuated with every hormonal induction, with the highest levels observed at the end of differentiation **(Fig. 10D)** .

Thiazolidinedione treatment enhances adipogenic conversion of hMSCs.

Treatment of pre-adipocytes with thiazolidinediones (TZDs), selective PPARγ ligands, enhances their differentiation, and in some cases, TZDs are required for their differentiation [207,234]. Troglitazone and BRL 49,653 enhanced differentiation, so at the end of the 21-day experiment, 80% of cells were Oil Red O positive, and lipid accumulation measured by Oil Red O method was two times higher than in controls **(Fig. 11A)** .

Rabbit serum supports adipogenesis.

As was previously demonstrated [235-237], rabbit serum enhances adipogenesis *in vitro*. We exposed hMSCs to the differentiation medium containing 15% rabbit serum. Rabbit serum alone failed to promote differentiation without induction by hormonal cocktail. In the presence of both rabbit serum and hormonal cocktail, hMSCs began to differentiate immediately (<24 hours) as compared with the FBS-containing medium. After 6 days, 90% of cells were Oil Red O positive, i.e., almost all cells were sensitive to adipogenic stimuli in the presence of rabbit serum **(Fig. 11B)** . At day 21, hMSCs differentiated in rabbit serum contained larger lipid droplets than under control conditions (not shown).

Inhibition of ERK1/2 facilitates differentiation of hMSCs into adipocytes.

Previous studies demonstrated that differentiation of hMSCs into osteoblasts or adipocytes is a mutually exclusive event [208]. MAPK (ERK1/2) promotes differentiation of hMSCs into osteoblasts. Previous reports suggested that blocking the activation of the MAPK pathway resulted in the spontaneous differentiation of hMSCs into adipocytes. Pretreatment with 50 μM PD98059, a specific inhibitor of MEK1/2 (an upstream activator of ERK1/2), before the onset of differentiation and subsequent treatment of hMSCs

throughout the course of differentiation with PD98059 resulted in 35% to 110% increase of adipogenesis as determined by Oil Red O staining. The positive effect of PD98059 was especially pronounced during the first week of differentiation **(Fig. 11C)**. When cells were allowed to differentiate for 21 days, the difference between control and PD98059-treated cells decreased due to the recruitment of new adipocytes after the third hormonal induction in the control medium.

In preliminary studies, we found that ERK1/2 was phosphorylated in the basal state, and the effect of PD 98059 was more pronounced at higher passages (data not shown). We evaluated the hypothesis that basal ERK1/2 activity is increased at higher passages, and consequently the inhibition of ERK1/2 phosphorylation by PD98059 would then be more efficient. To test this hypothesis, we used cells from three subsequent passages. 5-Day post-confluent cells were grown under identical conditions. Using ERK1/2-phospho-specific and ERK1/2-total antibodies, we found increased ERK1/2 activation in samples from cells at higher passages. The effect of PD98059 on differentiation increased with the passage number, whereas differentiation of hMSCs under control conditions decreased **(Fig. 12)**. This indicates that extensive passaging of cells is linked with higher ERK1/2 activation and has a suppressive effect on adipogenesis.

Clonal expansion is not required for terminal differentiation of hMSCs.

Clonal expansion after hormonal treatment is a very important event in the differentiation of 3T3 cell [225]. On the contrary, the number of human adipose tissue-derived pre-adipocytes remains the same after hormonal induction, and treatment with the replication inhibitor arabinosylcytosine (araC) cannot block the terminal differentiation [221].

To clarify the relevance of clonal expansion of hMSCs before terminal differentiation, we measured the expression of proliferation markers shortly after differentiation. Hormonal treatment was associated with transiently increased levels of PCNA mRNA (data not shown). Cyclin D1 mRNA levels increased slightly within the first 12 hours after hormonal induction and then decreased **(Fig. 13A)**. Importantly, treatment of cells with araC (1 to 3 pg/cell), a replication blocker, did not affect differentiation as measured by Oil Red O staining at day 21 **(Fig. 13B)**. Similarly the cell number did not differ from the control condition after 3 days (data not shown).
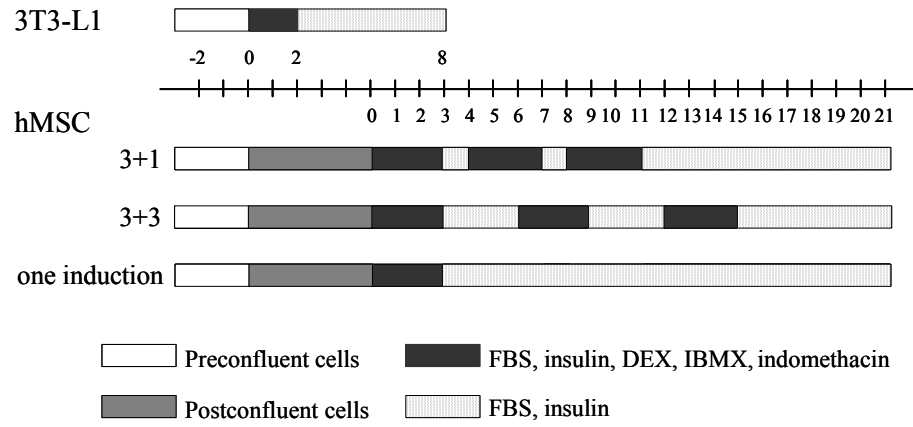
Fig. 7. Comparison of differentiation protocols for 3T3-L1 cells and hMSCs.
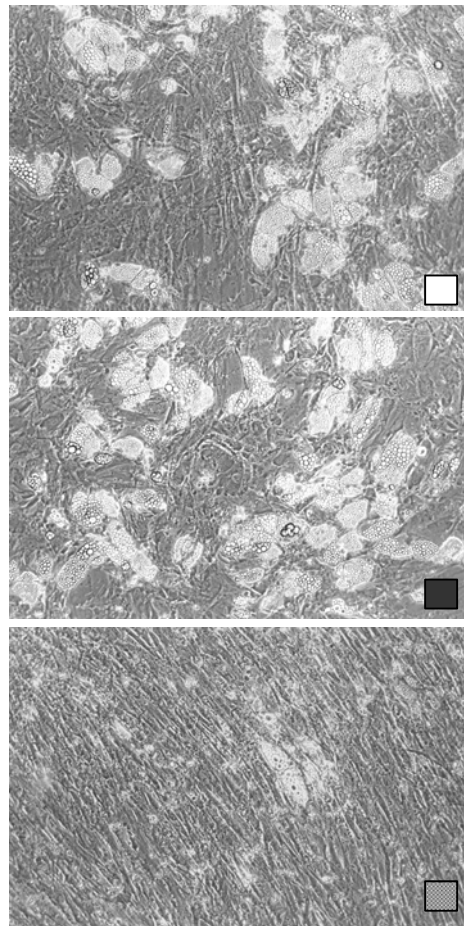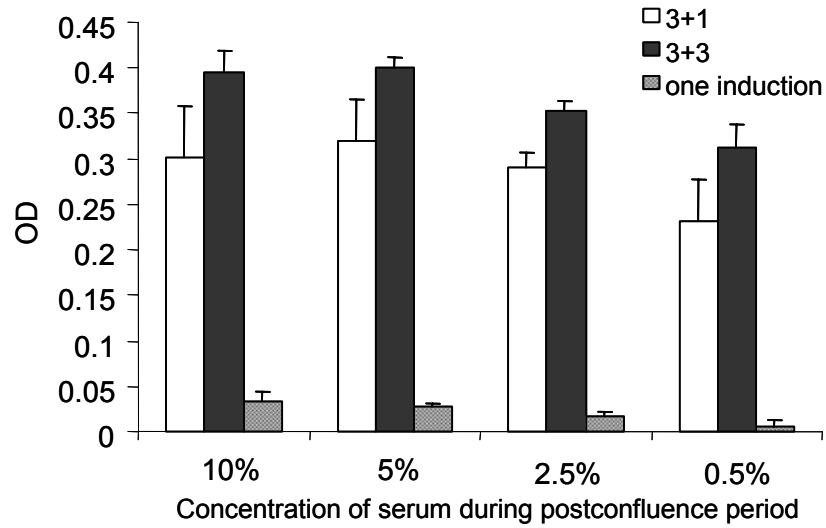
Fig. 8. Effect of serum concentration during post-confluence on differentiation.
Cells were fed 5 days after they reached 100% confluence with media containing 10%, 5%, 2.5%, or 0.5% FBS. For differentiation three protocols were used: "3 + 1" when induction medium was used for 3 days, whereas maintenance medium was used for only 1 day; "3 + 3" when both media were used for 3-day periods; and "one induction" when induction medium was used for only the first 3 days. After 21 days, the degree of differentiation was determined by Oil Red O staining (expressed as OD units). Photomicrographs representing cells maintained in 5% FBS during post-confluence are shown for each differentiation protocol.
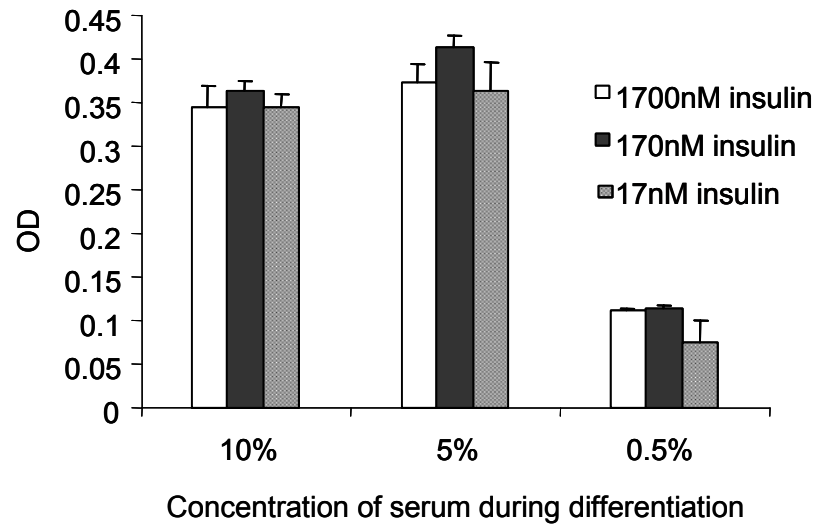
Fig. 9. Effect of serum and insulin concentration during differentiation on lipid accumulation.
Cells were differentiated in the presence of varying concentrations of FBS and human insulin. Lipid accumulation was determined by Oil Red O staining.
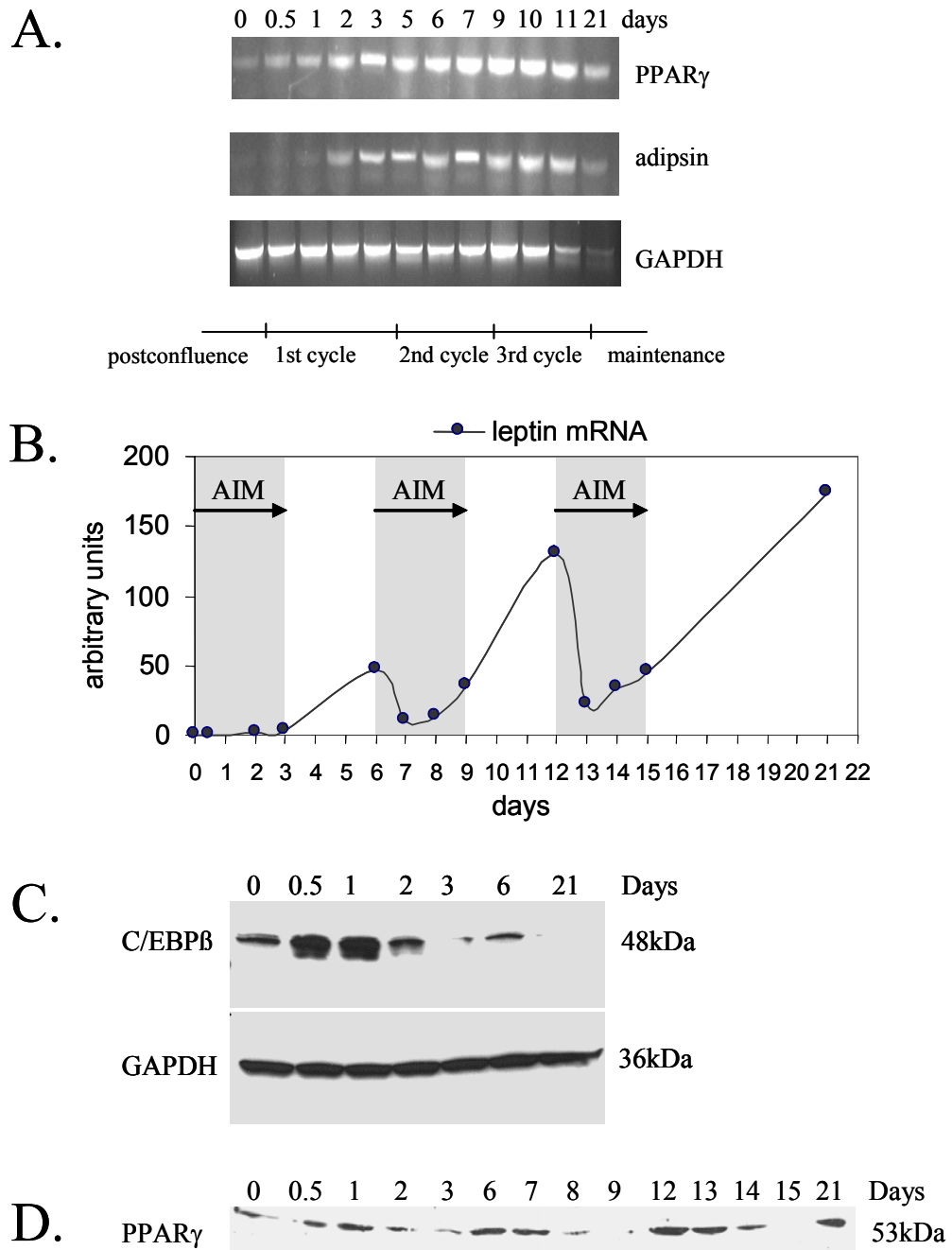
A.

B.

C.

D.

Fig. 10. Analysis of gene expression during differentiation of hMSCs.
(A) RT-PCR analysis of gene expression. Total RNA was reverse-transcribed, and gene-specific primers for PPARγ and adipsin were used for PCR reaction. GAPDH was used as a loading control. (B) Real-time RT-PCR analysis of leptin expression. 10 ng of total RNA from each time point was used as a template in one-step reaction. Gray blocks show time when cells were fed with AIM medium. (C) C/EBPß protein levels. Western blot using C/EBPß antibody was performed. Equal loading was confirmed when the same membrane was reprobed with GAPDH antibody. (D) PPARγ protein levels.
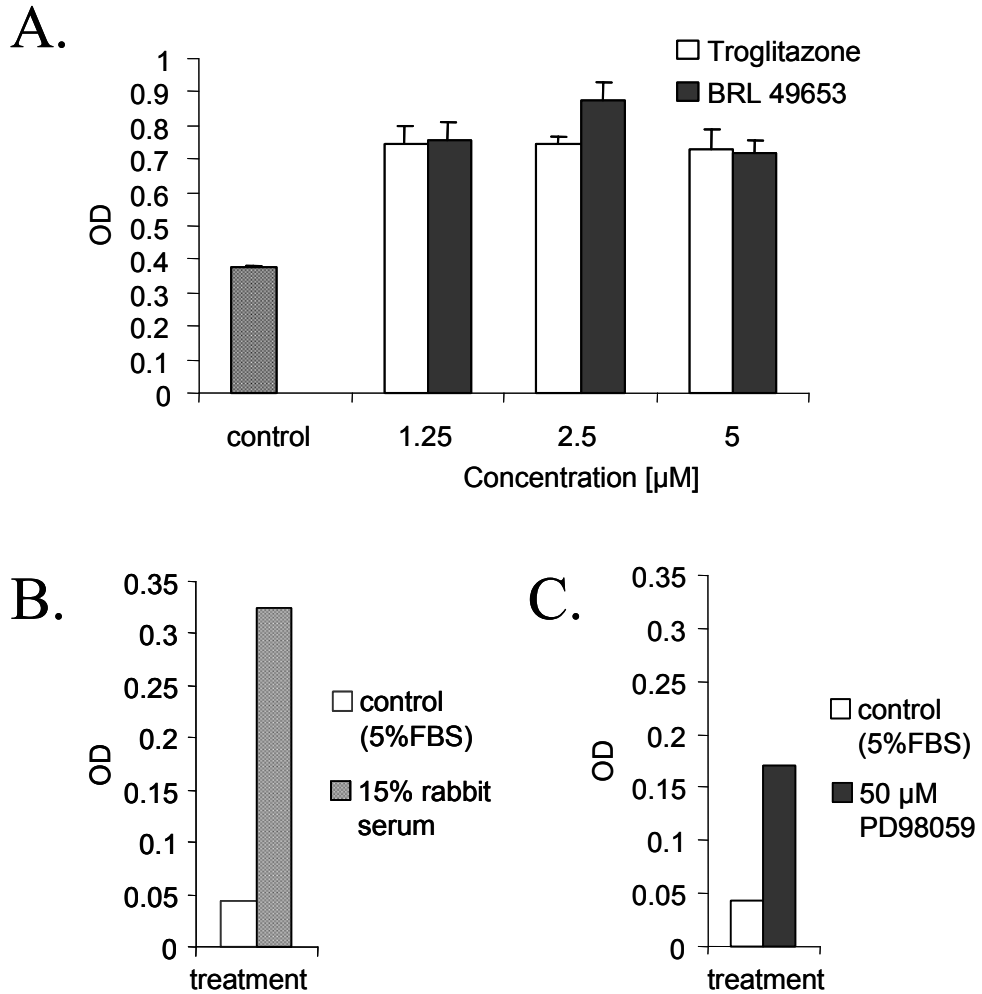
Fig. 11. The effects of different compounds on hMSC differentiation into adipocytes.
(A) TZD's effect on adipogenesis in hMSCs. Cells were differentiated in the absence or presence of varying concentrations of troglitazone or BRL 49,653. After 21 days of differentiation, cells were fixed and the degree of differentiation was determined by Oil Red O staining. The early effect of rabbit serum (B) and PD98059 (C) on hMSC differentiation. Cells (at passage 8) were differentiated in the presence or absence of 15% rabbit serum or 50 µM PD98059-supplemented AIM and AMM for 6 days. The degree of differentiation was determined by Oil Red O staining (expressed as OD units).
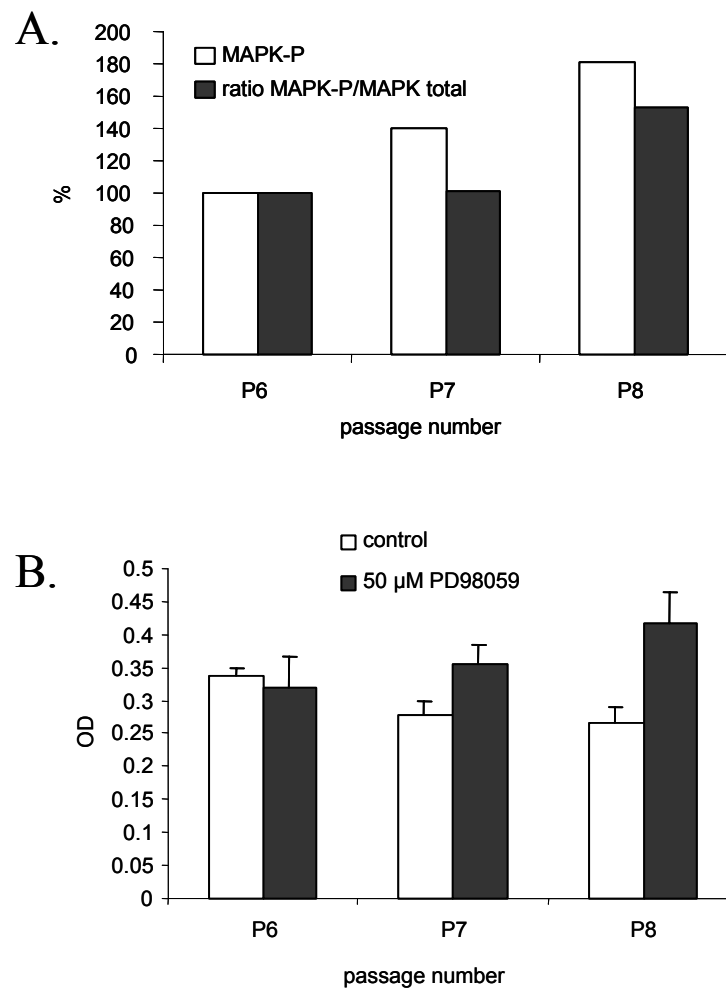
Fig. 12. The relationship among MAPK activity, population doublings and adipogenesis.
(A) Activity of ERK1/2 in cells with increasing number of population doublings. 5-day post-confluent cells harvested in the presence of phosphatase inhibitors. Samples were analyzed using Western blot and ERK1/2-phospho-specific and ERK1/2-total antibody. The percentage change of ERK1/2 phosphorylation alone or corrected with total ERK1/2 is shown. (B) Effect of MAPK inhibitor PD98059 on adipogenesis in cells with increasing population doublings. Cells from three subsequent passages were differentiated in the absence or presence of 50 µM PD98059. After 21 days, the degree of differentiation was determined by Oil Red O staining (expressed as OD units).
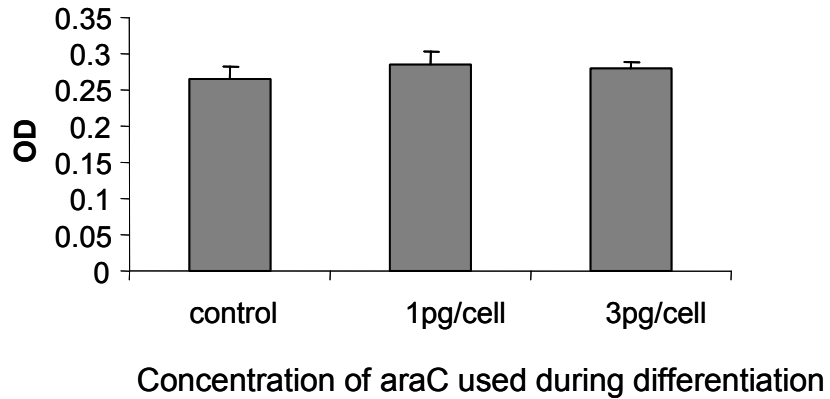
A.
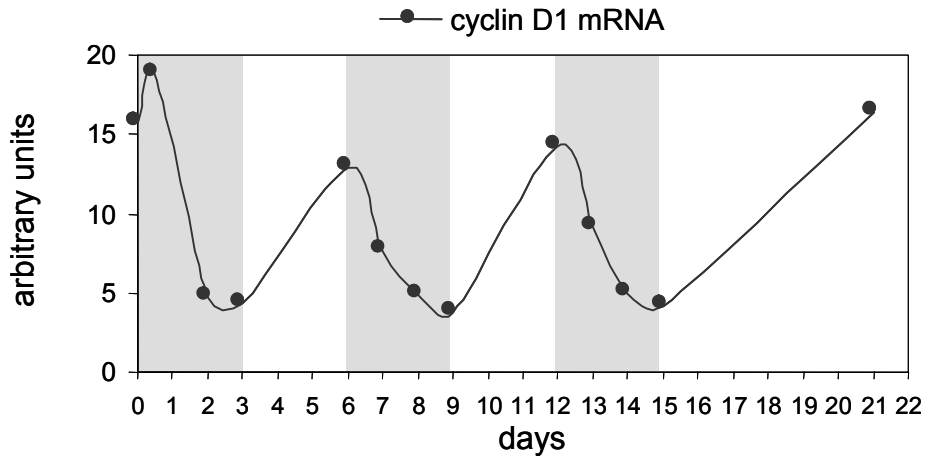
B.

Fig. 13. Analysis of cellular proliferation during adipogenic conversion of hMSC.
(A) Real-time RT-PCR analysis of leptin and cyclin D1 expression during the differentiation. 10 ng of total RNA from each time point was used as a template in one-step reaction. Gray blocks show time when cells were fed with AIM medium. (B) Effect of araC on adipogenesis. Cells were differentiated in the absence or presence of different concentrations of araC. After 21 days, the degree of differentiation was determined by Oil Red O staining (expressed as OD units).

5.2 Experimental part II

5.2.1 Introduction

Acute promyelocytic leukemia (APL) is a subtype of acute myeloid leukemia (AML) comprising of about 10% of AMLs [238]. The molecular basis of APL is characterized by a chromosomal translocation invariably involving retinoic acid receptor alpha (RARα) gene on the chromosome 17. The translocation partner for RARα is in 98% of APL cases represented by promyelocytic leukemia protein (PML) gene located on chromosome 15. The resulting fusion proteins are considered to be responsible for a differentiation block of myeloid line and for the subsequent accumulation of immature cells in bone marrow.

The molecular mechanism underlying APL was described previously [82,85,239]. Based on the fact that attached fusion partner causes a stronger interaction of fusion protein with corepressor complex recruiting histone deacetylases, it has been suggested that in addition to RA, HDAC inhibitors could be used for APL treatment in order to eliminate the repressing effect of HDACs. The observation that trichostatin A (TSA), a specific inhibitor of HDAC, caused reactivation of RA-inducible genes in APL cells [85] strongly supports this hypothesis. HDAC inhibitors have been tested as potent anticancer reagents in different types of solid tumor cell lines and in hematopoietic transformed cell lines. Several of them are in initial phases of clinical trials (for reviews, see [240,241]). HDAC inhibitors have also the ability to overcome a differentiation block in promyelocyte maturation - therefore they are intensively tested for a potential treatment of APL. However, eventhough several HDAC inhibitors have been shown to arrest cancer cell growth and/or induce apoptosis in doses that have little toxicity to normal cells, nothing is known about their impact on the expression of RARα translocation partners. Therefore, we aimed to characterize effects of HDAC inhibitors on PML expression of PML, the most frequent translocation partner of RARα, using the model of IFNα-inducible PML expression.

In this study, we describe the suppressive effect of HDAC inhibitors on IFNα-induced expression of PML and two other IFN-stimulated genes (ISGs), Sp100 and interferon regulatory factor 1 (IRF-1). As can be implicated from the known functions of PML NBs in cellular stress and from the role of ISGs in antiviral mechanisms, this suppressive effect should be taken into account as potential cause of therapeutic adverse effects of HDAC inhibitors currently tested or prepared in future for the clinical use.

5.2.2 Results

IFNα-induced increase of PML NBs number is suppressed by TSA.

When examining the effect of protein acetylation on the redistribution of specific proteins between nuclear compartments, we found that HDAC inhibitor TSA negatively affects IFNα-dependent increase of specific nuclear compartment, PML NBs. Since this finding is inconsistent with predominantly stimulatory action of TSA-mediated chromatin hyperacetylation on gene expression, we explored the effect of TSA on PML regulation in more detail. We followed the number of PML NBs in HeLa cells treated by IFNα, TSA or combination of both drugs by indirect immunofluorescence using antibodies recognizing the two main structural components of PML NBs - PML and Sp100 protein. As expected, we observed at least two-fold increase in PML NBs number in HeLa cells stimulated by IFNα for 24 hours [13]. However, this increase was completely suppressed when the cells were simultaneously treated with IFNα and TSA (see **Fig. 14A** for immunofluorescence data and **Fig. 14B** for quantification of PML NBs). The suppressive effect could be seen already after 12 hours of combined IFNα- and TSA-treatment **(Fig. 14C)**. Note that TSA alone did not influence noticeably the number of PML NBs in comparison to control untreated cells. When the cells were pretreated for 12 hours with IFNα and then exposed to TSA after IFNα removal, only insignificant decrease in PML NBs number was observed in comparison to cells treated with IFNα alone. The observation that once induced PML NBs remained stable for at least 12 hours even in presence of TSA (note also last column in **Fig. 14C**) suggests that TSA blocks only certain steps of PML expression and cannot cause PML NBs dissociation. Conversely, when the cells were exposed to TSA (12 h) prior to IFNα-treatment (12 h), the ability to increase PML NBs number was still observed, which indicates that the effect of TSA on IFNα pathway is reversible **(Fig. 14C)**. Taken together, these data clearly show that PML NBs are not induced by IFNα in the presence of HDAC inhibitor TSA and suggest that activation of PML gene by IFNα pathway is impaired by inhibition of protein deacetylation.

TSA inhibits PML transcription induced by IFNα.

To clarify whether the suppressive effect of TSA on IFNα-induced increase of PML NBs number is caused by the dispersion of PML and Sp100 proteins from bodies to nucleoplasm or by their decreased cell pool, we assessed cellular levels of both proteins by

specific antibodies on immunoblots in a similar experimental setup as described in the previous paragraph. As shown on **Fig. 15A**, TSA suppressed the IFNα-mediated induction of both proteins. For PML, identical results were obtained in human skin fibroblasts and HEK293 cells (not shown). In addition, PML was suppressed by TSA in mouse NIH-3T3 cells induced by IFNβ (not shown). Notably, IFNα-induced protein levels of IRF-1 were slightly decreased after TSA-treatment in HeLa cells **(Fig. 15A)**. These findings suggested that the inhibitory effect of TSA on the expression of these IFNα-induced genes is mediated at the transcriptional level. For further confirmation, we measured specific PML mRNA levels by real time RT-PCR. The primers were designed to cover the region of PML gene that is common to all PML isoforms (forward primer was designed over the junction of exon 2 and 3, reverse primer was positioned in the exon 3; first four exons are shared by all PML isoforms). PML mRNA levels were assessed in HeLa cells treated with IFNα, TSA or combination of both for 1, 4, 8, or 24 hours and normalized to GAPDH as endogenous control gene. As shown in **Fig. 15B**, the level of PML mRNA increased more than three times in comparison to control cells with a maximum approximately after 8 hours of IFNα-treatment, and returned back to the original level 24 hours after the start of treatment. Consistently with previous findings, IFNα-induced up-regulation of PML mRNA was substantially blocked in the cells treated simultaneously with TSA (within the whole range of concentrations: 30, 60, 125, 250, 500 ng/ml; not shown). Next, we performed PML mRNA analyses also with the SaOS-2, HSF, HEK293T, H1299, K562, and Jurkat cell lines. Notably, we observed a similar suppressive effect of TSA on IFNα-mediated induction of PML mRNA in all human cell lines tested **(Fig. 15C)**. In summary, these findings show that TSA blocks IFNα-mediated transcription of PML gene and that the suppressive effect of TSA is independent of cellular origin. Moreover, the same effect seen in mouse NIH-3T3 cells suggests an operation of a similar mechanism controlling IFNα-induced expression of PML and other ISGs in different species.

<u>Other histone deacetylase inhibitors suppress IFNα-induced PML up-regulation.</u>

As the individual types of HDACs differ in their sensitivity to various inhibitors [240], we tested the effect of selected HDAC inhibitors on IFNα-induced PML expression. Sodium butyrate (BUT; 5 mM; 24 hour) blocked IFNα-induction of PML protein in HeLa **(Fig. 16A)** and in HSF **(Fig. 16D)**. We were also interested if MS-275, SAHA and valproic acid (VA), the HDAC inhibitors currently used in the early phases of clinical trials, have the same suppressive effect on IFNα-induced PML expression as TSA and BUT. MS-275

at a concentration 0.3 μM (IC_{50} for HDAC1 [242]), 1 μM, or 8 μM (IC_{50} for HDAC3 [242]; not shown) showed only a slight inhibition of IFNα-induction of PML protein in HeLa **(Fig. 16B)** and HSF **(Fig. 16D)**. A slight inhibition was also observed with SAHA at the 1 μM concentration (**Fig. 16A**; only HeLa cells shown), whereas 2 μM and 10 μM (not shown) SAHA exhibited more pronounced suppression in both HeLa cells and HSF **(Fig. 16A, D)**. Valproic acid (VA), a suggested inhibitor of class I HDAC [243], had a mild suppressive effect on IFNα-induction of PML protein level at concentration up to 5 mM **(Fig. 16C)**, i.e. at the concentration reported to induce comparable levels of histone acetylation as 5 mM BUT or 100 nM TSA [243]. Because we observed variable intensity of suppression of IFNα-induced PML protein levels by different HDAC inhibitors (especially VA and MS-275), we decided to confirm and compare the effects of all inhibitors at the level of PML mRNA. PML mRNA levels in HeLa cells treated with IFNα alone or in a combination with particular HDAC inhibitor for 8 hours (i.e. at the time-interval when IFNα-induction of PML mRNA is peaking; see **Fig. 16B**) were measured by real time RT-PCR **(Fig. 16E)**. All tested inhibitors showed a significant suppression of PML mRNA in the following order: TSA > BUT/VA > SAHA > MS-275 (8 μM). With the exception of VA, these data well correspond with the suppressive effect of HDAC inhibitors observed at the protein level. In summary, all tested HDAC inhibitors showed, although in various extent, a significant suppressive effect on PML expression induced by IFNα.

TSA suppressive effect on IFNα-stimulation of PML is not caused by impaired translocation of STAT2 to nucleus.

It has been shown previously that TSA suppresses the response to viral infection in mice and concurrently inhibits cytoplasmic-nuclear relocalization of signal transducer and activator of transcription 2 (STAT2) in virus-infected L929 cells [244]. STAT2 is a component of IFN-stimulated gene factor 3 (ISGF3) complex, which is a transcription factor binding to ISRE elements in promoters of IFNα/β-induced genes. To test whether TSA has the same inhibitory effect on IFNα-induced translocation of STAT2 to the nucleus in our model, we performed immunoblot analysis of STAT2 localization in the nuclear fraction of HeLa cells treated with IFNα, TSA, or both. Consistently with the published data, we found that as soon as in 30 minutes after IFNα treatment, STAT2 appeared in the nuclear fraction **(Fig. 17A)**. STAT2 persisted in the nuclear fraction for at least 8 hours after IFNα-treatment, when a peak of PML mRNA induction was detected by real time RT-PCR. However, in the cells simultaneously treated by IFNα and TSA either

for 30 minutes or for 8 hours, STAT2 signal in the nuclear fraction was similar to that of the cells treated by IFNα alone **(Fig. 17A)**. This indicates that in our model TSA did not block IFNα-induced translocation of STAT2 into the nucleus.

TSA treatment does not impair STAT2 binding to ISRE element of PML promoter.

To investigate whether TSA affects the binding of ISGF3 complex to ISRE element of PML promoter *in vivo*, we performed chromatin immunoprecipitation of the PML promoter region containing ISRE element using STAT2 antibody in the control or in IFNα/TSA-treated HeLa cells. An increase of STAT2 bound to PML promoter in IFNα but also in IFNα+TSA treated cells was detected repeatedly in independent experiments when compared to control or TSA treated cells, where almost no signal was detected (see **Fig. 17B**). In summary, data from the cell fractionation and chromatin immunoprecipitation experiments suggest that in human cells TSA does not block translocation of STAT2 to the nucleus after IFNα stimulation and that TSA does not block STAT2 binding to PML promoter.
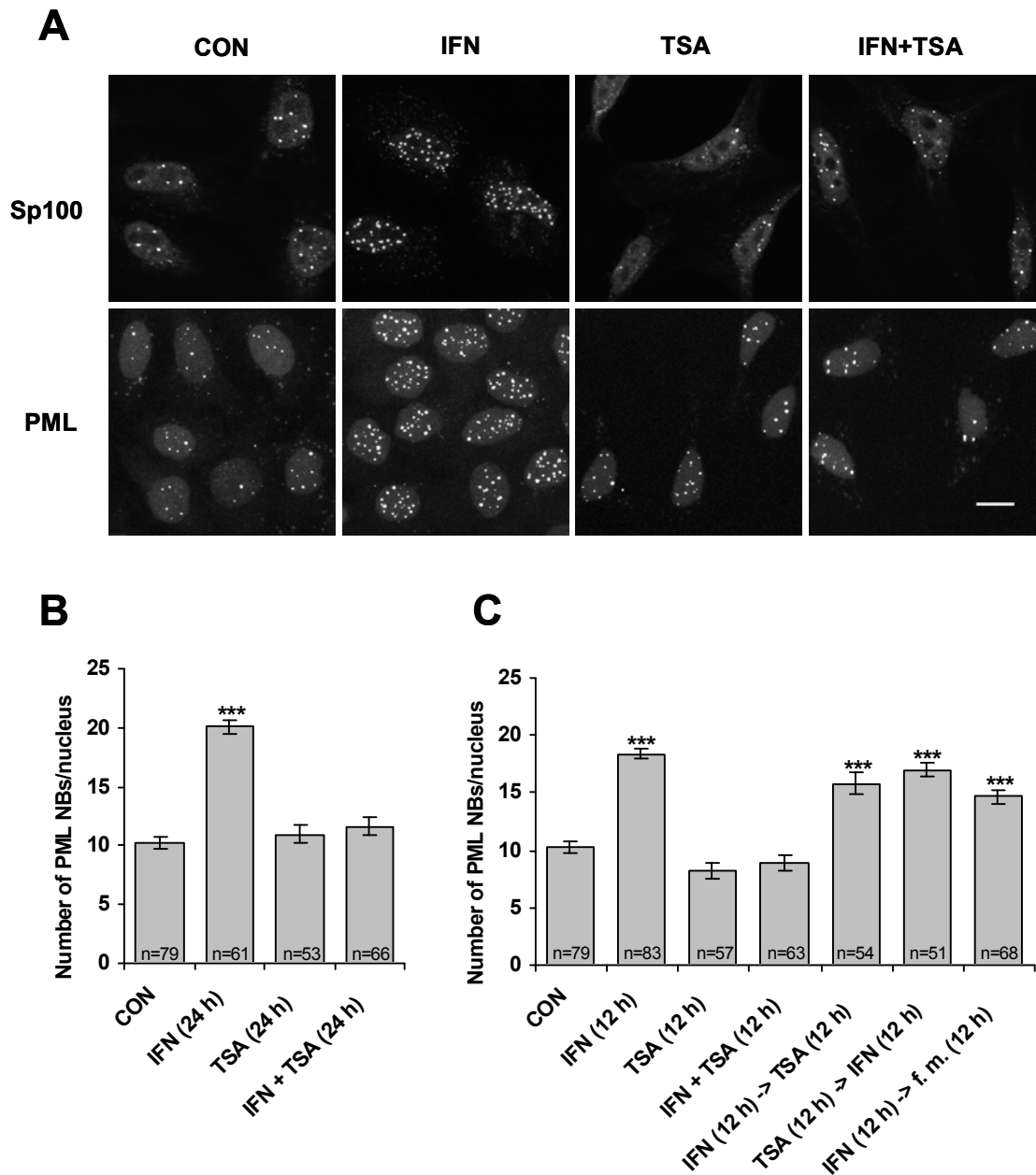
A

B

C

Fig. 14. IFNα-induced increase of PML NBs number is suppressed by TSA
(A) Confocal images of HeLa cells untreated (CON) or treated with 1000 U/ml interferon-α (IFN), 500 ng/ml trichostatin A (TSA), or their combination (IFN+TSA) for 24 h, immunostained with Sp100 or PML antibody; nuclei were co-stained with Sytox. Bar 10 μm. (B, C) Quantification of PML NBs. HeLa cells were treated with IFN, TSA, or IFN+TSA for the indicated time, or first incubated with one drug for a period of 12 hours and then after washing out with the second drug, or maintained in the fresh medium (f.m.) for the next 12 h as indicated for each column. The number of PML NBs per nucleus detected by PML antibody was counted on a total projection of confocal sections (1 section per 0.4 μm) through entire cell nucleus. n indicates the number of counted cells for each condition. Error bars represent standard error. Statistically significant differences to the control (untreated cells) are indicated by *** ($P < 0.001$).
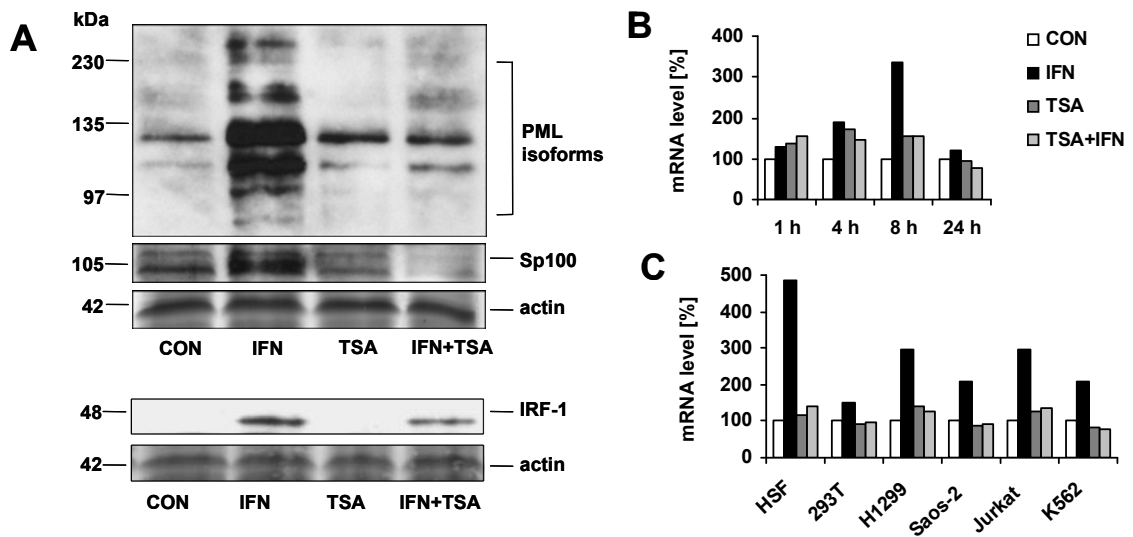
Fig. 15. TSA suppresses IFNα-induced PML transcription
(A) Western blot analysis of PML, Sp100 and IRF1 proteins in HeLa cells. Cell lysates (50 µg of total protein) were loaded on the SDS gels. Proteins were detected by the indicated antibodies; Coomassie- or Ponceau S- stained bands of actin were used as a loading control. (B,C) Real time RT-PCR quantification of PML mRNA. (B) HeLa cells were treated with 1000 U/ml interferon-α (IFN), 500 ng/ml trichostatin A (TSA) or both (IFN+TSA) for 1, 4, 8 and 24 hours. PML mRNA levels were normalized to GAPDH; the same results were obtained using other two control genes - actin and 18S rRNA (not shown). (C) Various cell lines were treated with IFN, TSA or IFN+TSA for 8 hours and PML mRNA was quantified by real time RT PCR relatively to GAPDH.
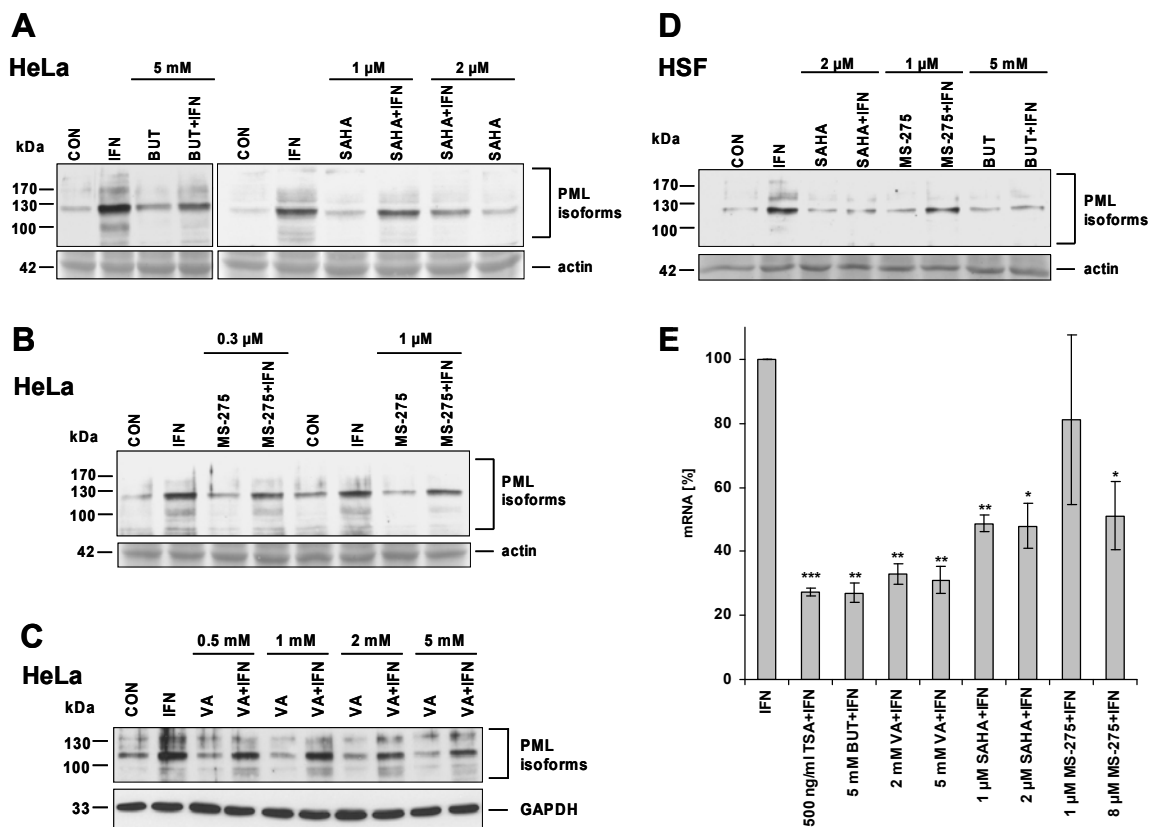
Fig. 16. HDAC inhibitors differ in their ability to suppress IFNα induction of PML

Western blot analysis of PML protein levels in HeLa (A, B, C) or HSF cells (D) simultaneously treated for 24 hours with IFNα and one of the following HDAC inhibitors: sodium butyrate (BUT), valproic acid (VA), SAHA, or MS-275. The final concentrations of the inhibitors are indicated. Cell protein lysates (25 μg of total protein) were loaded on 8% SDS gels (actin band of Ponceau S-stained membrane or GAPDH signal are shown to demonstrate equal loading). (E) Real time RT-PCR quantification of HDAC inhibitors' suppression of IFNα-induced PML mRNA. HeLa cells were treated with 1000 U/ml IFNα alone or simultaneously with a particular HDAC inhibitor for 8 hours. PML mRNA levels were normalized to GAPDH. Statistically significant differences compared to the IFNα-treated cells are indicated by *** ($P < 0.001$), ** ($P < 0.005$), or * ($P < 0.05$); three independent experiments were evaluated. Error bars represent standard error.
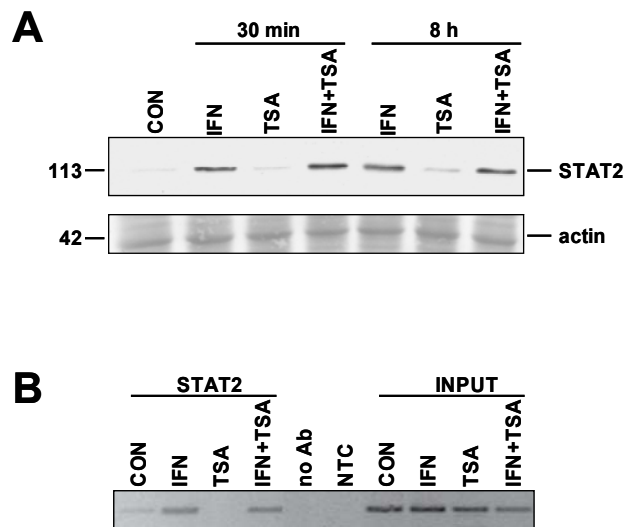
Fig. 17. TSA does not affect IFNα-induced translocation of STAT2 to nucleus and STAT2 binding to PML promoter
(A) Western blot analysis of STAT2 in nuclei of HeLa cells treated with 1000 U/ml IFNα, 500 ng/ml TSA, or both simultanously for either 30 minutes or 8 hours. Nuclear extracts (25 μg of total protein) were loaded on 8% SDS gels (Ponceau S stained band of actin is shown for equal loading). (B) Chromatin immunoprecipitation using STAT2 antibody and PCR amplification of PML promoter region containing ISRE element (located at +606 to +618 after the most 5′ major transcription start). To exclude unspecific binding to G-Sepharose beads we performed ChIP in the absence of the antibody (no Ab). The negative nontemplate control (NTC) reaction excluded unspecific PCR amplification. Cells were treated with the indicated drugs for 8 hours.

5.3 Experimental part III

5.3.1 Introduction

PML bodies are present in cells with different tissue origins, but PML protein level is diminished in most types of human tumors. This suggests different regulation of PML gene expression in tumor cells [31]. Nevertheless, most of *in vitro* studies on PML and PML bodies have been carried out on immortalized aneuploid cell lines with compromised ability to regulate their growth. This encouraged us to study PML bodies and protein on a model of normal diploid human mesenchymal stem cells - pluripotent precursor cells, which readily proliferate but also retain the ability to differentiate [191].

The nucleolus represents a structure that under optimal growth conditions supports cellular growth, and under the stress it mediates interactions of proteins with growth-regulating function. Therefore, any change in nucleolar structure or activity has a profound impact on the overall cell metabolism. Until recently, no link between PML and the nucleolus has been suggested. However, it could be expected that PML might be affected by or might affect nucleolar functions, similarly to tumor suppressors p53 and pRb, which are targeted to the nucleolus upon certain conditions and modulate rDNA transcription [113]. Indeed, a possible connection between PML and nucleolar proteins is now slowly emerging. It was reported that PML accumulates in the nucleolus upon inhibition of proteasomal degradation [245], and it was shown that upon extensive DNA damage PML relocalizes to the nucleolus where it sequesters MDM2 and thus blocks its interaction with p53 [50].

Here, we describe that PML associated with nucleoli upon standard growth conditions as well as after rRNA synthesis inhibition in human mesenchymal stem cells and human diploid fibroblasts. Moreover, PML binding to the nucleolus was enhanced in replicatively senescent hMSC. This association was severely diminished in transformed cell lines with various defects in the p53 and pRb tumor suppressor pathways, such as HeLa, H1299, SaOS-2, U-2 OS and A549. Intriguingly, in HeLa cells, PML association with the nucleolus was restored by long-term exposition of cell to 5-bromodeoxyuridine and distamycin A. This treatment causes premature cellular senescence accompanied by reactivation of the p53 and pRb tumor suppressor pathways [176,183]. Based on these data, we propose that in normal human cells or in senescent tumor cells PML responds to changes in the transcriptional activity and structure of the nucleolus by translocation to the

nucleolar surface and that this association could be important for the tumor suppressor activity of PML.

5.3.2 Results

Characterization of human mesenchymal stem cells as a model for PML studies.

To determine PML protein expression and localization in hMSC, we immunostained exponentially growing, confluent and differentiated hMSC with monoclonal antibody against human PML protein [246]. Similarly to other cell types [57], PML protein was found in hMSC both free in nucleoplasm and bound in PML bodies **(Fig. 18A)**. Although the number of PML bodies ranged from 10 to 70 per nucleus, the average numbers of PML bodies in confluent hMSC were dependent on the proliferation age of the culture. We found a strong positive correlation between PML NBs number and the passage number (during each passage, cells were split 1:3). The average number of PML NBs per cell in early passage cultures (P5), middle passage cultures (P10), and in late passage cultures (P18, reflecting terminal senescent state) was 13.9 ± 4.67 s.d., in 24.4 ± 7.12 s.d. 34.6 ± 11.22 s.d., respectively **(Fig. 18C, Fig. 19)**. This number of PML bodies was 3 times higher than was reported for HeLa cells [57]. Interestingly, the number of PML bodies seemed to be lowered in hMSC differentiated into adipocytes **(Fig. 18B)**, but the precise evaluation was not done due to substantial change of nuclear shape by accumulated lipid droplets. Ultrastructurally, PML bodies appeared as electron dense areas positively labeled with anti-PML antibody **(Fig. 18D, E)**, which is in agreement with previous reports [3].

It was well documented that *PML* gene expression in immortalized cell lines is stimulated by interferons [12,16]. To confirm this effect of interferons (IFN) on *PML* expression in hMSC, we compared mRNA and protein PML levels in control and IFNα-treated hMSC. Indeed, levels of *PML* (all isoforms) mRNA were increased compared to controls more than 4 times after 6 hours and 2.5 times after 24 and 48 hours of 1000 U/ml IFNα treatment **(Fig. 18F)**. PML protein levels followed closely mRNA levels, i.e. they were upregulated after 4-hour of IFNα treatment and peaked around 6 hours. But then, differently to mRNA, protein levels remained stable for up to 24 hours **(Fig. 18G)**. However, average number of PML bodies increased only about $18\% \pm 6.8$ s.d. suggesting that the newly synthesized PML protein was targeted mainly into original PML bodies.

This is in contrast to HeLa cells where IFN-treatment substantially increases number of PML bodies [14].

Together, these results show that growing, confluent or terminally differentiated hMSC readily express PML protein, which is targeted to PML bodies. Number of PML bodies per cell nucleus is dependent on the culture proliferative age.

PML forms donut-like structures that surround material of nucleolar origins.

Besides typical PML bodies, we noted presence of small PML bodies positioned on the surface of nucleoli as confirmed by 3-D reconstruction of nucleus using composite image from serial confocal sections **(Fig. 20A, B)**. This observation was made in 0.79% of early culture cells (P5), in 15.9% of middle culture cells (P12), and in 36.48% of senescent cells (P18). Although PML translocation to the nucleolus was previously described in cells treated with proteasome inhibitors and DNA damage inducing doxorubicin [50,245], to the best of our knowledge, this was for the first time, when PML was found in close connection with the nucleolus under standard growth conditions.

Moreover, in 1% of confluent middle passage hMSC (P12), we observed large donut-like PML bodies. PML protein in these large bodies colocalized with Sp100, SUMO-1 **(Fig. 20C,D)** and Daxx (data not shown) - proteins considered as PML bodies' markers [38,45,247]. The 3-D shape of these structures was either a sphere or an open barrel (as determined by 3-D reconstruction of nucleus using composite image from serial confocal sections). Intriguingly, donut-like PML bodies were often positioned close to nucleoli. Analysis of 78 PML donut-like bodies found in cells kept under standard growth conditions showed that 40 of them (i.e. 51%) were in close contact with the adjacent nucleoli as detected by confocal microscopy allowing the resolution of 0.2 μm. Additional 33% of donut-like bodies were detected within the 2 μm distance from the closest nucleolus, while the maximal distance of PML donut-like body from the nucleolus was 8 μm The distance from the closest nucleolus did not appear to be dependent on the size of the particular PML donut-like bodies (ranging from 0.9 to 5.02 μm, **Fig. 21**).

The relationship of these structures to nucleoli was further assessed by the detection of nucleolar proteins typically not observed in PML NBs. B23, the protein known to accumulate in granular component (GC) of the nucleolus [248], was found inside of all donut-like PML bodies **(Fig. 20E)**. Notably, B23 was often more concentrated within this donut-like PML body than in the adjacent nucleolus **(Fig. 20J)**. In 28.5% of donut-like PML bodies, UBF and RNA polymerase I [249,250] was found in one or two spots reminiscent of

fibrillar centers (FC) of the nucleolus (**Fig. 20F,** [141]). Moreover, in many instances we observed the structural continuity between nucleolar compartment and donut-like PML nuclear body appearing as a "bud" of the nucleolus (see **Fig. 20F, G**) when FCs and dense fibrillar component (DFC) were detected both at the base of such a bud, i.e. inside the donut-like PML body, and within the bud neck. In addition, FCs inside PML donut-like bodies were transcriptionally competent as determined by run-on transcription assay with 5-BrUTP in living cells **(Fig. 20I)**. Interestingly, another protein occasionally concentrated within the donut-like PML structure was nuclear DNA helicase II (NDHII, **Fig. 20H**) that is otherwise found mainly in nucleoplasm while in the nucleolus it is much less concentrated [219]. On the contrary to the "regular" PML NBs **(Fig. 20E, 22B)**, the donut-like PML bodies appeared ultrastructurally as an electron dense material resembling granular component of the nucleolus, which is encircled by a layer of positive PML labeling **(Fig. 22)**. Altogether, these findings show that PML protein interacts with proteins or nucleic acids on the nucleolar surface and it can surround large structures containing typical nucleolar proteins, which we therefore term as *PML-nucleolus-derived structure* (PML-NDS) in further text.

PML is attracted to segregated nucleoli.

Next, we were searching for conditions favoring formation of PML-NDS. Because it is known that PML negatively affects cellular proliferation, we thought that the assembly of PML-NDS could be an indication of decreased nucleolar activity. Therefore, we tested whether PML-NDS could be induced under the conditions inhibiting nucleolar activity and cellular growth. However, serum starvation (0.2% FBS for 2 and 10 days), which negatively affects Pol I-dependent transcription [149] and leads to growth arrest, did not induce PML-NDS formation in hMSC (not shown). Also treatment with rapamycin (20 and 100 nM) that blocks mTOR pathway [251] and consequently the initiation of rDNA transcription [146,252] failed to induce PML-NDS assembly (not shown).

To block rRNA synthesis more efficiently, we treated hMSC with actinomycin D (AMD) for 24 hours at concentrations that were shown to specifically inhibit Pol I-dependent transcription (5 to 40 nM) and that lead to the nucleolar segregation defined as separation of fibrillar and granular components [137,138]. To confirm similar sensitivity of hMSC to low doses of AMD, we performed run-on transcription assay in the presence of 10 nM AMD that revealed unaffected Pol II transcription, while nucleoli were inactive **(Fig. 23)**. Thus the conditions used for experimental block of Pol I did not affect Pol II

activity in hMSC.

Intriguingly, PML frequently encircled (partially or completely) segregated nucleoli in 14.8 and 15.8% cells treated with 5 and 40 nM AMD, respectively, compared to untreated cells where we did not observe such structures at all **(Fig. 24)**. When the cells were exposed to IFNα prior AMD treatment, the fraction of cells with PML encircling segregated nucleoli was further increased up to 31.5% **(Fig. 24B)**. Composition of these structures was similar but not identical to PML-NDS and therefore we will further call them *actinomycin-induced PML nucleolar coats* (APNCs). In detail, PML was found on the surface of segregated GC containing B23 protein together with FC and DFC segregated into nucleolar caps **(Fig. 25A-D, F)**. Differently to PML-NDS, NDHII was excluded from segregated nucleoli with APNCs **(Fig. 25E)**. On the ultrastructural level, we detected PML protein within an electron dense shell that was positioned around the segregated nucleolus **(Fig. 26G,H)**.

Thus, PML may not only interact with the transcriptionally active nucleolus but it also binds to the surface of AMD-inhibited nucleoli. However, the absence of NDHII from inactive nucleoli suggests that PML association with segregated nucleoli is functionally distinct from PML-NDS where NDHII is concentrated.

Translocation of PML to segregated nucleoli is a dynamic and reversible process.

We followed the dynamics of PML translocation to the surface of segregated nucleolus in a time-course experiment. Detectable levels of PML were found on the surface of the nucleolus soon after the onset of its segregation, i.e. within 2 to 4 hours of AMD treatment. APNCs remained stable during entire 24 hour-experiment **(Fig. 26A)**. To determine whether PML translocation towards nucleoli was reversible, the cells were first treated for 2 hours with 10 nM AMD, then extensively washed, and allowed to resume rRNA synthesis in the absence of AMD for 2, 4, 6, and 22 hours **(Fig. 26B)**. Two hours after the AMD removal nucleoli remained segregated and APNCs were even more compact. After 4 hours in the absence of AMD, nucleolar activity was partially restored (seen as an increase in FCs number) and a "breakage" of APNCs into two half-moon-like structures was often observed. Intriguingly, 6 hours after AMD removal, many APNCs were rearranged into structures very similar to PML-NDS, although they contained usually more than one FC. Finally, after 22 hours, APNCs disappeared while many PML-NDS with up to 2 fibrillar centers were present. The increased frequency of cells with PML-NDS compared to control cells was substantial as shown in **(Fig. 26C)**. To support the

hypothesis about transition of APNCs into PML-NDS we analyzed at least 50 PML nucleolar structures in each time point of AMD wash-out. Then we assigned each PML structure to one of four categories- a) APNCs; b) Type I (i.e. PML is located on the surface of nucleoli, FCs become separated and activated); c) Type II (i.e., PML surrounds portion of nucleolar material that is partially but not completely detached from the maternal nucleolus); d) PML-NDS. Distribution of individual forms is shown in **Fig. 26B**. There was a clear trend towards the formation of PML-NDS while intermediate forms were disappearing with increasing time after AMD wash-out.

Altogether, PML binds to the nucleolar surface when rRNA synthesis is blocked. Moreover, it appears that PML nucleolar coats may convert into PML-NDS upon restoration of rRNA transcription.

Association of PML with nucleoli is diminished in tumor-derived cells.

To determine whether PML interaction with nucleoli is common for different cell lines or whether it is cell type specific, we examined human skin fibroblasts, HeLa, U-2 OS, A549, SaOS-2 and H1299 cell lines. Similarly to hMSC, the presence of PML-NDS and formation of APNCs was observed in normal skin fibroblasts. However, both structures were absent in HeLa, U-2 OS, A549 **(Fig. 27A)** and were observed only rarely in SaOS-2 cell lines (PML-NDS in 0.4% of cell population) and in H1299 cells (PML-NDS in 0.4% and APNCs in 0.2% of cell population) (data not shown). In fact, the formation of APNCs in the tested cell lines could not be induced even by high doses of AMD (up to 500 nM, not shown).

To test the possibility that these cell lines cannot form PML-NDS or APNCs due to a low PML expression, we first treated them with 1000 U/ml IFNα for 18 hours to stimulate PML protein synthesis. Regardless of increased PML protein levels, we did not observe formation of PML-NDS or APNCs in HeLa and we detected these structures only rarely (0.4% of cell population) in U-2 OS and A549. Remarkably, IFNα treatment induced formation of both PML-NDS (2.9%) and APNCs (6.7%) in SaOS-2 cells (**Fig. 27A** and data not shown).

Together, PML association with the nucleolus is severely diminished in tumor-derived cell lines but in some cases it can be partially rescued under condition of IFNα-induced PML overexpression. Since the high and deregulated nucleolar activity is general characteristics of most tumor cells, this finding suggests that PML binding to the nucleolus is inversely related to the activity of the nucleolus. Moreover, the difference in PML

affinity to the nucleolus between normal and tumor cells also suggests that the tumor suppressor pathways inactivated in immortal cells might be important for the formation of the PML nucleolar compartment.

Induction of premature cellular senescence restores PML nucleolar association in tumor-derived cells.

To activate both p53 and pRb tumor suppressor pathways, we challenged HeLa cells simultaneously with 5-bromodeoxyuridine (5-BrdU) and distamycin A (DMA). This combined treatment promotes an expression of senescence-associated genes such as *pRb, p53, p21*$^{waf/sdi-1}$ and *p16*^{ink4a} and induces apoptosis and cellular senescence even in transformed cell lines [176,183]. Remarkably, after 1-week treatment with 10 μM 5-BrdU and 10 μM DMA, the surviving HeLa cells restored the ability to form either PML-NDS or APNCs **(Fig. 27C, 21B)**. At the same time, they exhibited increased p53, p21 and hypophosphorylated pRb protein levels and increased SA-ß-galactosidase activity **(Fig. 27B, 28A)**. Comparably, this treatment in hMSC led to the block of proliferation before cells reached the confluence, and after 3 weeks, it also strongly augmented the formation of PML-NDS (not shown). Moreover, replicatively senescent hMSC (P18) exhibited increased numbers of PML-NDS (4.9%) and PML nucleolar staining (36.4%). Our data suggest that activation of either p53 or pRb pathways with accompanying changes of cellular physiological status (cellular senescence) restore the ability of PML to associate with the nucleolus.

To verify it, the same experiment was performed on U-2 OS, H1299 and SaOS-2 cells, which bear various defects (i.e. partial or complete deletion) in tumor suppressors (Tab. 2). In H1299 cells with deletion of *p53* gene, 5-BrdU/DMA-treatment induced senescent phenotype (as assessed by senescence-associated β-galactosidase staining; not shown) and the occurrence of PML-NDS or APNCs were elevated in comparison to untreated cells **(Fig. 27C)**. SaOS-2 cells, which bear defects in both p53 and pRb, were massively dying upon the 5-BrdU/DMA-treatment and thus were not examined for PML association with the nucleolus. Intriguingly, no PML-NDS or APNCs were observed in surviving U-2 OS cells after 1-week treatment with 5-BrdU/DMA. Moreover, U-2 OS also did not show typical senescence-associated β-galactosidase staining (not shown).

Altogether, these data indicate that only tumor cells sensitive to induction of premature senescence by genotoxic stress are able to restore the PML nucleolar compartment. In addition, the observation made on H1299 cells treated with 5-BrdU/DMA

indicates that functional p53 is not necessary for senescence-induced PML association with the nucleolus.
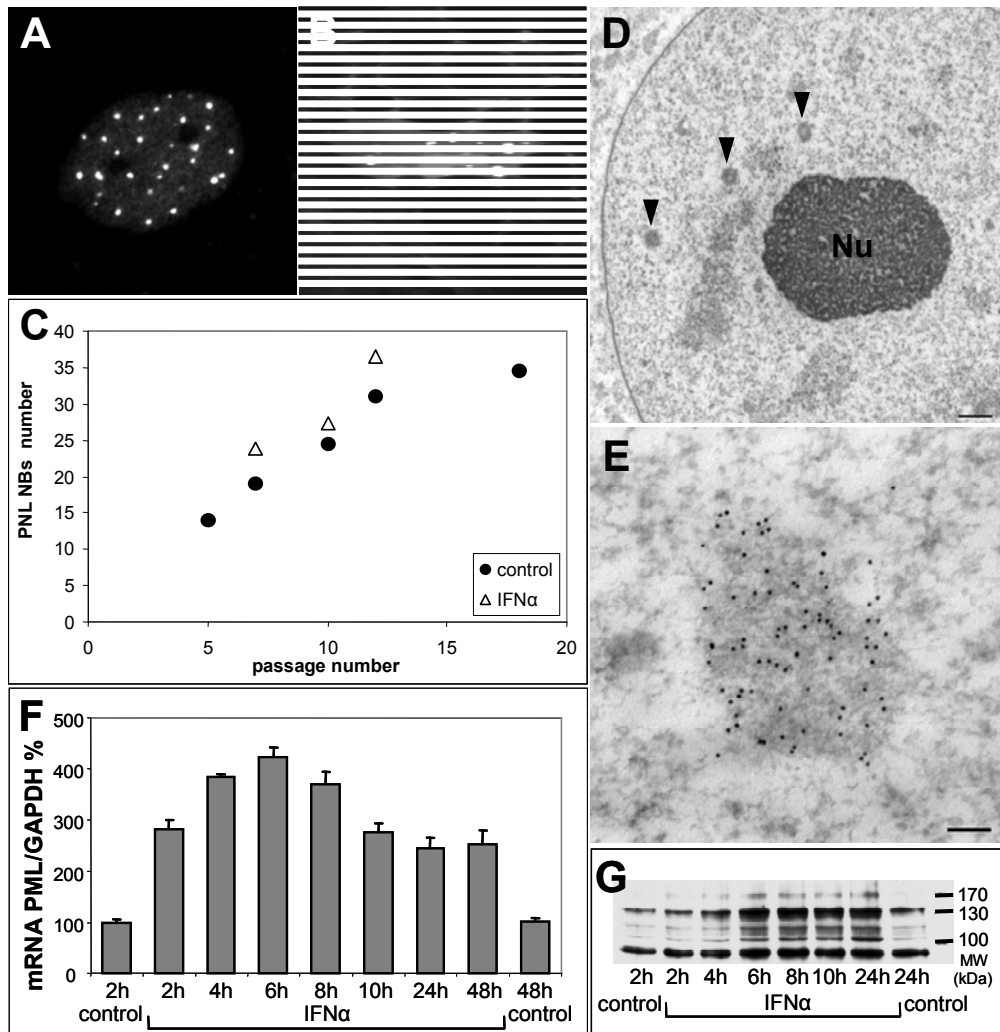
Fig. 18. PML is expressed in proliferating, differentiated and aging hMSC and is upregulated in response to IFNα.
Indirect immunofluorescence detection of PML bodies in confluent hMSC (A) and in hMSC differentiated into adipocytes (B). PML bodies were visualized by anti-PML (PG-M3) antibody (white), RNA by TOTO3 (gray). Lipid droplets are negatively stained with TOTO3. Bar, 2 μm. (C) Relationship between the PML NBs number and the age of hMSC. hMSC of indicated passage grown in standard medium or treated for 24 hours with 1000 U/ml IFNα were examined for PML NBs number by immunofluorescence. At each passage, PML NBs were counted in at least 50 cells. Average numbers of PML NBs are shown. (D) Electron micrograph of hMSC nucleus. PML bodies appeared as electron-dense structures (arrowheads) that were recognized by rabbit antibody against PML and visualized by secondary antibody conjugated with 12 nm gold particles (E). Bars, 1 μm for (D) and 100 nm for (E). (F) Quantification of PML mRNA levels. mRNA levels were upregulated already after 2 hours, reached the peak value after 6 hours and remained elevated for 48 hours of IFNα treatment. PML mRNA levels were measured by qRT-PCR and normalized to GAPDH in 2 independent experiments, error bars represent s.d. (G) Immunoblot analysis of PML expression in confluent hMSC. PML expression was induced by 1000 U/ml IFNα for indicated times.
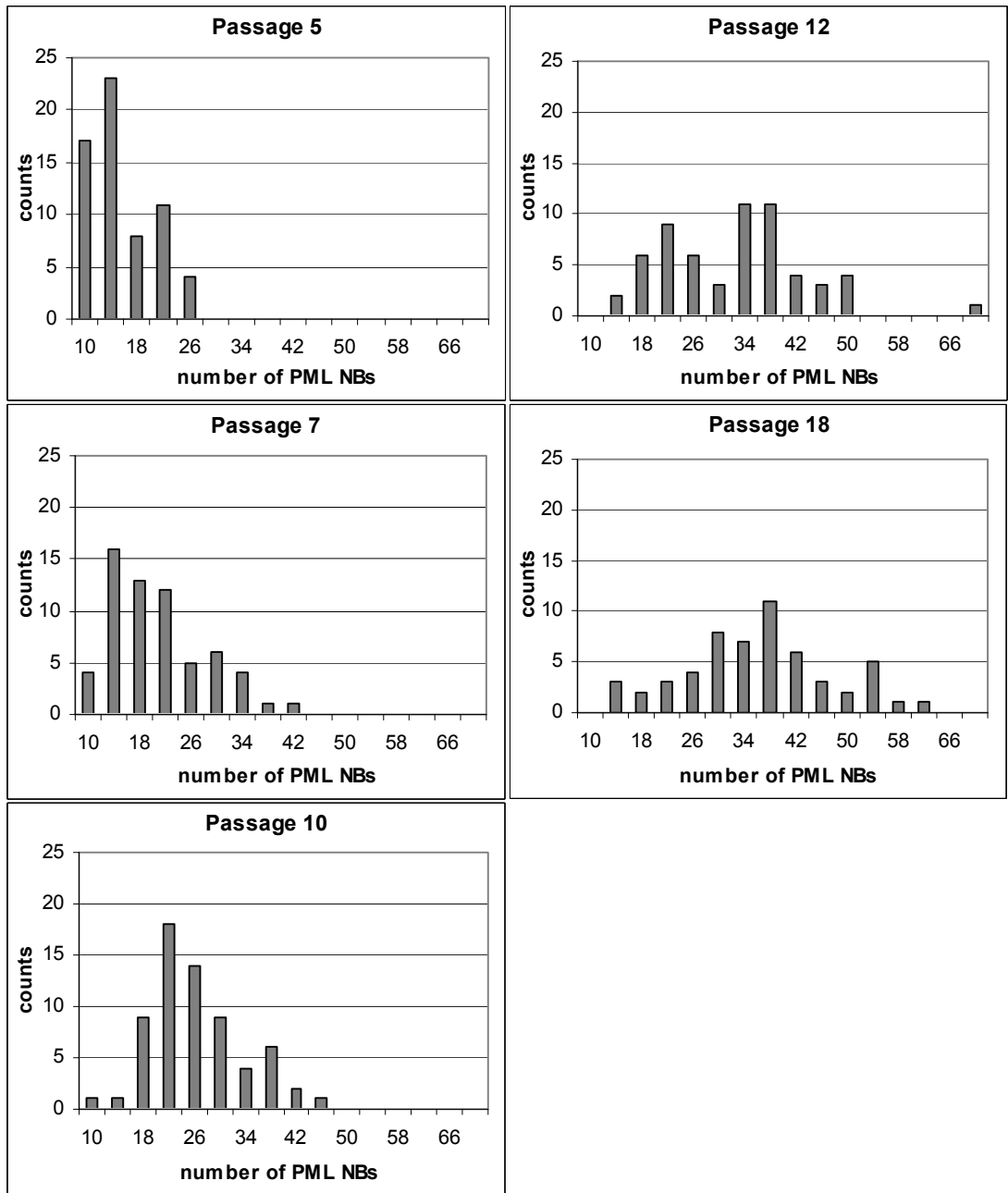
Passage 5

Passage 12

Passage 7

Passage 18

Passage 10

Fig. 19. Number of PML NBs is dependent on the replicative history of hMSC.
Sorted histograms showing frequency distribution of PML NBs per nucleus are based on the same experiment as shown in Fig. 18C. Briefly, PML was visualized by immunofluorescence and PML NBs were counted in at least 50 cell nuclei over several passages.
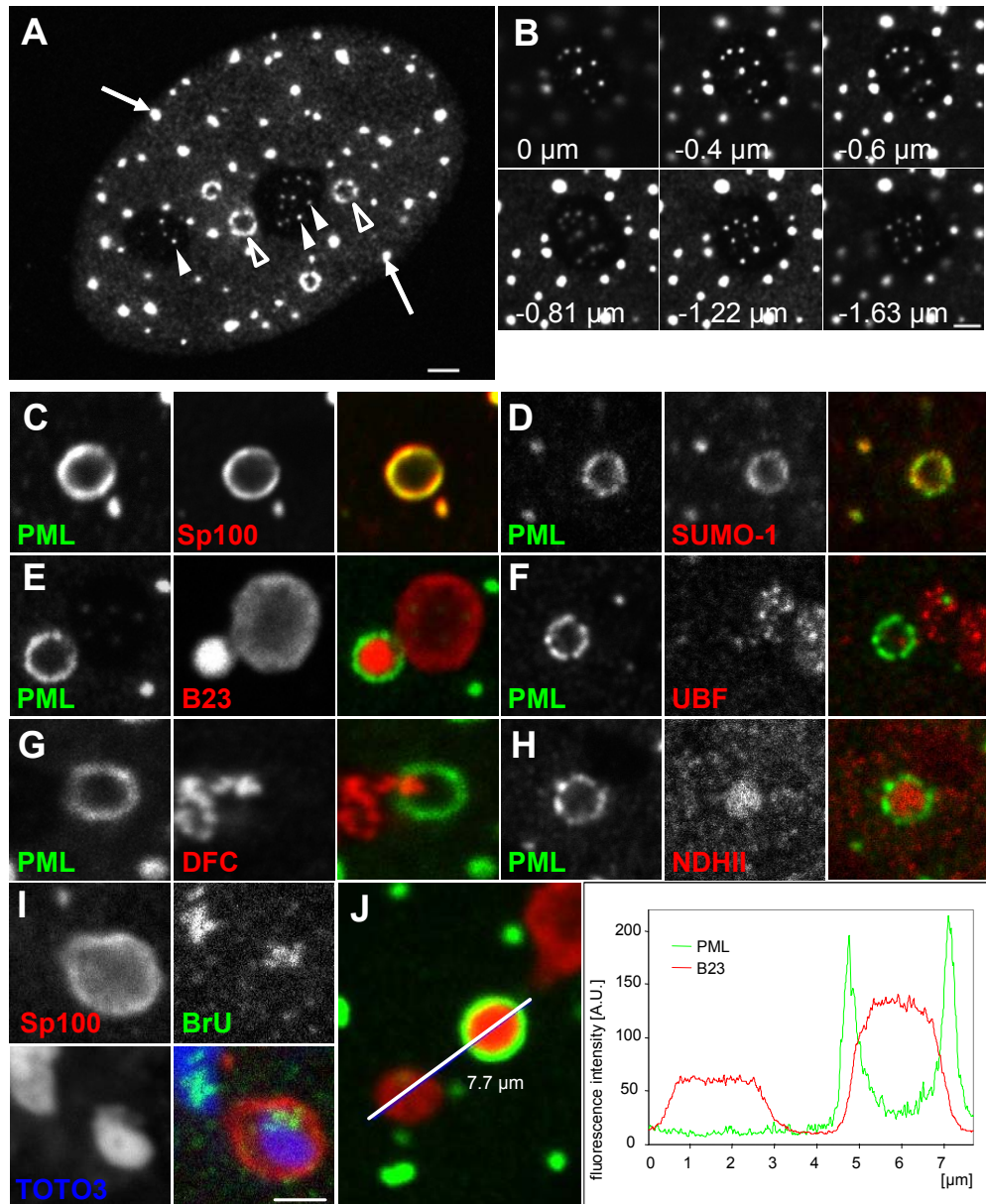
Fig. 20. PML associates with the nucleolus and nucleoli-derived structures in hMSC grown under standard conditions.
(A) Indirect immunofluorescence detection of PML in confluent hMSC. Cells were fixed and stained with anti-PML (PG-M3) antibody. Note small PML bodies on the surface of the nucleoli (full arrowheads). Open arrowheads point to nucleoli-derived structures that were encircled by PML protein (PML-NDS), arrows point to standard PML bodies. (B) Serial sections of the nucleus show the distribution of small PML bodies preferentially on the surface of the nucleolus. (C-J) PML-NDS composition: PML-NDS are similar but not identical to nucleoli. PML-NDS were visualized by indirect immunofluorescence using antibodies against two markers of PML bodies: Sp100 (C) and SUMO-1(D). Localization of PML-NDS and three nucleolar domains - GC, FC, DFC, and NDHII is shown (E-H). Merged images are shown in color. (I) *In vitro* transcription in PML-NDS. rDNA genes within PML-NDS were transcriptionally competent, i.e. nascent transcript containing BrU incorporated during run-on assay were detected by anti-BrdU antibody and are shown in green, Sp100 in red and TOTO3 in blue. (J) Profile of B23 and PML fluorescence intensity within nucleolus and PML-NDS. hMSC were stained as in (E), intensity of fluorescence for B23 is shown in red, PML in green. Note that B23 protein was concentrated within PML-NDS. Bars A-I, 2 µm.
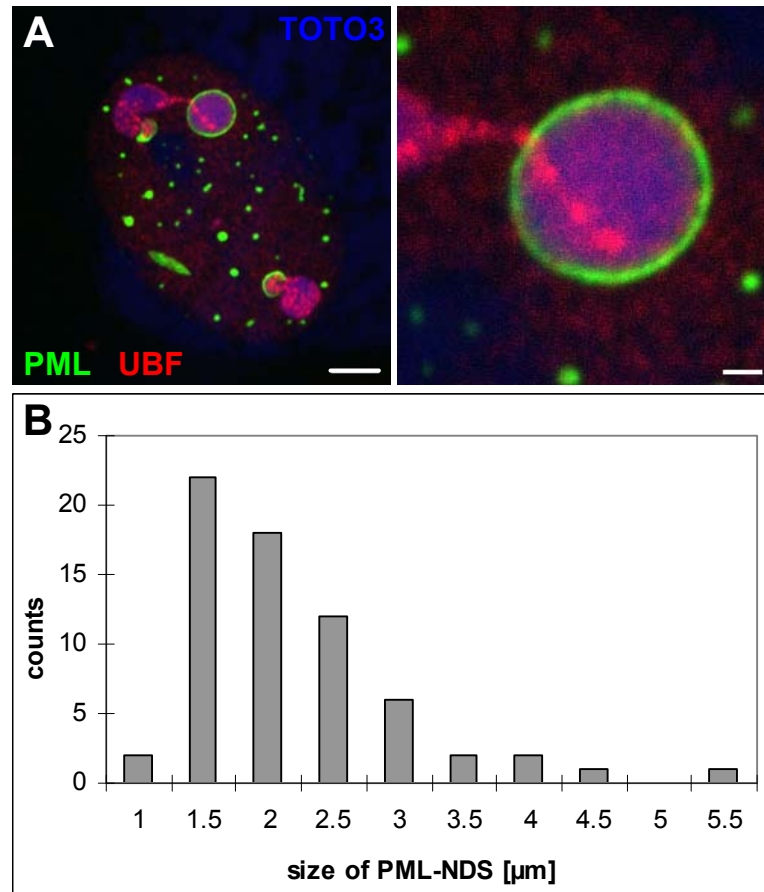
Fig. 21. PML-NDS reach the size up to 5 µm in diameter.
A. Confluent hMSC were fixed and PML-NDS were visualized by indirect immunofluorescence using antibodies against PML (PG-M3, green) and UBF (red). RNA stained by TOTO3 is shown in blue. Bars, 5 and 1 (inset) µm. B. Sorted histogram showing the size distribution of PML-NDS in confluent hMSC. For this dataset, 66 PML-NDS were visualized by immunofluorescence (using antibodies against PML and UBF and TOTO3 staining), scanned and analyzed using Leica software.
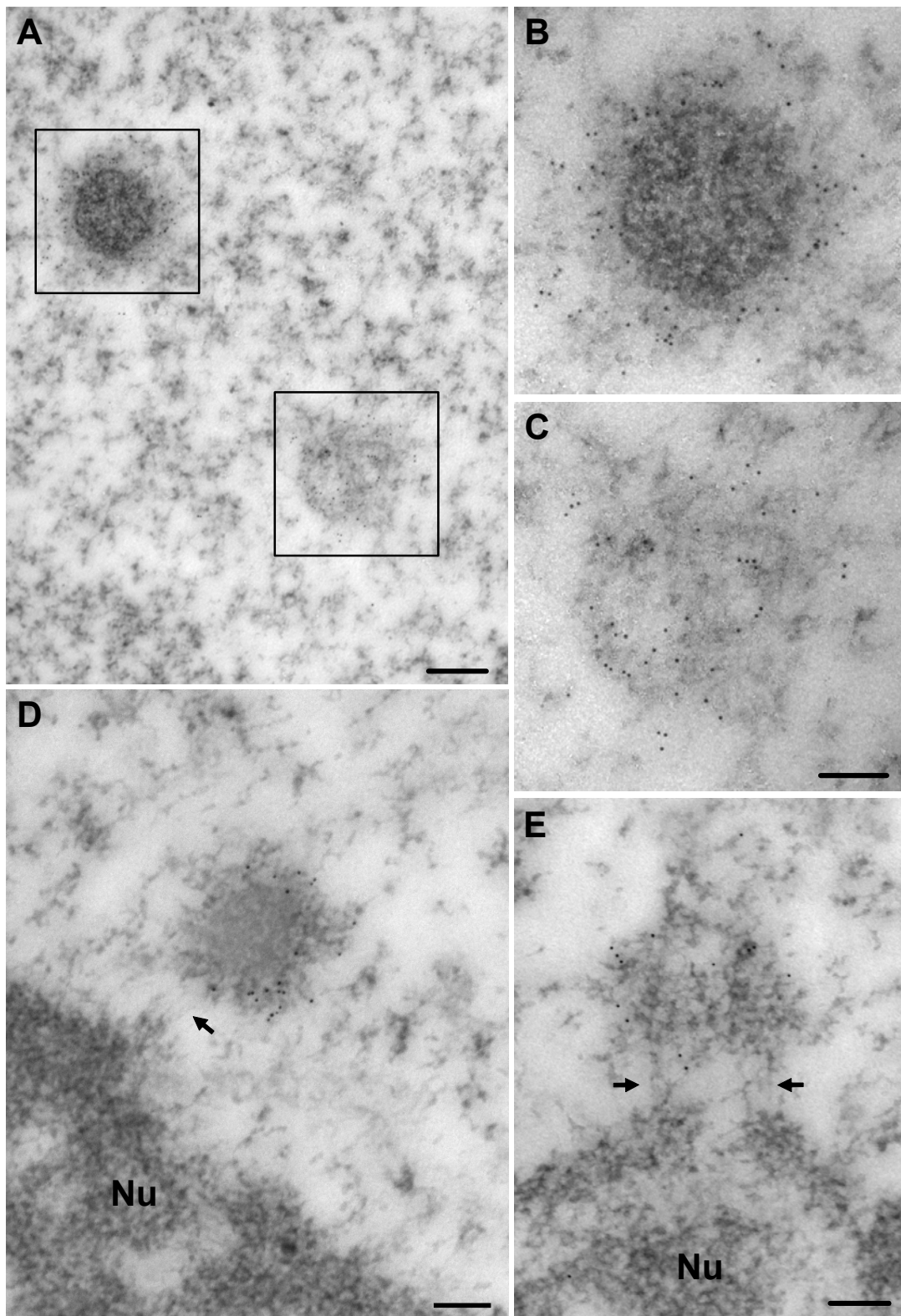
Fig. 22. Donut-like PML bodies differ from regular PML bodies on the ultrastructural level.
PML protein was detected by rabbit antibody against PML and visualized by secondary antibody conjugated with 5 nm gold particles. (A) Two PML bodies are shown; the upper one represents the donut-like body (also shown in B) and the lower one the regular PML body (also shown in C). (D,E) The donut-like PML body adjacent to the nucleolus (Nu). Note the fibrils connecting the nucleolus with the donut-like PML body (arrows). Bars, 200 nm for (A), 100 nm for (B-E).

Fig. 23. Transcription activity of AMD-treated hMSC.
In vitro transcription assay in control cells and cells treated for 18 hrs with low (10 nM) and high doses (100 nM) of AMD. Note, that cells t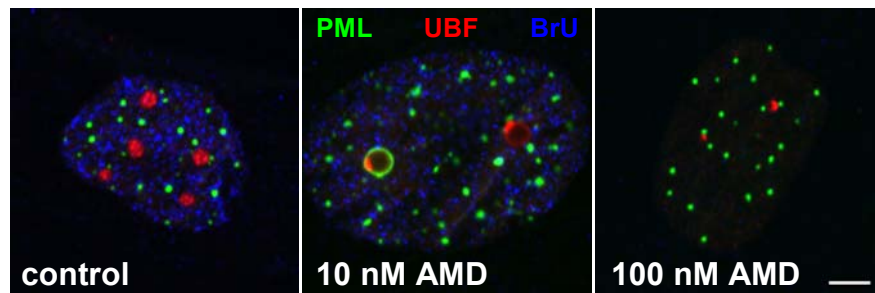reated with 10 nM AMD have inactive segregated nucleoli (UBF, red) while they still incorporate BrU into nascent Pol II transcripts (BrU, blue). Bar, 2 μm.
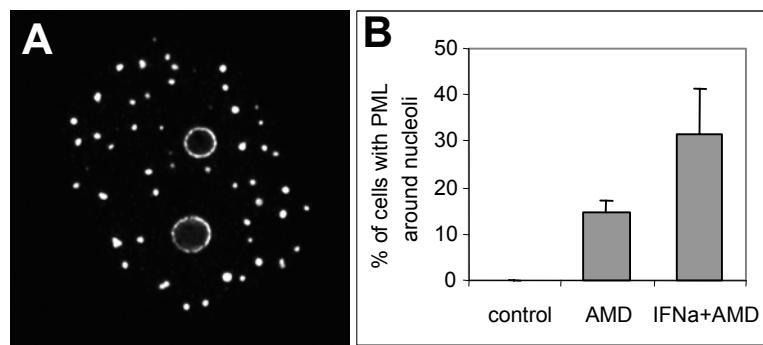
Fig. 24. PML associates with segregated nucleoli in hMSC cells.
(A) Indirect immunofluorescence detection of PML structures in confluent hMSC that were treated with 5 nM actinomycin D for 24 hours. After fixation, cells were stained with anti-PML (PG-M3) antibody. (B) Induction of PML aggregation on the surface of segregated nucleoli. Control cells or cells pretreated with 1000 U/ml IFNα for 18 hours were exposed to 5 nM actinomycin D for next 24 hours. For scoring, cells were stained with PG-M3 and UBF antibodies. 500 cells were scored in 3 independent experiments, error bars represent s.d.

81
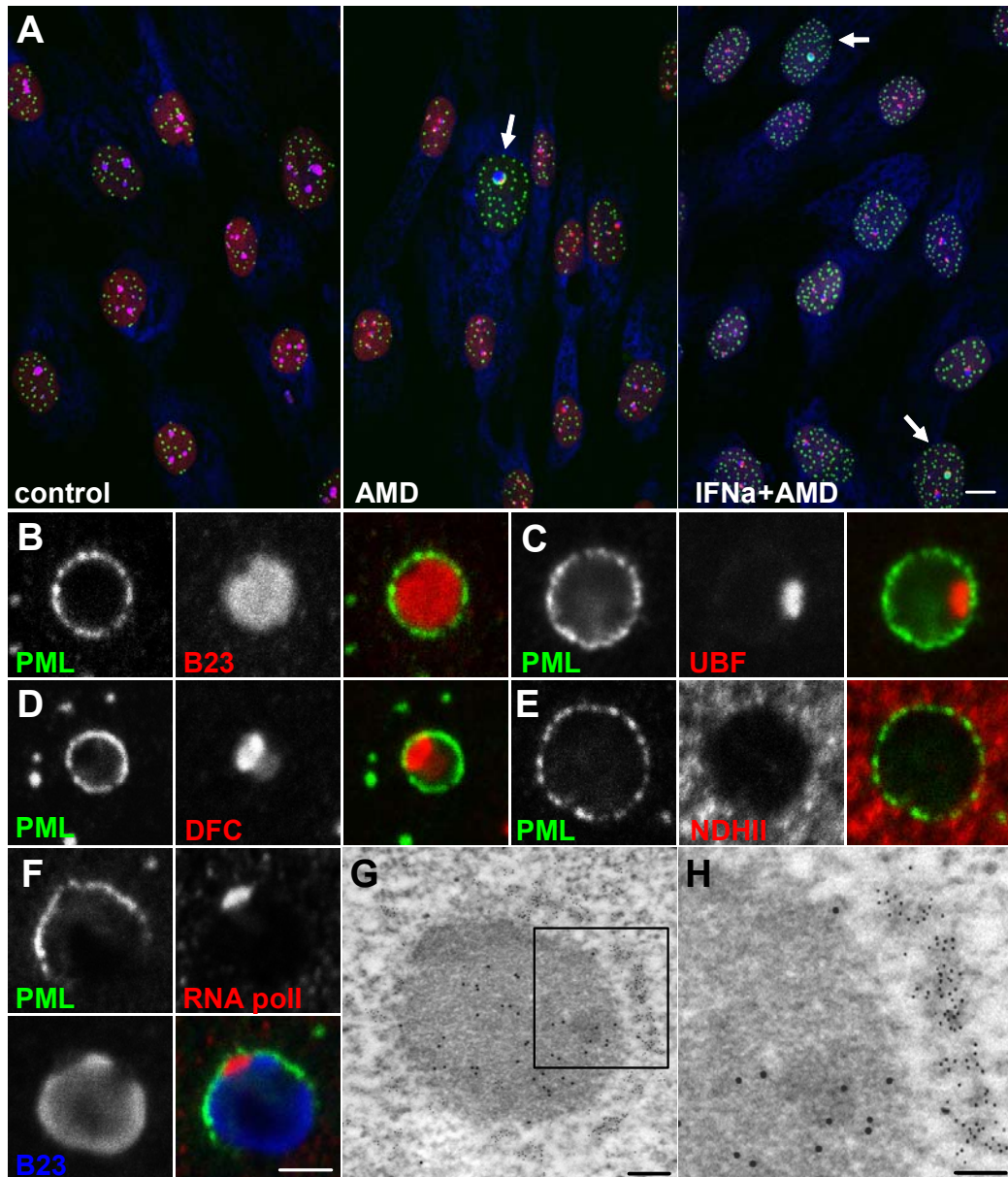
Fig. 25. AMD inhibition of PolI transcription causes formation of PML nucleolar coats.
(A) Representative images of control cells, cells exposed for 24 hours to 10 nM AMD without or after IFNα 24 hour-pretreatment. PML is shown in green, UBF in red, TOTO3 in blue, cells with PML nucleolar coats are highlighted by arrows. Bar, 10 μm. (B-E) Localization of PML and markers for GC, FC, DFC, and NDHII in actinomycin D inhibited nucleoli. Cells were stained with indicated antibodies. Merged images are shown in color. Note that NDHII was excluded from the segregated nucleolus. (F) Triple labeling of segregated nucleolus with RNA polI, B23 and PML antibody. Merged image is shown in color. Bars B-F, 2 μm. (G, H) Electron micrograph of APNCs. PML was labeled with rabbit PML antibody and secondary antibody coupled with 6 nm colloidal gold, GC compartment with anti-B23 antibody and secondary antibody conjugated with 12 nm colloidal gold. Bars, 200 nm in G, 100 nm in H.
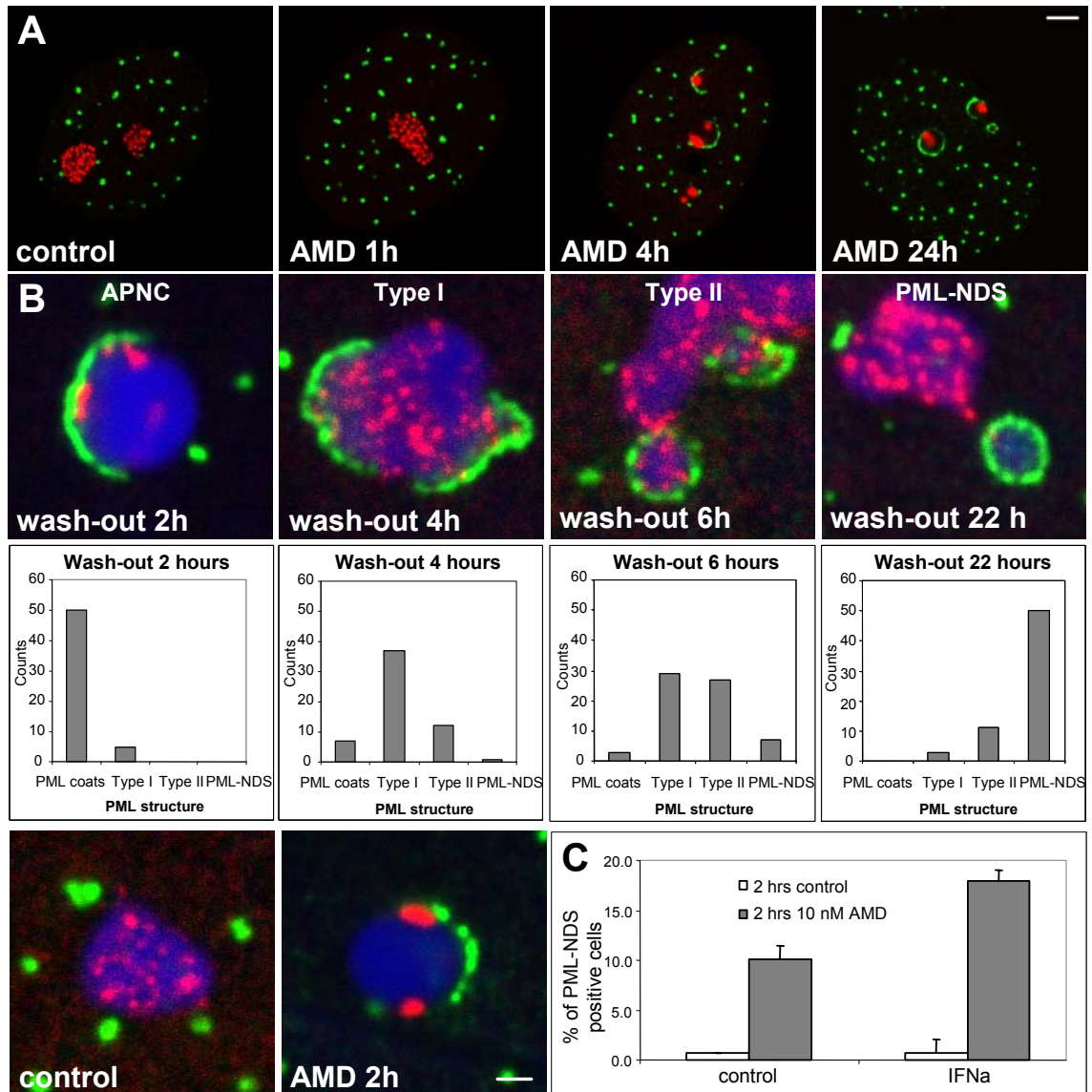
Fig. 26. PML association with the nucleolus is dynamic.
(A) Localization of PML and UBF during AMD treatment. hMSC were treated with 5 nM AMD and fixed at indicated times. PML (green) and UBF (red) were visualized with corresponding antibodies. Bar, 4 μm. (B) AMD wash-out experiment. hMSC were treated with 10 nM AMD for 2 hours, then washed and let to resume rRNA synthesis in the absence of AMD for specified times. Cells were then fixed and stained with anti-PML (green) and anti-UBF (red) antibodies. For quantification of different forms of PML associated with the nucleolus, at least 50 PML structures in each time point of AMD wash-out were analyzed and then assigned to one of four categories characterized by the image above. Bar, 1 μm. (C) Recovery of nucleolar activity after AMD wash-out induces the formation of PML-NDS. hMSC (control of pretreated with IFNα for 24 hours) were treated as in (Fig. 24B) and left to recover from AMD treatment for 22 hours. Then they were stained with anti-PML (PG-M3) and anti-B23 antibody and PML-NDS were counted. 500 cells were scored in 2 independent experiments. Error bars represent s.d.
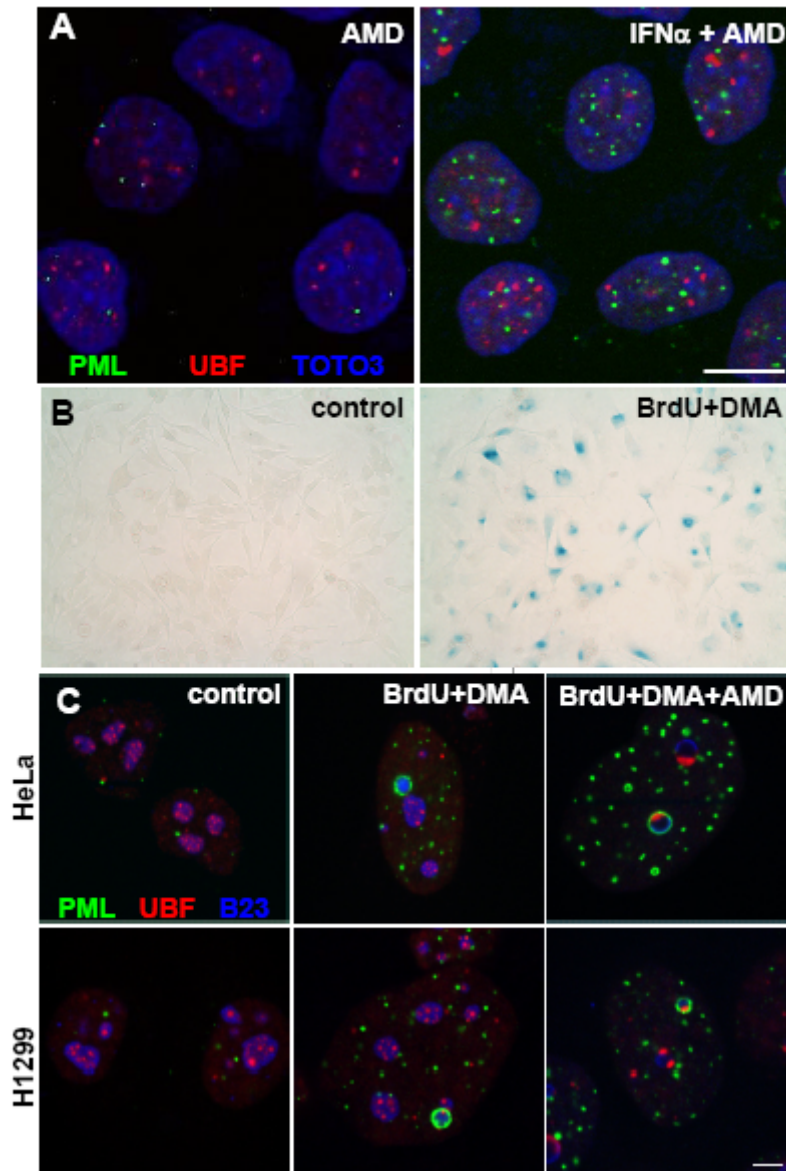
Fig. 27. PML does not associate with the segregated nucleolus in growing immortalized cell lines but this association is induced in prematurely senescent HeLa and H1299 cells.
(A) Indirect immunofluorescence detection of PML structures in HeLa. HeLa cells were treated with IFNα or vehicle for 24 hours, followed by treatment with 40 nM AMD for 24 hours. PML bodies were stained with anti-PML (PG-M3, green), FC with anti-UBF antibody (red) and RNA with TOTO3 (blue). Note that PML translocation to segregated nucleoli could not be induced in HeLa cells. Bar, 10 μm. (B) Model of BrdU and DMA-induced senescence. HeLa cells were treated with DMSO or 10 μM BrdU and 10 μM DMA for 6 days. Then, cells were fixed and stained to visualize SA-ß-galactosidase activity. (C) Indirect immunofluorescence detection of PML-NDS and APNCs in senescent HeLa and H1299 cells. Cells were treated with vehicle or 10 μM BrdU and 10 μM DMA for 6 days. For detection of APNCs, cells were treated with 5 nM AMD for the next 24 hours. Then PML, UBF and B23 were visualized with corresponding antibodies. Bar, 4 μm.
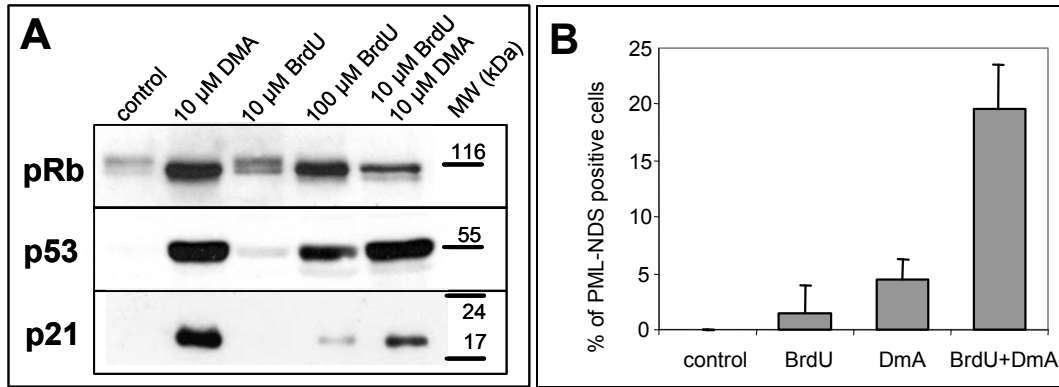
Fig. 28. BrdU and DMA-induced senescence is accompanied with elevated levels of tumor suppressor proteins and formation of PML-NDS.
(A) Immunoblot analysis of pRb, p53 and p21$^{waf/sdi-1}$ expression in prematurely-senescent HeLa. HeLa cells were treated as indicated for 6 days and then lysed. Note that anti-pRb antibody recognized both phosphorylated and hypophosphorylated pRb form. (B) HeLa cells were treated with 10 µM BrdU, 10 µM DMA or both for 6 days. Cells were then fixed, stained with anti-PML (PG-M3) and anti-B23 antibodies and PML-NDS were counted. For each condition, 100 cells were scored in 4 independent experiments. Error bars represent s. d.

Table 2. Characteristics of used cell lines with respect to the tumor suppressor expression.

Cell Line	pRb	ARF	p16	p53
U-2 OS	Expressed (wt)	No expression (methylated promoter)	No expression (methylated promoter)	Expressed (wt)
A549	Expressed (wt)	No expression (methylated promoter)	No expression (methylated promoter)	Expressed (wt)
H1299	Expressed (wt)	Expressed (wt)	No expression	No expression (deleted gene)
SaOS-2	No expression (mutant gene)	Expressed (wt)	Expressed (wt)	No expression (deleted gene)
HeLa	Inactivated by HPV-encoded E7	Expressed (wt)	Expressed (wt)	Inactivated by HPV-encoded E6

85

6 Discussion

The goal of this work was to extend current knowledge on the PML expression and behavior. Specifically, we focused on deciphering of the regulation of IFNα-induced transcription and on description of PML behavior in normal, tumor and senescent cells. To achieve these goals, we employed different *in vitro* models that we had to characterize first.

6.1 hMSC as a model for human adipogenesis

To characterize process of terminal differentiation of human cells we focused on adipogenic conversion of human mesenchymal stem cells. The regulation of terminal differentiation of adipocyte precursors is an important factor in the development of obesity and type II diabetes and therefore there has been a growing emphasis on understanding this process [253]. The validation of hMSC as an *in vitro* model for human adipogenesis was of importance as certain questions on human adipogenesis cannot be solved by using human preadipocytes. Because pre-adipocytes are unipotent, already committed cells, they cannot be used when it is important to investigate very early differentiation events, i.e., the recruitment of pre-adipocytes from multipotent precursors. As published [199], micro-serial analysis of gene expression of undifferentiated hMSCs revealed that hMSCs simultaneously express transcripts characteristic of various mesenchymal cell lineages. Several groups have examined the process of hMSC commitment and differentiation to the osteogenic lineage. However, less is known about culture conditions favoring adipogenic conversion. In Experimental part I, we confirm and extend the characterization of hMSC differentiation into adipocytes.

Insulin is classically viewed as a promoter of adipogenesis, but it is also important for chondrogenesis [198], growth of muscle satellite cells [254], and other cell types as well. High concentrations of insulin activate the IGF-I receptor and have a mitogenic effect. Moreover, insulin activates MAPK [226,255], a key factor in the osteogenic conversion of hMSCs [208]. In agreement with these observations, we have found that high concentrations of insulin slightly inhibit adipogenesis compared with 170 nM insulin. We also found that prolonged "resting periods" without dexamethasone, 3-isobutyl-1-methylxanthine, and indomethacin improved the differentiation process. This is consistent with the gene expression data showing that leptin mRNA was substantially increased during the rest periods and that the presence of hormonal mixture is important mainly for initiation of

86

differentiation, not for full development of adipocyte phenotype. C/EBPß and PPARγ protein are present in uncommitted hMSCs as was described previously also in other committed and uncommitted cells and cell lines [256-263]. The induction of these transcription factors after treatment with the differentiation cocktail is accordant with the adipocytic differentiation model as proposed by Rosen et al. [207]. We confirmed that hMSCs transiently increase expression of C/EBPß and exhibit inducible expression of PPARγ, GLUT4, and leptin genes, illustrating the complete transition from primitive precursor cells to the terminally differentiated adipocytes. The complete disappearance of the C/EBPß protein after three cycles of differentiation cocktail suggests that the majority of the hMSCs progressed through the adipocytic "commitment" stage. Given that many of these cells did not store lipid, this might represent commitment but not terminal differentiation.

As expected, activation of PPARγ is important for hMSC differentiation. Oil Red O staining was increased 2-fold in the presence of PPARγ ligands [206,234,264]. We also confirmed that, as reported by Diascro and others [235-237], rabbit serum enhances adipogenic conversion. Interestingly, the magnitude of the rabbit serum effect on differentiation was similar to the TZDs. The mechanism of its action remains unclear. It was reported that rabbit serum has a higher content of free fatty acids compared with FBS. Fatty acids are putative ligands of PPARγ and may enhance adipogenesis through the activation of the PPARγ system [265].

Activation of PPARγ is a critical event in adipogenesis [205,266]. MAPK can phosphorylate PPARγ and decrease its transcriptional activity [209,267]. Consistent with this observation, we observed that inhibition of MAPK pathway through inhibition of MEK1/2 phosphorylation facilitated adipogenesis. This effect was more pronounced in extensively passaged cells. Furthermore, we found that increased sensitivity to MAPK inhibitor PD98059 treatment coincides with increased basal activity of ERK1/2 in later passages of hMSCs. This supports the observation that the adipogenic potential of hMSCs is reversibly reduced with increasing cell doublings and that this might be due to activation of ERK1/2.

There is a considerable controversy regarding the necessity of clonal expansion to adipogenic conversion. Clonal expansion usually consists of one or two rounds of mitosis followed by terminal growth arrest. The transient increase in expression of PCNA and cyclin D1 could suggest a re-entry into the cell cycle prior the terminal differentiation, however the number of cells did not increase after the hormonal induction of adipogenesis and the block of proliferation caused by araC treatment [221] did not decrease the differentiation efficiency. Therefore we conclude that if clonal expansion occurs before

terminal differentiation, this phenomenon is not necessary for adipogenic differentiation. Further work on this problem is warranted.

6.2 The effect of HDAC inhibitors on PML expression

The basic mechanism of IFNα-induced transcription of PML has been clarified 11 years ago [16]. Now, we have brought the evidence that full transcriptional activation of PML by interferons is dependent on the deacetylation events. Although it is well accepted that chromatin hyperacetylation caused by HDAC inhibitors has prevailingly a stimulatory effect on gene expression [268,269], some genes including a subset of IFN-controlled genes are not stimulated but repressed [244,270,271]. Our findings that TSA and other HDAC inhibitors block IFNα-mediated induction of PML NBs components further support and extend these reports. They indicate that many if not all IFN-inducible genes might be affected by HDAC inhibitors through a common mechanism operating during the propagation of interferon type I and type II signaling pathways. Although a direct deacetylation-regulated target has not yet been identified, Genin et al. [244] showed that TSA impairs STAT2 translocation into the nucleus and the formation/nuclear translocation of ISGF3, a trimeric complex of STAT1, STAT2 and IRF9, in virus-infected murine cells [272]. Our data show, however, that at least in HeLa cells the entry of STAT2 into the nucleus after IFNα-stimulation was not blocked by TSA. Moreover, as proved by the ChIP analysis, STAT2 was bound to PML ISRE element to the same extent as in the cells treated by IFNα alone, even when PML expression was simultaneously suppressed by TSA. In addition, the transcription of IRF-1 gene, which is regulated by GAF/AAF (γ-interferon activated factor/α-interferon activated factor) through GAS element after IFN stimulation, was also partially suppressed by TSA. This indicates that the effect is not mediated exclusively via ISGF3. Thus, our results are in accordance with the study of Nusinzon and Horvath showing no effect of pharmacological doses of TSA on STAT activation, heterodimerization and subcellular trafficking [271].

As we excluded STAT pathway as a major cause of HDAC effect on the attenuation of IFNα-induced PML expression, we propose that IRF1 is another possible target for further analysis of this suppressive effect of HDAC inhibitors. This factor participates in a delayed interferon response and as such might be a potential transcription regulator of PML gene. This idea is supported by the fact that the maximal levels of IFNα-induced PML mRNA are observed 8 hours after interferon stimulus; the levels of IRF1

protein are peaking within 2 and 4 hours after IFNα stimulation (ref. [273] and our observation). Since IRF-1 up-regulation by IFNα was partially inhibited by TSA and we also identified binding of IRF-1 to ISRE element of PML promoter by ChIP (our unpublished observation), we can speculate that the inhibition of PML expression can be caused, at least partially, by suppression of IRF-1 cellular level.

Although HDAC inhibitors used in this study are thought to be nonselective or poorly selective inhibitors of all or most of class I (HDAC1, HDAC2, HDAC3, HDAC8 and HDAC11 - newly classified into class IV) and class II (HDAC4, HDAC5, HDAC6, HDAC7, HDAC9 and HDAC10) enzymes [274], the discrimination of the specific HDAC involved in the regulation of interferon-stimulated genes would be the next step in our understanding of the transcriptional regulation of interferon-dependent genes.

6.3 *PML association with nucleolar structures*

The shortage of appropriate *in vitro* models for the study of PML with respect to its behaviour upon DNA damage, cell cycle progression and establishment of cellular senescence was a strong impuls for us to utilize hMSC for such studies. Human mesenchymal stem cells possess features of typical stem cells and moreover they have intact cell cycle and DNA damage checkpoints and thus represent a unique model for a study of various biological processes such as cell differentiation and aging. Here, we showed that hMSC expressed PML and formed PML bodies when proliferating, growth arrested, or differentiated into adipocytes. Remarkably, the number of PML bodies strongly correlated with the proliferative age of hMSC which could be explained by the PML role in the cellular senescence [46]. However, what initiates PML expression in aging cells remains unclear. One possible explanation is that PML is upregulated in response to accumulating DNA damage observed in replicatively senescent cells [275]. DNA damage is the signal for stabilization of p53 that may in turn stimulate PML expression [24]. The increase of PML NBs number with culture age of hMSC could therefore reflect the accumulation of DNA damage and activation of DNA damage checkpoints.

Interferon α also enhanced *PML* expression in hMSC. However, given that number of PML bodies did not increase as profoundly as levels of PML mRNA and protein, newly synthesized protein was targeted mainly to the original PML bodies. Thus, we can speculate that there is a limited number of places where PML bodies can be assembled and that these places become mostly occupied already when hMSC reach the confluence. This

is in agreement with observation that upon heat shock PML bodies disassemble and they reform in the original locations upon recovery [65].

Apart from expected localization of PML in nucleoplasm and PML bodies, we found PML in close connection with the nucleolus and nucleolus-derived structures in hMSC grown under standard conditions. To our knowledge this was the first observation of the PML association with structures of nucleolar origin in untreated cells. Until now, translocation of PML to the nucleolus was observed only after proteasome inhibition [245], doxorubicin or mitomycin C treatment [50] or after treatment with high doses of AMD [137]. All these treatments strongly affect nucleolar functions that inevitably initiate changes in the nucleolar structure. Proteasome inhibitors block late processing of rRNA precursors, DNA damage induced by doxorubicin leads to p53 upregulation, which in turn inactivates Pol I, and high doses of AMD block Pol I and II and cause nucleolar segregation and dispersal of many nucleolar proteins into the nucleoplasm. Quite distinctly, we have found small PML bodies on the nucleolar surface and PML-NDS in cells with normal nucleolar structure associated with ongoing rRNA synthesis as revealed by UBF staining and run-on transcription assay. Remarkably, the association of PML with the nucleolus was not found in HeLa, U-2 OS, A549, and SaOS-2 cell lines under standard growth conditions. In fact, several reports showed that in addition to loss or mutation of well-known tumor suppressors, PML is frequently deregulated in tumor cells *in vivo* [18,31]. For this reason, we hypothesize that the association of PML with the active nucleolus might represent one of the common mechanisms important for sensing or regulation of nucleolar activity that is partially or completely lost in tumor cells. The exact basis of this PML function is unknown but two observations we present here could offer a partial explanation. First, B23 protein - a marker of granular compartment - was frequently found enriched in PML-NDS compared to the adjacent nucleolus. Second, NDHII that usually locates to the nucleoplasm and in low levels to the nucleolus was also occasionally concentrated in PML-NDS. Thus, it seems that PML surrounds specifically enriched nucleolar material. Given the fact that both B23 and NDHII are RNA binding proteins and PML-NDS are readily stained with TOTO3 that has affinity to RNA, it is tempting to speculate that PML-NDS sequester rRNA requiring special processing and offer an appropriate environment where this processing could be carried out by accumulated proteins.

In the presence of low concentration of AMD (5-40 nM [138], Pol I-dependent synthesis of 47S rRNA precursor is completely abolished and nucleolar compartments segregate. We showed that segregated nucleoli in hMSC attracted PML that was organized

into donut-like structures on the nucleolar surface. Similar structures were described by Bernardi *et al*. after doxorubicin and mitomycin C treatment of MEF and WI-38 fibroblasts [50]. Both chemicals cause significant DNA damage affecting also rDNA genes. In our experiments, we used low doses of AMD and there is no convincing evidence that low doses of AMD could cause significant DNA damage. Besides, AMD-induced PML binding to the nucleolus was reversible and strongly dependent on the block of Pol I transcription. Therefore, we believe that it was the inhibition of rRNA synthesis and not the DNA damage what was the primary cause of PML nucleolar translocation in AMD-treated hMSC.

It is well documented that PML is important for cell cycle arrest, apoptosis and cellular senescence, mainly due to its ability to stabilize and activate p53 and pRb [46,88,91]. In tumor-derived cells, these PML effects are ineffective because of inactivation of either *p53* or *pRb* and as a result these cells are mostly insensitive to the induction of senescence or apoptosis. It is possible that tumor cells have lost also other PML downstream effects that are not directly related to activation of *p53* and *pRb* but have an impact on cellular growth. We propose that such an effect could be the binding of PML to the nucleolus that is severely reduced in tumor-derived cells. This hypothesis is based on the observation that in HeLa cells, the treatment causing senescence not only normalizes p53, pRb and p21 levels but it also restores PML binding to the nucleolus. It is possible that a specific PML modification, which occurs only in the presence of intact p53 and pRb pathways, may be required for its binding to the nucleolus. Taking into consideration PML binding properties, it is likely that PML may regulate flow of proteins into or out of the nucleolus and thus control nucleolar processes indirectly.

6.4 General discussion

In summary, we have shown that hMSCs exhibit true adipogenic phenotype *in vitro* that can be fully expressed under proper adipogenesis-favoring conditions. When cultured under the appropriate conditions (with TZDs, PD98059, or rabbit serum), ~80% of these cells differentiate into adipocytes. hMSCs express several key adipogenic genes in a sequence consistent with other models of adipogenesis. Thus, hMSC represent a unique model to follow the expression of any protein of interest during the conversion of proliferating stem cell into highly specialized terminally differentiated cell. Using hMSC, we determined the expression of PML in terminally differentiated cells. The presence of PML bodies in terminally differentiated cells *in vitro* or *in vivo* [18] emphasize the

91

importance of other PML functions apart from regulation of cell proliferation and senescence as terminally differentiated cells are permanently growth arrested and there is no evidence that they could become senescent.

Next, we have brought the evidence that full transcriptional activation of PML by interferons is dependent on the deacetylation events. We excluded STAT pathway as a major cause of HDAC effect on the attenuation of IFNα-induced PML expression and therefore we propose that IRF1 is a possible target for the suppressive effect of HDAC inhibitors. Since several HDAC inhibitors are currently in clinical trials as anticancer agents (for reviews, see [240,241]), our data showing adverse effect of TSA on the induction of PML by interferons are of practical importance for cancer therapy as can be implied from known antiviral and anticancer effects of interferons (for a recent review on interferons in cancer therapy, see, e.g. ref. [276]). Regarding the importance of interferon system for the maintenance of an organism homeostasis, our data could be important for the design or selection of antitumor HDAC inhibitors that would not perturbe the interferon pathway.

Finally, our data showed that in normal diploid human cells PML interacts with the nucleolus and that this interaction is dependent on nucleolar activity. We suggest that PML binding to the nucleolus might be important for the regulation of cellular growth or senescence, but the exact relationship between PML and nucleolar metabolism remains to be elucidated.

7 Conclusions

Ad Aim1: To optimize the culture conditions enhancing adipogenesis in hMSC and then to validate hMSC as an in vitro model of human adipogenesis.

We have established that differentiation medium for hMSC based on medium 199 and containing 170 nM insulin, 0.5 mM 3-isobutyl-1-methylxanthine, 0.2 mM indomethacin, 1 μM dexamethasone, and 5% fetal bovine serum was optimal. The replacement of fetal bovine serum with rabbit serum (15%) led to further enhancement of differentiation and the inhibition of mitogen-activated protein kinase activation also facilitated adipogenic conversion of hMSCs.

We have shown that hMSCs exhibit true adipogenic phenotype *in vitro* that can be fully expressed under proper adipogenesis-favoring conditions. We have documented that the pattern of genes expressed during hMSC differentiation into adipocytes (adipsin, peroxisome proliferator-activated receptor-γ, CCAAT/enhancer-binding protein-ß, GLUT4, and leptin) was similar to that observed in other *in vitro* adipocyte models. Thus, hMSCs represent a new model for the study of human adipogenesis.

Ad Aim 2: To examine the role of chromatin acetylation in the expression of PML gene.

We have shown that the action of histone deacetylases is necessary for the full IFNα-stimulated transcriptional activation of *PML* and *Sp100* genes since histone deacetylases inhibitors (trichostatin A, sodium butyrate, MS-275, SAHA, and valproic acid) attenuated the response of PML and Sp100 to interferon-α. In detail, trichostatin A blocked the increase of PML NBs number and suppressed up-regulation of PML mRNA and protein levels in several human cell lines and in normal diploid skin fibroblasts.

We have examined two components of the pathway responsible for IFNα/β-dependent gene transcription, i.e. STAT2 and IRF1. We have not detected any defects in STAT2 cytoplasmic-nuclear transport or binding of STAT2 to ISRE element of PML promoter, thus excluding STAT2-dependent mechanism of TSA effect on PML transcription. On the other hand, we have found that TSA, although incompletely, inhibited IFNα-induction of IRF1, putative transcription activator of *PML* gene. Thus, the effect of HDAC inhibition on PML expression can be at least partially explained by the impairment of delayed interferon response driven by IRF1.

Ad Aim3: To describe the PML expression and nuclear compartmentalization in growing,
differentiated and senescent hMSC and in other prematurely senescent cells.

We have documented that PML was expressed in growing, confluent or terminally differentiated hMSC. The expression of PML was strongly induced by IFNα both at the mRNA and protein level, while the number of PML NBs was increased only modestly. Importantly, the number of PML bodies per cell nucleus was found to be dependent on the culture proliferative age, further supporting the role of PML in cellular senescence.

We have described various forms of a novel nuclear PML compartment associated with nucleoli that was found under growth-permitting conditions in human mesenchymal stem cells and skin fibroblasts but not in several immortal cell lines with defects in the p53 and pRb pathways. In addition, we have observed PML translocation to the surface of segregated nucleoli in response to the shut-off of rRNA synthesis induced by actinomycin D. The absence of nucleolar PML compartment in rapidly growing tumor-derived cells suggests that PML association with the nucleolus might be important for the cell cycle regulation.

We have found that the induction of premature senescence in HeLa cells restored PML binding to nucleoli-derived structures and to the surface of segregated nucleoli. These findings indicate that PML may be involved in nucleolar functions of senescent cells.

8 References

1. de The H, Lavau C, Marchio A, Chomienne C, Degos L, Dejean A. The PML-RAR alpha fusion mRNA generated by the t(15;17) translocation in acute promyelocytic leukemia encodes a functionally altered RAR. Cell. 1991;66:675-684

2. Kakizuka A, Miller WH, Jr., Umesono K, Warrell RP, Jr., Frankel SR, Murty VV, Dmitrovsky E, Evans RM. Chromosomal translocation t(15;17) in human acute promyelocytic leukemia fuses RAR alpha with a novel putative transcription factor, PML. Cell. 1991;66:663-674

3. Maul GG, Negorev D, Bell P, Ishov AM. Review: properties and assembly mechanisms of ND10, PML bodies, or PODs. J Struct Biol. 2000;129:278-287

4. GeneCards. an integrated database of human genes, an academic web site of the Weizmann Institute of Science in association with Xennex. Vol. http://www.genecards.org/

5. Fagioli M, Alcalay M, Pandolfi PP, Venturini L, Mencarelli A, Simeone A, Acampora D, Grignani F, Pelicci PG. Alternative splicing of PML transcripts predicts coexpression of several carboxy-terminally different protein isoforms. Oncogene. 1992;7:1083-1091

6. Jensen K, Shiels C, Freemont PS. PML protein isoforms and the RBCC/TRIM motif. Oncogene. 2001;20:7223-7233

7. Condemine W, Takahashi Y, Zhu J, Puvion-Dutilleul F, Guegan S, Janin A, de The H. Characterization of endogenous human promyelocytic leukemia isoforms. Cancer Res. 2006;66:6192-6198

8. Goddard AD, Borrow J, Freemont PS, Solomon E. Characterization of a zinc finger gene disrupted by the t(15;17) in acute promyelocytic leukemia. Science. 1991;254:1371-1374

9. Ruggero D, Wang ZG, Pandolfi PP. The puzzling multiple lives of PML and its role in the genesis of cancer. Bioessays. 2000;22:827-835

10. Borden KL. Pondering the promyelocytic leukemia protein (PML) puzzle: possible functions for PML nuclear bodies. Mol Cell Biol. 2002;22:5259-5269

11. Dellaire G, Bazett-Jones DP. PML nuclear bodies: dynamic sensors of DNA damage and cellular stress. Bioessays. 2004;26:963-977

12. Regad T, Chelbi-Alix MK. Role and fate of PML nuclear bodies in response to interferon and viral infections. Oncogene. 2001;20:7274-7286

13. Chelbi-Alix MK, Pelicano L, Quignon F, Koken MH, Venturini L, Stadler M, Pavlovic J, Degos L, de The H. Induction of the PML protein by interferons in normal and APL cells. Leukemia. 1995;9:2027-2033

14. Lavau C, Marchio A, Fagioli M, Jansen J, Falini B, Lebon P, Grosveld F, Pandolfi PP, Pelicci PG, Dejean A. The acute promyelocytic leukaemia-associated PML gene is induced by interferon. Oncogene. 1995;11:871-876

15. Grotzinger T, Sternsdorf T, Jensen K, Will H. Interferon-modulated expression of genes encoding the nuclear-dot-associated proteins Sp100 and promyelocytic leukemia protein (PML). Eur J Biochem. 1996;238:554-560

16. Stadler M, Chelbi-Alix MK, Koken MH, Venturini L, Lee C, Saib A, Quignon F, Pelicano L, Guillemin MC, Schindler C, et al. Transcriptional induction of the PML growth suppressor gene by interferons is mediated through an ISRE and a GAS element. Oncogene. 1995;11:2565-2573

17. Pelicano L, Li F, Schindler C, Chelbi-Alix MK. Retinoic acid enhances the expression of interferon-induced proteins: evidence for multiple mechanisms of action. Oncogene. 1997;15:2349-2359

18. Gambacorta M, Flenghi L, Fagioli M, Pileri S, Leoncini L, Bigerna B, Pacini R, Tanci LN, Pasqualucci L, Ascani S, Mencarelli A, Liso A, Pelicci PG, Falini B. Heterogeneous nuclear expression of the promyelocytic leukemia (PML) protein in normal and neoplastic human tissues. Am J Pathol. 1996;149:2023-2035

19. Gongora C, David G, Pintard L, Tissot C, Hua TD, Dejean A, Mechti N. Molecular cloning of a new interferon-induced PML nuclear body-associated protein. J Biol Chem. 1997;272:19457-19463

20. Gongora C, Degols G, Espert L, Hua TD, Mechti N. A unique ISRE, in the TATA-less human Isg20 promoter, confers IRF-1-mediated responsiveness to both interferon type I and type II. Nucleic Acids Res. 2000;28:2333-2341

21. Fabunmi RP, Wigley WC, Thomas PJ, DeMartino GN. Interferon gamma regulates accumulation of the proteasome activator PA28 and immunoproteasomes at nuclear PML bodies. J Cell Sci. 2001;114:29-36

22. Koken MH, Linares-Cruz G, Quignon F, Viron A, Chelbi-Alix MK, Sobczak-Thepot J, Juhlin L, Degos L, Calvo F, de The H. The PML growth-suppressor has an altered expression in human oncogenesis. Oncogene. 1995;10:1315-1324

23. Terris B, Baldin V, Dubois S, Degott C, Flejou JF, Henin D, Dejean A. PML nuclear bodies are general targets for inflammation and cell proliferation. Cancer Res. 1995;55:1590-1597

24. de Stanchina E, Querido E, Narita M, Davuluri RV, Pandolfi PP, Ferbeyre G, Lowe SW. PML is a direct p53 target that modulates p53 effector functions. Mol Cell. 2004;13:523-535

25. Pearson M, Carbone R, Sebastiani C, Cioce M, Fagioli M, Saito S, Higashimoto Y, Appella E, Minucci S, Pandolfi PP, Pelicci PG. PML regulates p53 acetylation and premature senescence induced by oncogenic Ras. Nature. 2000;406:207-210

26. Chan JY, Li L, Fan YH, Mu ZM, Zhang WW, Chang KS. Cell-cycle regulation of DNA damage-induced expression of the suppressor gene PML. Biochem Biophys Res Commun. 1997;240:640-646

27. Topisirovic I, Capili AD, Borden KL. Gamma interferon and cadmium treatments modulate eukaryotic initiation factor 4E-dependent mRNA transport of cyclin D1 in a PML-dependent manner. Mol Cell Biol. 2002;22:6183-6198

28. Zhang H, Melamed J, Wei P, Cox K, Frankel W, Bahnson RR, Robinson N, Pyka R, Liu Y, Zheng P. Concordant down-regulation of proto-oncogene PML and major histocompatibility antigen HLA class I expression in high-grade prostate cancer. Cancer Immun. 2003;3:2

29. Yu JH, Nakajima A, Nakajima H, Diller LR, Bloch KD, Bloch DB. Restoration of promyelocytic leukemia protein-nuclear bodies in neuroblastoma cells enhances retinoic acid responsiveness. Cancer Res. 2004;64:928-933

30. Villagra NT, Berciano J, Altable M, Navascues J, Casafont I, Lafarga M, Berciano MT. PML bodies in reactive sensory ganglion neurons of the Guillain-Barre syndrome. Neurobiol Dis. 2004;16:158-168

31. Gurrieri C, Capodieci P, Bernardi R, Scaglioni PP, Nafa K, Rush LJ, Verbel DA, Cordon-Cardo C, Pandolfi PP. Loss of the tumor suppressor PML in human cancers of multiple histologic origins. J Natl Cancer Inst. 2004;96:269-279

32. Reymond A, Meroni G, Fantozzi A, Merla G, Cairo S, Luzi L, Riganelli D, Zanaria E, Messali S, Cainarca S, Guffanti A, Minucci S, Pelicci PG, Ballabio A. The tripartite motif family identifies cell compartments. Embo J. 2001;20:2140-2151

33. Borden KL, CampbellDwyer EJ, Salvato MS. The promyelocytic leukemia protein PML has a pro-apoptotic activity mediated through its RING domain. FEBS Lett. 1997;418:30-34

34. Fagioli M, Alcalay M, Tomassoni L, Ferrucci PF, Mencarelli A, Riganelli D, Grignani F, Pozzan T, Nicoletti I, Pelicci PG. Cooperation between the RING + B1-B2 and coiled-coil domains of PML is necessary for its effects on cell survival. Oncogene. 1998;16:2905-2913

35. Boddy MN, Duprez E, Borden KL, Freemont PS. Surface residue mutations of the PML RING finger domain alter the formation of nuclear matrix-associated PML bodies. J Cell Sci. 1997;110 (Pt 18):2197-2205

36. Le XF, Yang P, Chang KS. Analysis of the growth and transformation suppressor domains of promyelocytic leukemia gene, PML. J Biol Chem. 1996;271:130-135

37. Henderson BR, Eleftheriou A. A comparison of the activity, sequence specificity, and CRM1-dependence of different nuclear export signals. Exp Cell Res. 2000;256:213-224

38. Duprez E, Saurin AJ, Desterro JM, Lallemand-Breitenbach V, Howe K, Boddy MN, Solomon E, de The H, Hay RT, Freemont PS. SUMO-1 modification of the acute promyelocytic leukaemia protein PML: implications for nuclear localisation. J Cell Sci. 1999;112 (Pt 3):381-393

39. Kamitani T, Nguyen HP, Kito K, Fukuda-Kamitani T, Yeh ET. Covalent modification of PML by the sentrin family of ubiquitin-like proteins. J Biol Chem. 1998;273:3117-3120

40. Fu C, Ahmed K, Ding H, Ding X, Lan J, Yang Z, Miao Y, Zhu Y, Shi Y, Zhu J, Huang H, Yao X. Stabilization of PML nuclear localization by conjugation and oligomerization of SUMO-3. Oncogene. 2005;24:5401-5413

41. Kamitani T, Kito K, Nguyen HP, Wada H, Fukuda-Kamitani T, Yeh ET. Identification of three major sentrinization sites in PML. J Biol Chem. 1998;273:26675-26682

42. Zhong S, Muller S, Ronchetti S, Freemont PS, Dejean A, Pandolfi PP. Role of SUMO-1-modified PML in nuclear body formation. Blood. 2000;95:2748-2752

43. Gong L, Yeh ET. Characterization of a family of nucleolar SUMO-specific proteases with preference for SUMO-2 or SUMO-3. J Biol Chem. 2006;281:15869-15877

44. Seeler JS, Dejean A. SUMO: of branched proteins and nuclear bodies. Oncogene. 2001;20:7243-7249

45. Ishov AM, Sotnikov AG, Negorev D, Vladimirova OV, Neff N, Kamitani T, Yeh ET, Strauss JF, 3rd, Maul GG. PML is critical for ND10 formation and recruits the PML-interacting protein daxx to this nuclear structure when modified by SUMO-1. J Cell Biol. 1999;147:221-234

46. Bischof O, Kirsh O, Pearson M, Itahana K, Pelicci PG, Dejean A. Deconstructing PML-induced premature senescence. Embo J. 2002;21:3358-3369

47. Shen TH, Lin HK, Scaglioni PP, Yung TM, Pandolfi PP. The Mechanisms of PML-Nuclear Body Formation. Mol Cell. 2006;24:331-339

48. Everett RD, Lomonte P, Sternsdorf T, van Driel R, Orr A. Cell cycle regulation of PML modification and ND10 composition. J Cell Sci. 1999;112 (Pt 24):4581-4588

49. Yang S, Kuo C, Bisi JE, Kim MK. PML-dependent apoptosis after DNA damage is regulated by the checkpoint kinase hCds1/Chk2. Nat Cell Biol. 2002;4:865-870

50. Bernardi R, Scaglioni PP, Bergmann S, Horn HF, Vousden KH, Pandolfi PP. PML regulates p53 stability by sequestering Mdm2 to the nucleolus. Nat Cell Biol. 2004;6:665-672

51. Dellaire G, Ching RW, Ahmed K, Jalali F, Tse KC, Bristow RG, Bazett-Jones DP. Promyelocytic leukemia nuclear bodies behave as DNA damage sensors whose response to DNA double-strand breaks is regulated by NBS1 and the kinases ATM, Chk2, and ATR. J Cell Biol. 2006;175:55-66

52. Scaglioni PP, Yung TM, Cai LF, Erdjument-Bromage H, Kaufman AJ, Singh B, Teruya-Feldstein J, Tempst P, Pandolfi PP. A CK2-dependent mechanism for degradation of the PML tumor suppressor. Cell. 2006;126:269-283

53. Zhang P, Chin W, Chow LT, Chan AS, Yim AP, Leung SF, Mok TS, Chang KS, Johnson PJ, Chan JY. Lack of expression for the suppressor PML in human small cell lung carcinoma. Int J Cancer. 2000;85:599-605

54. Beech SJ, Lethbridge KJ, Killick N, McGlincy N, Leppard KN. Isoforms of the promyelocytic leukemia protein differ in their effects on ND10 organization. Experimental Cell Research. 2005;In Press, Corrected Proof

55. Xu ZX, Zou WX, Lin P, Chang KS. A role for PML3 in centrosome duplication and genome stability. Mol Cell. 2005;17:721-732

56. Lin HK, Bergmann S, Pandolfi PP. Cytoplasmic PML function in TGF-beta signalling. Nature. 2004;431:205-211

57. Ascoli CA, Maul GG. Identification of a novel nuclear domain. J Cell Biol. 1991;112:785-795

58. Bernstein RM, Neuberger JM, Bunn CC, Callender ME, Hughes GR, Williams R. Diversity of autoantibodies in primary biliary cirrhosis and chronic active hepatitis. Clin Exp Immunol. 1984;55:553-560

59. Szostecki C, Guldner HH, Will H. Autoantibodies against "nuclear dots" in primary biliary cirrhosis. Semin Liver Dis. 1997;17:71-78

60. Dellaire G, Ching RW, Dehghani H, Ren Y, Bazett-Jones DP. The number of PML nuclear bodies increases in early S phase by a fission mechanism. J Cell Sci. 2006;119:1026-1033

61. Boisvert FM, Hendzel MJ, Bazett-Jones DP. Promyelocytic leukemia (PML) nuclear bodies are protein structures that do not accumulate RNA. J Cell Biol. 2000;148:283-292

62. LaMorte VJ, Dyck JA, Ochs RL, Evans RM. Localization of nascent RNA and CREB binding protein with the PML-containing nuclear body. Proc Natl Acad Sci U S A. 1998;95:4991-4996

63. Luciani JJ, Depetris D, Usson Y, Metzler-Guillemain C, Mignon-Ravix C, Mitchell MJ, Megarbane A, Sarda P, Sirma H, Moncla A, Feunteun J, Mattei MG. PML nuclear bodies are highly organised DNA-protein structures with a function in heterochromatin remodelling at the G2 phase. J Cell Sci. 2006;119:2518-2531

64. Eskiw CH, Dellaire G, Bazett-Jones DP. Chromatin contributes to structural integrity of promyelocytic leukemia bodies through a SUMO-1-independent mechanism. J Biol Chem. 2004;279:9577-9585

65. Eskiw CH, Dellaire G, Mymryk JS, Bazett-Jones DP. Size, position and dynamic behavior of PML nuclear bodies following cell stress as a paradigm for supramolecular trafficking and assembly. J Cell Sci. 2003;116:4455-4466

66. Shiels C, Islam SA, Vatcheva R, Sasieni P, Sternberg MJ, Freemont PS, Sheer D. PML bodies associate specifically with the MHC gene cluster in interphase nuclei. J Cell Sci. 2001;114:3705-3716

67. Wang J, Shiels C, Sasieni P, Wu PJ, Islam SA, Freemont PS, Sheer D. Promyelocytic leukemia nuclear bodies associate with transcriptionally active genomic regions. J Cell Biol. 2004;164:515-526

68. Dellaire G, Farrall R, Bickmore WA. The Nuclear Protein Database (NPD): sub-nuclear localisation and functional annotation of the nuclear proteome. Nucleic Acids Res. 2003;31:328-330

69. Bischof O, Kim SH, Irving J, Beresten S, Ellis NA, Campisi J. Regulation and localization of the Bloom syndrome protein in response to DNA damage. J Cell Biol. 2001;153:367-380

70. Carbone R, Pearson M, Minucci S, Pelicci PG. PML NBs associate with the hMre11 complex and p53 at sites of irradiation induced DNA damage. Oncogene. 2002;21:1633-1640

71. Blander G, Zalle N, Daniely Y, Taplick J, Gray MD, Oren M. DNA damage-induced translocation of the Werner helicase is regulated by acetylation. J Biol Chem. 2002

72. Grobelny JV, Godwin AK, Broccoli D. ALT-associated PML bodies are present in viable cells and are enriched in cells in the G(2)/M phase of the cell cycle. J Cell Sci. 2000;113 Pt 24:4577-4585

73. Wu WS, Vallian S, Seto E, Yang WM, Edmondson D, Roth S, Chang KS. The growth suppressor PML represses transcription by functionally and physically interacting with histone deacetylases. Mol Cell Biol. 2001;21:2259-2268

74. Doucas V, Tini M, Egan DA, Evans RM. Modulation of CREB binding protein function by the promyelocytic (PML) oncoprotein suggests a role for nuclear bodies in hormone signaling. Proc Natl Acad Sci U S A. 1999;96:2627-2632

75. Maul GG, Yu E, Ishov AM, Epstein AL. Nuclear domain 10 (ND10) associated proteins are also present in nuclear bodies and redistribute to hundreds of nuclear sites after stress. J Cell Biochem. 1995;59:498-513

76. Hofmann TG, Moller A, Sirma H, Zentgraf H, Taya Y, Droge W, Will H, Schmitz ML. Regulation of p53 activity by its interaction with homeodomain-interacting protein kinase-2. Nat Cell Biol. 2002;4:1-10

77. Fogal V, Gostissa M, Sandy P, Zacchi P, Sternsdorf T, Jensen K, Pandolfi PP, Will H, Schneider C, Del Sal G. Regulation of p53 activity in nuclear bodies by a specific PML isoform. Embo J. 2000;19:6185-6195

78. von Mikecz A, Zhang S, Montminy M, Tan EM, Hemmerich P. CREB-binding protein (CBP)/p300 and RNA polymerase II colocalize in transcriptionally active domains in the nucleus. J Cell Biol. 2000;150:265-273

79. Ishov AM, Stenberg RM, Maul GG. Human cytomegalovirus immediate early interaction with host nuclear structures: definition of an immediate transcript environment. J Cell Biol. 1997;138:5-16

80. Nabetani A, Yokoyama O, Ishikawa F. Localization of hRad9, hHus1, hRad1, and hRad17 and caffeine-sensitive DNA replication at the alternative lengthening of telomeres-associated promyelocytic leukemia body. J Biol Chem. 2004;279:25849-25857

81. Piazza F, Gurrieri C, Pandolfi PP. The theory of APL. Oncogene. 2001;20:7216-7222

82. Grignani F, De Matteis S, Nervi C, Tomassoni L, Gelmetti V, Cioce M, Fanelli M, Ruthardt M, Ferrara FF, Zamir I, Seiser C, Lazar MA, Minucci S, Pelicci PG. Fusion proteins of the retinoic acid receptor-alpha recruit histone deacetylase in promyelocytic leukaemia. Nature. 1998;391:815-818

83. Villa R, De Santis F, Gutierrez A, Minucci S, Pelicci PG, Di Croce L. Epigenetic gene silencing in acute promyelocytic leukemia. Biochem Pharmacol. 2004;68:1247-1254

84. Yoshida H, Kitamura K, Tanaka K, Omura S, Miyazaki T, Hachiya T, Ohno R, Naoe T. Accelerated degradation of PML-retinoic acid receptor alpha (PML-RARA) oncoprotein by all-trans-retinoic acid in acute promyelocytic leukemia: possible role of the proteasome pathway. Cancer Res. 1996;56:2945-2948

85. Lin RJ, Nagy L, Inoue S, Shao W, Miller WH, Jr., Evans RM. Role of the histone deacetylase complex in acute promyelocytic leukaemia. Nature. 1998;391:811-814

86. Wang ZG, Ruggero D, Ronchetti S, Zhong S, Gaboli M, Rivi R, Pandolfi PP. PML is essential for multiple apoptotic pathways. Nat Genet. 1998;20:266-272

87. Wang ZG, Delva L, Gaboli M, Rivi R, Giorgio M, Cordon-Cardo C, Grosveld F, Pandolfi PP. Role of PML in cell growth and the retinoic acid pathway. Science. 1998;279:1547-1551

88. Mallette FA, Goumard S, Gaumont-Leclerc MF, Moiseeva O, Ferbeyre G. Human fibroblasts require the Rb family of tumor suppressors, but not p53, for PML-induced senescence. Oncogene. 2004;23:91-99

89. Bischof O, Nacerddine K, Dejean A. Human papillomavirus oncoprotein E7 targets the promyelocytic leukemia protein and circumvents cellular senescence via the Rb and p53 tumor suppressor pathways. Mol Cell Biol. 2005;25:1013-1024

90. Takahashi Y, Lallemand-Breitenbach V, Zhu J, de The H. PML nuclear bodies and apoptosis. Oncogene. 2004;23:2819-2824

91. Ferbeyre G, de Stanchina E, Querido E, Baptiste N, Prives C, Lowe SW. PML is induced by oncogenic ras and promotes premature senescence. Genes Dev. 2000;14:2015-2027

92. He D, Mu ZM, Le X, Hsieh JT, Pong RC, Chung LW, Chang KS. Adenovirus-mediated expression of PML suppresses growth and tumorigenicity of prostate cancer cells. Cancer Res. 1997;57:1868-1872

93. Le XF, Vallian S, Mu ZM, Hung MC, Chang KS. Recombinant PML adenovirus suppresses growth and tumorigenicity of human breast cancer cells by inducing G1 cell cycle arrest and apoptosis. Oncogene. 1998;16:1839-1849

94. Mu ZM, Le XF, Vallian S, Glassman AB, Chang KS. Stable overexpression of PML alters regulation of cell cycle progression in HeLa cells. Carcinogenesis. 1997;18:2063-2069

95. Rousseau D, Kaspar R, Rosenwald I, Gehrke L, Sonenberg N. Translation initiation of ornithine decarboxylase and nucleocytoplasmic transport of cyclin D1 mRNA are increased in cells overexpressing eukaryotic initiation factor 4E. Proc Natl Acad Sci U S A. 1996;93:1065-1070

96. Lai HK, Borden KL. The promyelocytic leukemia (PML) protein suppresses cyclin D1 protein production by altering the nuclear cytoplasmic distribution of cyclin D1 mRNA. Oncogene. 2000;19:1623-1634

97. Cohen N, Sharma M, Kentsis A, Perez JM, Strudwick S, Borden KL. PML RING suppresses oncogenic transformation by reducing the affinity of eIF4E for mRNA. Embo J. 2001;20:4547-4559

98. Culjkovic B, Topisirovic I, Skrabanek L, Ruiz-Gutierrez M, Borden KL. eIF4E is a central node of an RNA regulon that governs cellular proliferation. J Cell Biol. 2006;175:415-426

99. Alcalay M, Tomassoni L, Colombo E, Stoldt S, Grignani F, Fagioli M, Szekely L, Helin K, Pelicci PG. The promyelocytic leukemia gene product (PML) forms stable complexes with the retinoblastoma protein. Mol Cell Biol. 1998;18:1084-1093

100. Bode AM, Dong Z. Post-translational modification of p53 in tumorigenesis. Nat Rev Cancer. 2004;4:793-805

101. Langley E, Pearson M, Faretta M, Bauer UM, Frye RA, Minucci S, Pelicci PG, Kouzarides T. Human SIR2 deacetylates p53 and antagonizes PML/p53-induced cellular senescence. Embo J. 2002;21:2383-2396

102.   Moller A, Sirma H, Hofmann TG, Rueffer S, Klimczak E, Droge W, Will H, Schmitz ML. PML is required for homeodomain-interacting protein kinase 2 (HIPK2)-mediated p53 phosphorylation and cell cycle arrest but is dispensable for the formation of HIPK domains. Cancer Res. 2003;63:4310-4314

103.   D'Orazi G, Cecchinelli B, Bruno T, Manni I, Higashimoto Y, Saito S, Gostissa M, Coen S, Marchetti A, Del Sal G, Piaggio G, Fanciulli M, Appella E, Soddu S. Homeodomain-interacting protein kinase-2 phosphorylates p53 at Ser 46 and mediates apoptosis. Nat Cell Biol. 2002;4:11-19

104.   Kurki S, Latonen L, Laiho M. Cellular stress and DNA damage invoke temporally distinct Mdm2, p53 and PML complexes and damage-specific nuclear relocalization. J Cell Sci. 2003;116:3917-3925

105.   Webley K, Bond JA, Jones CJ, Blaydes JP, Craig A, Hupp T, Wynford-Thomas D. Posttranslational modifications of p53 in replicative senescence overlapping but distinct from those induced by DNA damage. Mol Cell Biol. 2000;20:2803-2808

106.   Toledo F, Wahl GM. Regulating the p53 pathway: in vitro hypotheses, in vivo veritas. Nat Rev Cancer. 2006;6:909-923

107.   Mittnacht S. The retinoblastoma protein--from bench to bedside. Eur J Cell Biol. 2005;84:97-107

108.   Wei X, Yu ZK, Ramalingam A, Grossman SR, Yu JH, Bloch DB, Maki CG. Physical and functional interactions between PML and MDM2. J Biol Chem. 2003;278:29288-29297

109.   Everett RD, Meredith M, Orr A. The ability of herpes simplex virus type 1 immediate-early protein Vmw110 to bind to a ubiquitin-specific protease contributes to its roles in the activation of gene expression and stimulation of virus replication. J Virol. 1999;73:417-426

110.   Li M, Chen D, Shiloh A, Luo J, Nikolaev AY, Qin J, Gu W. Deubiquitination of p53 by HAUSP is an important pathway for p53 stabilization. Nature. 2002;416:648-653

111.   Son SH, Yu E, Choi EK, Lee H, Choi J. Promyelocytic leukemia protein-induced growth suppression and cell death in liver cancer cells. Cancer Gene Ther. 2005;12:1-11

112.   Cairo S, De Falco F, Pizzo M, Salomoni P, Pandolfi PP, Meroni G. PML interacts with Myc, and Myc target gene expression is altered in PML-null fibroblasts. Oncogene. 2005;24:2195-2203

113.   White RJ. RNA polymerases I and III, growth control and cancer. Nat Rev Mol Cell Biol. 2005;6:69-78

114.   Smith KP, Byron M, O'Connell BC, Tam R, Schorl C, Guney I, Hall LL, Agrawal P, Sedivy JM, Lawrence JB. c-Myc localization within the nucleus: evidence for association with the PML nuclear body. J Cell Biochem. 2004;93:1282-1296

115.   Seker H, Rubbi C, Linke SP, Bowman ED, Garfield S, Hansen L, Borden KL, Milner J, Harris CC. UV-C-induced DNA damage leads to p53-dependent nuclear trafficking of PML. Oncogene. 2003;22:1620-1628

116.   Xu ZX, Timanova-Atanasova A, Zhao RX, Chang KS. PML colocalizes with and stabilizes the DNA damage response protein TopBP1. Mol Cell Biol. 2003;23:4247-4256

117.   Sancar A, Lindsey-Boltz LA, Unsal-Kacmaz K, Linn S. Molecular mechanisms of mammalian DNA repair and the DNA damage checkpoints. Annu Rev Biochem. 2004;73:39-85

118.   Nyberg KA, Michelson RJ, Putnam CW, Weinert TA. Toward maintaining the genome: DNA damage and replication checkpoints. Annu Rev Genet. 2002;36:617-656

119.   Shiloh Y. The ATM-mediated DNA-damage response: taking shape. Trends in Biochemical Sciences. 2006;31:402-410

120.   Abraham RT. Cell cycle checkpoint signaling through the ATM and ATR kinases. Genes Dev. 2001;15:2177-2196

121.   Yang J, Xu ZP, Huang Y, Hamrick HE, Duerksen-Hughes PJ, Yu YN. ATM and ATR: sensing DNA damage. World J Gastroenterol. 2004;10:155-160

122.   Bartek J, Lukas J. Mammalian G1- and S-phase checkpoints in response to DNA damage. Curr Opin Cell Biol. 2001;13:738-747

123.   Yang S, Jeong JH, Brown AL, Lee CH, Pandolfi PP, Chung JH, Kim MK. Promyelocytic leukemia activates Chk2 by mediating Chk2 autophosphorylation. J Biol Chem. 2006;281:26645-26654

124. Louria-Hayon I, Grossman T, Sionov RV, Alsheich O, Pandolfi PP, Haupt Y. The promyelocytic leukemia protein protects p53 from Mdm2-mediated inhibition and degradation. J Biol Chem. 2003;278:33134-33141

125. Guo A, Salomoni P, Luo J, Shih A, Zhong S, Gu W, Pandolfi PP. The function of PML in p53-dependent apoptosis. Nat Cell Biol. 2000;2:730-736

126. d'Adda di Fagagna F, Reaper PM, Clay-Farrace L, Fiegler H, Carr P, Von Zglinicki T, Saretzki G, Carter NP, Jackson SP. A DNA damage checkpoint response in telomere-initiated senescence. Nature. 2003;426:194-198

127. Henson JD, Neumann AA, Yeager TR, Reddel RR. Alternative lengthening of telomeres in mammalian cells. Oncogene. 2002;21:598-610

128. Dunham MA, Neumann AA, Fasching CL, Reddel RR. Telomere maintenance by recombination in human cells. Nat Genet. 2000;26:447-450

129. Wu G, Lee WH, Chen PL. NBS1 and TRF1 colocalize at promyelocytic leukemia bodies during late S/G2 phases in immortalized telomerase-negative cells. Implication of NBS1 in alternative lengthening of telomeres. J Biol Chem. 2000;275:30618-30622

130. Yeager TR, Neumann AA, Englezou A, Huschtscha LI, Noble JR, Reddel RR. Telomerase-negative immortalized human cells contain a novel type of promyelocytic leukemia (PML) body. Cancer Res. 1999;59:4175-4179

131. Takai H, Smogorzewska A, de Lange T. DNA damage foci at dysfunctional telomeres. Curr Biol. 2003;13:1549-1556

132. Wai LK. Telomeres, telomerase, and tumorigenesis--a review. MedGenMed. 2004;6:19

133. Melese T, Xue Z. The nucleolus: an organelle formed by the act of building a ribosome. Curr Opin Cell Biol. 1995;7:319-324

134. Raska I, Shaw PJ, Cmarko D. Structure and function of the nucleolus in the spotlight. Curr Opin Cell Biol. 2006;18:325-334

135. Schwarzacher HG, Mosgoeller W. Ribosome biogenesis in man: current views on nucleolar structures and function. Cytogenet Cell Genet. 2000;91:243-252

136. Alvarez M, Quezada C, Molina A, Krauskopf M, Vera MI, Thiry M. Ultrastructural changes of the carp (Cyprinus carpio) hepatocyte nucleolus during seasonal acclimatization. Biol Cell. 2006;98:457-463

137. Shav-Tal Y, Blechman J, Darzacq X, Montagna C, Dye BT, Patton JG, Singer RH, Zipori D. Dynamic Sorting of Nuclear Components into Distinct Nucleolar Caps during Transcriptional Inhibition. Mol Biol Cell. 2005;16:2395-2413

138. Iapalucci-Espinoza S, Franze-Fernandez MT. Effect of protein synthesis inhibitors and low concentrations of actinomycin D on ribosomal RNA synthesis. FEBS Lett. 1979;107:281-284

139. Robles SJ, Adami GR. Agents that cause DNA double strand breaks lead to p16INK4a enrichment and the premature senescence of normal fibroblasts. Oncogene. 1998;16:1113-1123

140. Nelson WG, Kastan MB. DNA strand breaks: the DNA template alterations that trigger p53-dependent DNA damage response pathways. Mol Cell Biol. 1994;14:1815-1823

141. Olson MO. The Nucleolus. Molecular Biology Intelligence Unit: Landes Biosciences, Kluwer Academic; 2004

142. Fromont-Racine M, Senger B, Saveanu C, Fasiolo F. Ribosome assembly in eukaryotes. Gene. 2003;313:17-42

143. Bachellerie JP, Cavaille J, Huttenhofer A. The expanding snoRNA world. Biochimie. 2002;84:775-790

144. Russell J, Zomerdijk JC. RNA-polymerase-I-directed rDNA transcription, life and works. Trends Biochem Sci. 2005;30:87-96

145. Grummt I. Life on a planet of its own: regulation of RNA polymerase I transcription in the nucleolus. Genes Dev. 2003;17:1691-1702

146. Mayer C, Zhao J, Yuan X, Grummt I. mTOR-dependent activation of the transcription factor TIF-IA links rRNA synthesis to nutrient availability. Genes Dev. 2004;18:423-434

147. Savkur RS, Olson MO. Preferential cleavage in pre-ribosomal RNA byprotein B23 endoribonuclease. Nucleic Acids Res. 1998;26:4508-4515

148. Olson MO, Dundr M, Szebeni A. The nucleolus: an old factory with unexpected capabilities. Trends Cell Biol. 2000;10:189-196

149. Grummt I. Regulation of mammalian ribosomal gene transcription by RNA polymerase I. Prog Nucleic Acid Res Mol Biol. 1999;62:109-154

150. Ruggero D, Pandolfi PP. Does the ribosome translate cancer? Nat Rev Cancer. 2003;3:179-192

151. Hannan KM, Kennedy BK, Cavanaugh AH, Hannan RD, Hirschler-Laszkiewicz I, Jefferson LS, Rothblum LI. RNA polymerase I transcription in confluent cells: Rb downregulates rDNA transcription during confluence-induced cell cycle arrest. Oncogene. 2000;19:3487-3497

152. Mayer C, Grummt I. Cellular stress and nucleolar function. Cell Cycle. 2005;4:1036-1038

153. Zhao J, Yuan X, Frodin M, Grummt I. ERK-dependent phosphorylation of the transcription initiation factor TIF-IA is required for RNA polymerase I transcription and cell growth. Mol Cell. 2003;11:405-413

154. Yuan X, Zhou Y, Casanova E, Chai M, Kiss E, Grone HJ, Schutz G, Grummt I. Genetic inactivation of the transcription factor TIF-IA leads to nucleolar disruption, cell cycle arrest, and p53-mediated apoptosis. Mol Cell. 2005;19:77-87

155. Roussel MF. The INK4 family of cell cycle inhibitors in cancer. Oncogene. 1999;18:5311-5317

156. David-Pfeuty T, Nouvian-Dooghe Y. Human p14(Arf): an exquisite sensor of morphological changes and of short-lived perturbations in cell cycle and in nucleolar function. Oncogene. 2002;21:6779-6790

157. Weber JD, Taylor LJ, Roussel MF, Sherr CJ, Bar-Sagi D. Nucleolar Arf sequesters Mdm2 and activates p53. Nat Cell Biol. 1999;1:20-26

158. Llanos S, Clark PA, Rowe J, Peters G. Stabilization of p53 by p14ARF without relocation of MDM2 to the nucleolus. Nat Cell Biol. 2001;3:445-452

159. Zhang Y, Xiong Y. Mutations in human ARF exon 2 disrupt its nucleolar localization and impair its ability to block nuclear export of MDM2 and p53. Mol Cell. 1999;3:579-591

160. Itahana K, Bhat KP, Jin A, Itahana Y, Hawke D, Kobayashi R, Zhang Y. Tumor suppressor ARF degrades B23, a nucleolar protein involved in ribosome biogenesis and cell proliferation. Mol Cell. 2003;12:1151-1164

161. Iaquinta PJ, Aslanian A, Lees JA. Regulation of the Arf/p53 tumor surveillance network by E2F. Cold Spring Harb Symp Quant Biol. 2005;70:309-316

162. Lindstrom MS, Zhang Y. B23 and ARF: friends or foes? Cell Biochem Biophys. 2006;46:79-90

163. Colombo E, Marine JC, Danovi D, Falini B, Pelicci PG. Nucleophosmin regulates the stability and transcriptional activity of p53. Nat Cell Biol. 2002;4:529-533

164. Bhat KP, Itahana K, Jin A, Zhang Y. Essential role of ribosomal protein L11 in mediating growth inhibition-induced p53 activation. Embo J. 2004;23:2402-2412

165. Zhang Y, Wolf GW, Bhat K, Jin A, Allio T, Burkhart WA, Xiong Y. Ribosomal protein L11 negatively regulates oncoprotein MDM2 and mediates a p53-dependent ribosomal-stress checkpoint pathway. Mol Cell Biol. 2003;23:8902-8912

166. Dai MS, Zeng SX, Jin Y, Sun XX, David L, Lu H. Ribosomal protein L23 activates p53 by inhibiting MDM2 function in response to ribosomal perturbation but not to translation inhibition. Mol Cell Biol. 2004;24:7654-7668

167. Dai MS, Lu H. Inhibition of MDM2-mediated p53 ubiquitination and degradation by ribosomal protein L5. J Biol Chem. 2004;279:44475-44482

168. Rubbi CP, Milner J. Disruption of the nucleolus mediates stabilization of p53 in response to DNA damage and other stresses. Embo J. 2003;22:6068-6077

169. Van Zant G, Liang Y. The role of stem cells in aging. Exp Hematol. 2003;31:659-672

170. Campisi J. The biology of replicative senescence. Eur J Cancer. 1997;33:703-709

171. Dimri GP, Lee X, Basile G, Acosta M, Scott G, Roskelley C, Medrano EE, Linskens M, Rubelj I, Pereira-Smith O, et al. A biomarker that identifies senescent human cells in culture and in aging skin in vivo. Proc Natl Acad Sci U S A. 1995;92:9363-9367

172. Lloyd AC. Limits to lifespan. Nat Cell Biol. 2002;4:E25-27

173. Schmitt CA. Cellular senescence and cancer treatment. Biochim Biophys Acta. 2007;1775:5-20

174. Anisimov VN, Osipova G. Two-step carcinogenesis induced by neonatal exposure to 5-bromo-2'-deoxyuridine and subsequent administration of urethan in BALB/c mice. Cancer Lett. 1992;64:75-82

175. Suzuki T, Minagawa S, Michishita E, Ogino H, Fujii M, Mitsui Y, Ayusawa D. Induction of senescence-associated genes by 5-bromodeoxyuridine in HeLa cells. Exp Gerontol. 2001;36:465-474

176. Michishita E, Nakabayashi K, Suzuki T, Kaul SC, Ogino H, Fujii M, Mitsui Y, Ayusawa D. 5-Bromodeoxyuridine induces senescence-like phenomena in mammalian cells regardless of cell type or species. J Biochem (Tokyo). 1999;126:1052-1059

177. Minagawa S, Nakabayashi K, Fujii M, Scherer SW, Ayusawa D. Functional and chromosomal clustering of genes responsive to 5-bromodeoxyuridine in human cells. Exp Gerontol. 2004;39:1069-1078

178. Michishita E, Matsumura N, Kurahashi T, Suzuki T, Ogino H, Fujii M, Ayusawa D. 5-Halogenated thymidine analogues induce a senescence-like phenomenon in HeLa cells. Biosci Biotechnol Biochem. 2002;66:877-879

179. Rotstein JB, Kresnak MT, Samadashwily GM, Davidson RL. Analysis of sequence specificity of 5-bromodeoxyuridine-induced reversion in cells containing multiple copies of a mutant gpt gene. Somat Cell Mol Genet. 1992;18:179-188

180. Wojcik A, von Sonntag C, Obe G. Application of the biotin-dUTP chromosome labelling technique to study the role of 5-bromo-2'-deoxyuridine in the formation of UV-induced sister chromatid exchanges in CHO cells. J Photochem Photobiol B. 2003;69:139-144

181. Baraldi PG, Bovero A, Fruttarolo F, Preti D, Tabrizi MA, Pavani MG, Romagnoli R. DNA minor groove binders as potential antitumor and antimicrobial agents. Med Res Rev. 2004;24:475-528

182. Satou W, Suzuki T, Noguchi T, Ogino H, Fujii M, Ayusawa D. AT-hook proteins stimulate induction of senescence markers triggered by 5-bromodeoxyuridine in mammalian cells. Exp Gerontol. 2004;39:173-179

183. Suzuki T, Michishita E, Ogino H, Fujii M, Ayusawa D. Synergistic induction of the senescence-associated genes by 5-bromodeoxyuridine and AT-binding ligands in HeLa cells. Exp Cell Res. 2002;276:174-184

184. Liebich I, Bode J, Reuter I, Wingender E. Evaluation of sequence motifs found in scaffold/matrix-attached regions (S/MARs). Nucleic Acids Res. 2002;30:3433-3442

185. Ogino H, Satou W, Fujii M, Suzuki T, He Y, Michishita E, Ayusawa D. The Human MYOD1 Transgene Is Suppressed by 5-Bromodeoxyuridine in Mouse Myoblasts. J Biochem (Tokyo). 2002;132:953-959

186. Ito F, Sartwell AD, Chou JY. 5-Bromo-2'-deoxyuridine induces placental alkaline phosphatase biosynthesis in cultured choriocarcinoma cells. Arch Biochem Biophys. 1984;233:830-837

187. Cohen H, Andre J, Grenot C, Guillaumot P, Pascal O. Induction (or stimulation) of prolactin and growth hormone production in a rat pituitary tumor cell line by bromodeoxyuridine. Endocrinology. 1982;110:421-427

188. Comi P, Ottolenghi S, Giglioni B, Migliaccio G, Migliaccio AR, Bassano E, Amadori S, Mastroberardino G, Peschle C. Bromodeoxyuridine treatment of normal adult erythroid colonies: an in vitro model for reactivation of human fetal globin genes. Blood. 1986;68:1036-1041

189. Munger K, Baldwin A, Edwards KM, Hayakawa H, Nguyen CL, Owens M, Grace M, Huh K. Mechanisms of human papillomavirus-induced oncogenesis. J Virol. 2004;78:11451-11460

190.   Shyu WC, Lee YJ, Liu DD, Lin SZ, Li H. Homing genes, cell therapy and stroke. Front Biosci. 2006;11:899-907

191.   Pittenger MF, Mackay AM, Beck SC, Jaiswal RK, Douglas R, Mosca JD, Moorman MA, Simonetti DW, Craig S, Marshak DR. Multilineage potential of adult human mesenchymal stem cells. Science. 1999;284:143-147

192.   Bruder SP, Jaiswal N, Haynesworth SE. Growth kinetics, self-renewal, and the osteogenic potential of purified human mesenchymal stem cells during extensive subcultivation and following cryopreservation. J Cell Biochem. 1997;64:278-294

193.   Lee K, Majumdar MK, Buyaner D, Hendricks JK, Pittenger MF, Mosca JD. Human mesenchymal stem cells maintain transgene expression during expansion and differentiation. Mol Ther. 2001;3:857-866

194.   Majumdar MK, Thiede MA, Mosca JD, Moorman M, Gerson SL. Phenotypic and functional comparison of cultures of marrow-derived mesenchymal stem cells (MSCs) and stromal cells. J Cell Physiol. 1998;176:57-66

195.   Conget PA, Minguell JJ. Phenotypical and functional properties of human bone marrow mesenchymal progenitor cells. J Cell Physiol. 1999;181:67-73

196.   Jaiswal N, Haynesworth SE, Caplan AI, Bruder SP. Osteogenic differentiation of purified, culture-expanded human mesenchymal stem cells in vitro. J Cell Biochem. 1997;64:295-312

197.   Zhao LR, Duan WM, Reyes M, Keene CD, Verfaillie CM, Low WC. Human bone marrow stem cells exhibit neural phenotypes and ameliorate neurological deficits after grafting into the ischemic brain of rats. Exp Neurol. 2002;174:11-20

198.   Mackay AM, Beck SC, Murphy JM, Barry FP, Chichester CO, Pittenger MF. Chondrogenic differentiation of cultured human mesenchymal stem cells from marrow. Tissue Eng. 1998;4:415-428

199.   Tremain N, Korkko J, Ibberson D, Kopen GC, DiGirolamo C, Phinney DG. MicroSAGE analysis of 2,353 expressed genes in a single cell-derived colony of undifferentiated human mesenchymal stem cells reveals mRNAs of multiple cell lineages. Stem Cells. 2001;19:408-418

200.   Toma C, Pittenger MF, Cahill KS, Byrne BJ, Kessler PD. Human mesenchymal stem cells differentiate to a cardiomyocyte phenotype in the adult murine heart. Circulation. 2002;105:93-98

201.   Mikkers H, Frisen J. Deconstructing stemness. Embo J. 2005;24:2715-2719

202.   Muraglia A, Cancedda R, Quarto R. Clonal mesenchymal progenitors from human bone marrow differentiate in vitro according to a hierarchical model. J Cell Sci. 2000;113 (Pt 7):1161-1166

203.   Sekiya I, Larson BL, Smith JR, Pochampally R, Cui JG, Prockop DJ. Expansion of human adult stem cells from bone marrow stroma: conditions that maximize the yields of early progenitors and evaluate their quality. Stem Cells. 2002;20:530-541

204.   Rosen ED, Spiegelman BM. Adipocytes as regulators of energy balance and glucose homeostasis. Nature. 2006;444:847-853

205.   Rosen ED, Sarraf P, Troy AE, Bradwin G, Moore K, Milstone DS, Spiegelman BM, Mortensen RM. PPAR gamma is required for the differentiation of adipose tissue in vivo and in vitro. Mol Cell. 1999;4:611-617

206.   Spiegelman BM. PPAR-gamma: adipogenic regulator and thiazolidinedione receptor. Diabetes. 1998;47:507-514

207.   Rosen ED, MacDougald OA. Adipocyte differentiation from the inside out. Nat Rev Mol Cell Biol. 2006;7:885-896

208.   Jaiswal RK, Jaiswal N, Bruder SP, Mbalaviele G, Marshak DR, Pittenger MF. Adult human mesenchymal stem cell differentiation to the osteogenic or adipogenic lineage is regulated by mitogen-activated protein kinase. J Biol Chem. 2000;275:9645-9652

209.   Hu E, Kim JB, Sarraf P, Spiegelman BM. Inhibition of adipogenesis through MAP kinase-mediated phosphorylation of PPARgamma. Science. 1996;274:2100-2103

210.   Janderova L, McNeil M, Murrell AN, Mynatt RL, Smith SR. Human mesenchymal stem cells as an in vitro model for human adipogenesis. Obes Res. 2003;11:65-74

211. Farmer SR. Transcriptional control of adipocyte formation. Cell Metab. 2006;4:263-273

212. Greer EL, Brunet A. FOXO transcription factors at the interface between longevity and tumor suppression. Oncogene. 2005;24:7410-7425

213. Nakae J, Kitamura T, Kitamura Y, Biggs WH, 3rd, Arden KC, Accili D. The forkhead transcription factor Foxo1 regulates adipocyte differentiation. Dev Cell. 2003;4:119-129

214. Guo W, Lasky JL, 3rd, Wu H. Cancer stem cells. Pediatr Res. 2006;59:59R-64R

215. Roufa DJ. 5-bromodeoxyuridine-DNA strand symmetry and the repair of photolytic breaks in Chinese hamster cell chromosomes. Proc Natl Acad Sci U S A. 1976;73:3905-3909

216. Serrano M, Lin AW, McCurrach ME, Beach D, Lowe SW. Oncogenic ras provokes premature cell senescence associated with accumulation of p53 and p16INK4a. Cell. 1997;88:593-602

217. Ramirez-Zacarias JL, Castro-Munozledo F, Kuri-Harcuch W. Quantitation of adipose conversion and triglycerides by staining intracytoplasmic lipids with Oil red O. Histochemistry. 1992;97:493-497

218. Livak KJ, Schmittgen TD. Analysis of relative gene expression data using real-time quantitative PCR and the 2(-Delta Delta C(T)) Method. Methods. 2001;25:402-408

219. Fuchsova B, Hozak P. The localization of nuclear DNA helicase II in different nuclear compartments is linked to transcription. Exp Cell Res. 2002;279:260-270

220. Hozak P, Cook PR, Schofer C, Mosgoller W, Wachtler F. Site of transcription of ribosomal RNA and intranucleolar structure in HeLa cells. J Cell Sci. 1994;107 (Pt 2):639-648

221. Entenmann G, Hauner H. Relationship between replication and differentiation in cultured human adipocyte precursor cells. Am J Physiol. 1996;270:C1011-1016

222. Hauner H, Entenmann G. Regional variation of adipose differentiation in cultured stromal-vascular cells from the abdominal and femoral adipose tissue of obese women. Int J Obes. 1991;15:121-126

223. Wilmut I, Schnieke AE, McWhir J, Kind AJ, Campbell KH. Viable offspring derived from fetal and adult mammalian cells. Nature. 1997;385:810-813

224. Hauner H, Skurk T, Wabitsch M. Cultures of human adipose precursor cells. Methods Mol Biol. 2001;155:239-247

225. Ailhaud G. Adipose cell differentiation in culture. Mol Cell Biochem. 1982;49:17-31

226. Qiu Z, Wei Y, Chen N, Jiang M, Wu J, Liao K. DNA synthesis and mitotic clonal expansion is not a required step for 3T3-L1 preadipocyte differentiation into adipocytes. J Biol Chem. 2001;276:11988-11995

227. Min HY, Spiegelman BM. Adipsin, the adipocyte serine protease: gene structure and control of expression by tumor necrosis factor. Nucleic Acids Res. 1986;14:8879-8892

228. Leroy P, Dessolin S, Villageois P, Moon BC, Friedman JM, Ailhaud G, Dani C. Expression of ob gene in adipose cells. Regulation by insulin. J Biol Chem. 1996;271:2365-2368

229. Descombes P, Schibler U. A liver-enriched transcriptional activator protein, LAP, and a transcriptional inhibitory protein, LIP, are translated from the same mRNA. Cell. 1991;67:569-579

230. Kaestner KH, Christy RJ, Lane MD. Mouse insulin-responsive glucose transporter gene: characterization of the gene and trans-activation by the CCAAT/enhancer binding protein. Proc Natl Acad Sci U S A. 1990;87:251-255

231. Williams LB, Fawcett RL, Waechter AS, Zhang P, Kogon BE, Jones R, Inman M, Huse J, Considine RV. Leptin production in adipocytes from morbidly obese subjects: stimulation by dexamethasone, inhibition with troglitazone, and influence of gender. J Clin Endocrinol Metab. 2000;85:2678-2684

232. Bradley RL, Cheatham B. Regulation of ob gene expression and leptin secretion by insulin and dexamethasone in rat adipocytes. Diabetes. 1999;48:272-278

233. Masuzaki H, Ogawa Y, Hosoda K, Miyawaki T, Hanaoka I, Hiraoka J, Yasuno A, Nishimura H, Yoshimasa Y, Nishi S, Nakao K. Glucocorticoid regulation of leptin synthesis and secretion in humans: elevated plasma leptin levels in Cushing's syndrome. J Clin Endocrinol Metab. 1997;82:2542-2547

234. Wabitsch M, Brenner RE, Melzner I, Braun M, Moller P, Heinze E, Debatin KM, Hauner H. Characterization of a human preadipocyte cell strain with high capacity for adipose differentiation. Int J Obes Relat Metab Disord. 2001;25:8-15

235. Diascro DD, Jr., Vogel RL, Johnson TE, Witherup KM, Pitzenberger SM, Rutledge SJ, Prescott DJ, Rodan GA, Schmidt A. High fatty acid content in rabbit serum is responsible for the differentiation of osteoblasts into adipocyte-like cells. J Bone Miner Res. 1998;13:96-106

236. Hicok KC, Thomas T, Gori F, Rickard DJ, Spelsberg TC, Riggs BL. Development and characterization of conditionally immortalized osteoblast precursor cell lines from human bone marrow stroma. J Bone Miner Res. 1998;13:205-217

237. Houghton A, Oyajobi BO, Foster GA, Russell RG, Stringer BM. Immortalization of human marrow stromal cells by retroviral transduction with a temperature sensitive oncogene: identification of bipotential precursor cells capable of directed differentiation to either an osteoblast or adipocyte phenotype. Bone. 1998;22:7-16

238. Stone RM, O'Donnell MR, Sekeres MA. Acute myeloid leukemia. Hematology (Am Soc Hematol Educ Program). 2004:98-117

239. He LZ, Guidez F, Tribioli C, Peruzzi D, Ruthardt M, Zelent A, Pandolfi PP. Distinct interactions of PML-RARalpha and PLZF-RARalpha with co-repressors determine differential responses to RA in APL. Nat Genet. 1998;18:126-135

240. Marks P, Rifkind RA, Richon VM, Breslow R, Miller T, Kelly WK. Histone deacetylases and cancer: causes and therapies. Nat Rev Cancer. 2001;1:194-202

241. Kelly WK, O'Connor OA, Marks PA. Histone deacetylase inhibitors: from target to clinical trials. Expert Opin Investig Drugs. 2002;11:1695-1713

242. Hu E, Dul E, Sung CM, Chen Z, Kirkpatrick R, Zhang GF, Johanson K, Liu R, Lago A, Hofmann G, Macarron R, de los Frailes M, Perez P, Krawiec J, Winkler J, Jaye M. Identification of novel isoform-selective inhibitors within class I histone deacetylases. J Pharmacol Exp Ther. 2003;307:720-728

243. Gottlicher M, Minucci S, Zhu P, Kramer OH, Schimpf A, Giavara S, Sleeman JP, Lo Coco F, Nervi C, Pelicci PG, Heinzel T. Valproic acid defines a novel class of HDAC inhibitors inducing differentiation of transformed cells. Embo J. 2001;20:6969-6978

244. Genin P, Morin P, Civas A. Impairment of interferon-induced IRF-7 gene expression due to inhibition of ISGF3 formation by trichostatin A. J Virol. 2003;77:7113-7119

245. Mattsson K, Pokrovskaja K, Kiss C, Klein G, Szekely L. Proteins associated with the promyelocytic leukemia gene product (PML)-containing nuclear body move to the nucleolus upon inhibition of proteasome-dependent protein degradation. Proc Natl Acad Sci U S A. 2001;98:1012-1017

246. Flenghi L, Fagioli M, Tomassoni L, Pileri S, Gambacorta M, Pacini R, Grignani F, Casini T, Ferrucci PF, Martelli MF, et al. Characterization of a new monoclonal antibody (PG-M3) directed against the aminoterminal portion of the PML gene product: immunocytochemical evidence for high expression of PML proteins on activated macrophages, endothelial cells, and epithelia. Blood. 1995;85:1871-1880

247. Sternsdorf T, Jensen K, Will H. Evidence for covalent modification of the nuclear dot-associated proteins PML and Sp100 by PIC1/SUMO-1. J Cell Biol. 1997;139:1621-1634

248. Grisendi S, Mecucci C, Falini B, Pandolfi PP. Nucleophosmin and cancer. Nat Rev Cancer. 2006;6:493-505

249. Olson MO, Dundr M. The moving parts of the nucleolus. Histochem Cell Biol. 2005;123:203-216

250. Dundr M, Hoffmann-Rohrer U, Hu Q, Grummt I, Rothblum LI, Phair RD, Misteli T. A kinetic framework for a mammalian RNA polymerase in vivo. Science. 2002;298:1623-1626

251. Rohde J, Heitman J, Cardenas ME. The TOR kinases link nutrient sensing to cell growth. J Biol Chem. 2001;276:9583-9586

252. Hannan KM, Brandenburger Y, Jenkins A, Sharkey K, Cavanaugh A, Rothblum L, Moss T, Poortinga G, McArthur GA, Pearson RB, Hannan RD. mTOR-dependent regulation of ribosomal gene transcription requires S6K1 and is mediated by phosphorylation of the carboxy-terminal activation domain of the nucleolar transcription factor UBF. Mol Cell Biol. 2003;23:8862-8877

253. Danforth E, Jr. Failure of adipocyte differentiation causes type II diabetes mellitus? Nat Genet. 2000;26:13

254. Shoubridge EA, Johns T, Boulet L. Use of myoblast cultures to study mitochondrial myopathies. Methods Enzymol. 1996;264:465-475

255. Font de Mora J, Porras A, Ahn N, Santos E. Mitogen-activated protein kinase activation is not necessary for, but antagonizes, 3T3-L1 adipocytic differentiation. Mol Cell Biol. 1997;17:6068-6075

256. Gutierrez S, Javed A, Tennant DK, van Rees M, Montecino M, Stein GS, Stein JL, Lian JB. CCAAT/enhancer-binding proteins (C/EBP) beta and delta activate osteocalcin gene transcription and synergize with Runx2 at the C/EBP element to regulate bone-specific expression. J Biol Chem. 2002;277:1316-1323

257. Lekstrom-Himes J, Xanthopoulos KG. Biological role of the CCAAT/enhancer-binding protein family of transcription factors. J Biol Chem. 1998;273:28545-28548

258. Bordji K, Grillasca JP, Gouze JN, Magdalou J, Schohn H, Keller JM, Bianchi A, Dauca M, Netter P, Terlain B. Evidence for the presence of peroxisome proliferator-activated receptor (PPAR) alpha and gamma and retinoid Z receptor in cartilage. PPARgamma activation modulates the effects of interleukin-1beta on rat chondrocytes. J Biol Chem. 2000;275:12243-12250

259. Fahmi H, Di Battista JA, Pelletier JP, Mineau F, Ranger P, Martel-Pelletier J. Peroxisome proliferator--activated receptor gamma activators inhibit interleukin-1beta-induced nitric oxide and matrix metalloproteinase 13 production in human chondrocytes. Arthritis Rheum. 2001;44:595-607

260. Gupta RA, Brockman JA, Sarraf P, Willson TM, DuBois RN. Target genes of peroxisome proliferator-activated receptor gamma in colorectal cancer cells. J Biol Chem. 2001;276:29681-29687

261. Auwerx J, Cock TA, Knouff C. PPAR-gamma: a thrifty transcription factor. Nucl Recept Signal. 2003;1:e006

262. Gimble JM, Robinson CE, Wu X, Kelly KA, Rodriguez BR, Kliewer SA, Lehmann JM, Morris DC. Peroxisome proliferator-activated receptor-gamma activation by thiazolidinediones induces adipogenesis in bone marrow stromal cells. Mol Pharmacol. 1996;50:1087-1094

263. Ahdjoudj S, Lasmoles F, Oyajobi BO, Lomri A, Delannoy P, Marie PJ. Reciprocal control of osteoblast/chondroblast and osteoblast/adipocyte differentiation of multipotential clonal human marrow stromal F/STRO-1(+) cells. J Cell Biochem. 2001;81:23-38

264. Adams M, Montague CT, Prins JB, Holder JC, Smith SA, Sanders L, Digby JE, Sewter CP, Lazar MA, Chatterjee VK, O'Rahilly S. Activators of peroxisome proliferator-activated receptor gamma have depot-specific effects on human preadipocyte differentiation. J Clin Invest. 1997;100:3149-3153

265. Ibrahimi A, Teboul L, Gaillard D, Amri EZ, Ailhaud G, Young P, Cawthorne MA, Grimaldi PA. Evidence for a common mechanism of action for fatty acids and thiazolidinedione antidiabetic agents on gene expression in preadipose cells. Mol Pharmacol. 1994;46:1070-1076

266. Barroso I, Gurnell M, Crowley VE, Agostini M, Schwabe JW, Soos MA, Maslen GL, Williams TD, Lewis H, Schafer AJ, Chatterjee VK, O'Rahilly S. Dominant negative mutations in human PPARgamma associated with severe insulin resistance, diabetes mellitus and hypertension. Nature. 1999;402:880-883

267. Rangwala SM, Lazar MA. Transcriptional control of adipogenesis. Annu Rev Nutr. 2000;20:535-559

268. Chiba T, Yokosuka O, Arai M, Tada M, Fukai K, Imazeki F, Kato M, Seki N, Saisho H. Identification of genes up-regulated by histone deacetylase inhibition with cDNA microarray and exploration of epigenetic alterations on hepatoma cells. J Hepatol. 2004;41:436-445

269. Van Lint C, Emiliani S, Verdin E. The expression of a small fraction of cellular genes is changed in response to histone hyperacetylation. Gene Expr. 1996;5:245-253

270. Sakamoto S, Potla R, Larner AC. Histone deacetylase activity is required to recruit RNA polymerase II to the promoters of selected interferon-stimulated early response genes. J Biol Chem. 2004;279:40362-40367

271. Nusinzon I, Horvath CM. Interferon-stimulated transcription and innate antiviral immunity require deacetylase activity and histone deacetylase 1. Proc Natl Acad Sci U S A. 2003;100:14742-14747

272. Fu XY, Schindler C, Improta T, Aebersold R, Darnell JE, Jr. The proteins of ISGF-3, the interferon alpha-induced transcriptional activator, define a gene family involved in signal transduction. Proc Natl Acad Sci U S A. 1992;89:7840-7843

273. Lehtonen A, Lund R, Lahesmaa R, Julkunen I, Sareneva T, Matikainen S. IFN-alpha and IL-12 activate IFN regulatory factor 1 (IRF-1), IRF-4, and IRF-8 gene expression in human NK and T cells. Cytokine. 2003;24:81-90

274. Johnstone RW. Histone-deacetylase inhibitors: novel drugs for the treament of cancer. Nature Rev. Drug Discov. 2002;1:287-299

275. Sedelnikova OA, Horikawa I, Zimonjic DB, Popescu NC, Bonner WM, Barrett JC. Senescing human cells and ageing mice accumulate DNA lesions with unrepairable double-strand breaks. Nat Cell Biol. 2004;6:168-170

276. Borden EC, Lindner D, Dreicer R, Hussein M, Peereboom D. Second-generation interferons for cancer: clinical targets. Semin Cancer Biol. 2000;10:125-144

9 Appendix

Research paper I
<u>Janderová L</u>, McNeil M, Murrell AN, Mynatt RL, Smith SR.: Human mesenchymal stem cells as an in vitro model for human adipogenesis. Obes Res. 2003 Jan;11(1):65-74.

Obesity Research IF 2003 3.409

Research paper II
Vlasáková J, Nováková Z, **<u>Rossmeislová L</u>**, Kahle M, Hozák P, Hodný Z.: Histone deacetylase inhibitors suppress IFNα-induced up-regulation of promyelocytic leukemia protein. Blood. 2007 Feb 15;109(4):1373-80. Epub 2006 Oct 24.

Blood IF 2005 10.131

Research paper III
<u>Janderová-Rossmeislová L</u>, Nováková Z, Vlasáková J, Philimonenko V, Hozák P, Hodný Z.: PML protein association with specific nucleolar structures differs in normal, tumor and senescent human cells. J Struct Biol. 2007 Jul;159(1):56-70. Epub 2007 Mar 12

Journal of Structural Biology IF 2005 3.49